Welding Research

SPONSORED BY THE WELDING RESEARCH COUNCIL
OF THE ENGINEERING FOUNDATION

W. SPRARAGEN, DIRECTOR

SUPPLEMENT TO THE WELDING JOURNAL, APRIL, 1956

RUPTURE PROPERTIES OF INCONEL WELDMENTS AT 1400, 1600 AND 1800° F

Joint efficiencies up to 10,000-hr rupture life established for Inconel weldments operating in the temperature range of 1400 to 1800° F

BY D. A. SCOTT

ABSTRACT. A rupture testing program was carried out to determine the joint efficiency up to 10,000-hr rupture life of Inconel weldments at 1400, 1600 and 1800° F. Metal-arc coated electrode Inconel welding rod was used to join $^3/_8$-in. thick Inconel plate, in the fine- and coarse-grained conditions. Inert-gas consumable electrode Inconel welding rod was used to join $^3/_8$-in. thick fine-grained Inconel plate. Samples of plate, weldments and weld metal were tested in standard creep-rupture machines. At 1400° F joint efficiencies up to 10,000-hr rupture life were 100%. At 1600° F, joint efficiencies varied between 100% at 500 hr and 80–85% at 10,000-hr rupture life. At 1800° F. inert-gas joint efficiencies were 95% at all times, but metal-arc joint efficiencies varied as follows: (1) 85% at 500 hr to 100% at 10,000 hr rupture life in fine-grained plate; and (2) 75% at 500 hr to 85% at 10,000 hr in coarse-grained plate. Post-welding treatment of fine-grained plate weldments at 2050° F for 2 hr showed marked improvement of weldment rupture life at 1800° F and high-stress levels.

Introduction

Many high-temperature alloys are fabricated into weldments for service in the temperature range 1400 to 1800° F. No information can be found in the literature relating to joint efficiencies which could lead to proper assessment for design purposes. Much of the design work is based on either room temperature properties or welder preference tests. Some time ago the International Nickel Co., Inc., had occasion to run casual rupture tests on Inconel X weldments, and were surprised to find that the weldment rupture strength ran some 30–40% lower than that of the plate. It was felt necessary, therefore, to examine the rupture properties of high-temperature alloy weldments. As a result of this, a rupture testing program for Inconel weldments was initiated to establish joint efficencies up to 10,000-hr rupture life at 1400,1600 and 1800° F.

Material for Testing

A number of weld samples were prepared by welding together pieces of Inconel, measuring 4- x 11- x $^3/_8$-in., along the 11 in. edge. In all cases, radiographs showed that the welds chosen for testing were completely sound.

Two types of plate used were: (1) hot-rolled and mill-annealed 2 hr at 1650° F (fine-grained); and (2) as in (1) but subsequently grain-coarsened for 2 hr at 2050° F. Two welding methods used were: (1) coated-electrode metallic-arc; and (2) inert-gas consumable-electrode, the former method being used for both plate grain sizes, the latter only with fine-grained plate.

Typical analyses of materials tested are as follows:

Elements	*C*	*Mn*	*Fe*	*S*	*Si*	*Cu*	*Ni*	*Cr*	*Cb*
Inconel plate	0.03	0.33	7.79	0.007	0.21	0.14	75.80	15.67	...
Metal-arc weld metal	0.10	0.35	9.50	0.007	0.50	0.15	71.5	15.0	2.50
Inert-gas weld metal	0.05	0.25	7.0	0.007	0.40	0.15	74.5	15.0	2.00

Method of Testing

Rupture tests were performed on plate, weld metal and weldment samples machined from the above-mentioned weldments. The plate samples were taken from material remaining after removing the weld metal samples.

Rupture samples were machined to 0.375 in. diam along a 2 in. gage length. Although rupture ductilities of weldments will vary according to the gage length of the test bar, the 2 in. length was chosen as a standard for comparison of plate and weldments. The weldment samples were chosen to include the weld at the center of the gage length without any reinforcement.

Test temperatures used were 1400, 1600 and 1800° F. Stresses were chosen on the basis of available data on Inconel plate. Rupture lives of 500 hr or more were attempted; where adequate test samples were available sufficient data was obtained to allow an assessment of behavior at 10,000-hr rupture life by means of a reasonable extrapolation.

Results of Tests

The results of rupture tests of plate, weldments and weld-metal are listed in Table 1. Plots of log stress–log rupture time are shown in Figs. 1 and 2. All of the weldment data are compared with

D. A. Scott is Metallurgist, International Nickel Co. of Canada, Ltd., Ottawa, Ontario.

To be presented at AWS 1956 National Spring Meeting in Buffalo, N. Y., May 7–11, 1956.

Table 1—Test Data on Plate, Weldments and Weld-Metal

Material tested	Test temperature, ° F.	Stress, psi	Rupture life, hr	Rupture Elongation, % in 2 in.	Position of fracture
Fine-grained plate	1400	8500	666	85.2	.....
	1400	7000	1874	77	.....
	1600	4000	631	52	.....
	1600	3500	1176	31	.....
	1800	2000	506	54	.....
	1800	2000	399	47	.....
	1800	1600	1146	75	.....
	1800	1300	3669	99	.....
Coarse-grained plate	1400	8500	582	93	.....
	1400	7000	2469	52	.....
	1600	4000	642	41	.....
	1600	3000	2402	28	.....
	1800	2000	914	16	.....
	1800	1400	6502	75	.....
Metal-arc weldment in fine-grained plate	1400	8500	720	42	Base metal
	1400	7000	2073	40	" "
	1600	4000	515	9	Fusion line
	1600	3500	789	6	" "
	1600	2750	1725	4	" "
	1800	2000	285	6	" "
	1800	2000	188	3	" "
	1800	2000	177	4	" "
	1800	1750	363	6	" "
	1800	1750	423	10	" "
	1800	1450	2184	70	Base metal
	1800	1500	3866	100	" "
Metal-arc weldments in coarse-grained plate	1400	8500	723	24	Base metal
	1600	4000	656	11	Fusion line
	1600	3000	1491	3	" "
	1800	2000	271	6	" "
	1800	1200	7330	18	Weld metal
Inert-gas weldment in fine-grained plate	1400	8500	644	44	Base metal
	1600	4000	601	16	Fusion line
	1800	2000	340	15	Base metal
	1800	1500	1312	32	" "
Metal-arc weld metal	1400	8000	4862	1	.....
	1600	4000	707	2	.....
	1800	2000	330	4	.....
	1800	1750	1147	13	.....
	1800	1500	1413	7	.....
Inert-gas weld metal	1800	2000	632	2	.....
	1800	1750	843	12	.....

plate in Fig. 1 and weld-metal data are compared with fine-grained plate in Fig. 2.

The results of tests showing the effect of post-welding heat treatments are listed in Table 2.

Table 2—2000 psi, 1800° F Rupture Tests, Post-Welding Heat Treatment

Test material	Temp. of 2-hr post-welding treatment	Hours to rupture	Rupture elongation, % in 2 in.	Min creep rate in/in./hr. × 10^{-6}	Start of 3rd stage creep, hr.
Metal-arc weldment in fine-grained plate	No treatment	278	10	...	...
	1950° F	454	32	...	...
	2050° F	644	34	...	...
Inert-gas weld metal	No treatment	425	6	13	75
	1950° F	577	8	17	100
	2050° F	646	10	10	140

Behavior at 1400° F

All of the materials except the weld metal have similar rupture lives at 1400° F; the weld-metal is much stronger than the plate and this, together with high plate ductility, accounts for weldment breakages occurring in the plate. The total ductility of weldments is lower than that of the plate because of the fact that a portion of the gage length comprises very low ductility weld metal. Joint efficiencies of all weldments are 100% at all times up to 10,000 hr.

Behavior at 1600° F

Rupture strength of weldments at 1600° F is less than that of the plate. At 500-hr rupture life metal-arc weldments made in fine-grained plate have some 95% of the plate rupture strength, whereas inert-gas weldments in fine-grained plate and metal-arc weldments made in coarse-grained plate have 100% of the plate strength. However, with increasing rupture life the weldments become increasingly weaker than the plate so that at 10,000-hr rupture life joint efficiencies are between 80 and 85% for all weldments. Weld-metal has the same rupture strength as the plate. The lower strength of the weldments is not due to lower weld-metal strength but to weakening at the fusion line, where all fractures occurred. This is attributed to stress concentration in the fusion zone where the relatively high-ductility plate and the very low-ductility weld-metal behave differently under load.

Rupture ductilities of plate and of all weldments are lower with increasing rupture life, and it is suggested that this is due to carbide precipitation at the grain boundaries, such precipitation being slow at 1600° F and accelerating with time at temperature.

Behavior at 1800° F

The behavior at 1800° F is somewhat more complicated than that at the two lower temperatures. The first complicating factor is that the coarse-grained plate has some 15% greater rupture strength than the fine-grained plate. Both types of weld-metal have about the same rupture strength as the fine-grained plate (Fig. 2). Therefore, it would be expected that all of the weldments made in fine-grained plate would have rupture lives controlled by either plate or weld-metal behavior, and that weldments made in coarse-grained plate would be controlled only by the lower rupture strength of the weld-metal. However, metal-arc weldments made in fine-grained plate, tested at 2000 psi and 1750 psi, ruptured at some $^1/_2$ to $^1/_2$ of the plate rupture life, and a metal-arc weldment made in coarse-grained plate, tested at 2000 psi, had $^1/_2$ the plate rupture life. All of these broke at the fusion line with very low rupture ductility and hence it is a stress concentration factor which governs at short rupture life at 1800° F, as it does at 1600° F at long rupture life. It was found that at 1800° F carbide precipitation is very rapid and this is certainly a cause of very low plate and weldment ductility at high-stress levels (low-rupture life).

In contrast to the above, rupture ductilities at lower stress levels are much

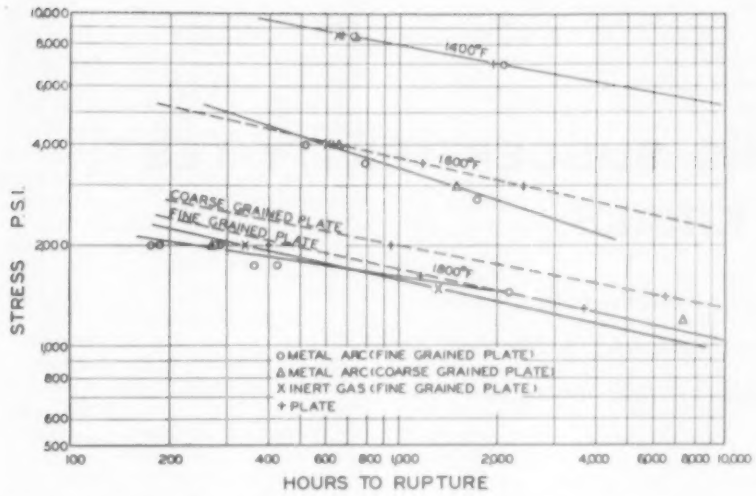

Fig. 1 Stress-rupture data of Inconel weldments compared with plate data

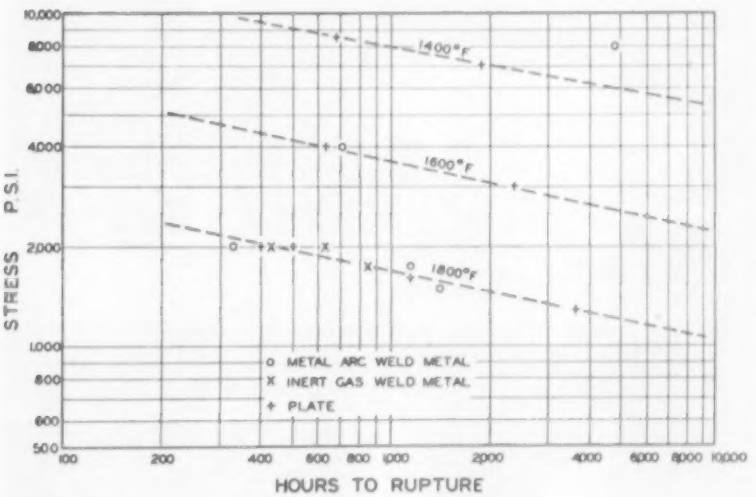

Fig. 2 Stress-rupture data of Inconel weld metal compared with fine-grained plate data

higher, and this is attributed to the fact that longer times at 1800° F result in carbide spheroidization and decarburization both, in the plate material. Coupled with the effect on carbides is considerable grain growth occurring in the fine-grained plate and grain boundary migration in both types of plate.

Two metal-arc weldments in fine-grained plate, tested at 1500 psi, broke in base metal, one with the same rupture life as the plate, the other, surprisingly, with almost double the plate life. A similar weldment in coarse-grained plate, on the other hand, when tested at 1200 psi, broke in weld-metal; this rupture point, if considered in Fig. 2, falls within reasonable limits of the weld-metal strength.

Metal-arc weldment joint efficiencies are: at 500-hr rupture life, 85% for fine-grained plate weldments and 75% for coarse-grained plate weldments; at 10,000-hr rupture life, 100% for fine-grained plate weldments and 85% for coarse-grained plate weldments. Because of breakage in either plate or weld-metal the solid curve in Fig. 1 for metal-arc weldments has been drawn at low-stress levels to coincide with the fine-grained plate curve.

The inert-gas weldments made in fine-grained plate, tested at 1800° F, broke in the base metal (in contrast to the performance of highly stressed metal-arc weldments). Based on the two points plotted in Fig. 1, joint efficiencies are 95% at all rupture times. No tests were made of inert-gas weldments in coarse-grained plate, but undoubtedly the lower rupture strength of the weld-metal would produce a joint efficiency of such weldments of close to 85% at 10,000-hr rupture life.

Post-Welding Heat Treatment

The behavior of metal-arc weldments in fine-grained plate at high-stress levels, at 1800° F, led to some cursory tests showing the effect of post-welding heat treatment on rupture life. The immediate effect of heat treatments of 2 hr at 1950 and 2050° F, is to coarsen fine-grained plate, and thus increase its creep resistance and rupture strength. The data on Table 2 indicate that the rupture life of metal-arc weldments at 2000 psi can be doubled with a considerable improvement in the rupture ductility. Fracture still occurs at the fusion line. Tests of inert-gas weld-metal show some improvement in its rupture life resulting from heat treatment. Thus, at 2000 psi and 1800° F, 100% joint efficiency has been achieved for metal-arc weldments and it is possible that some of the other types of weldments might be similarly, or at least somewhat, improved by a like treatment. However, it is felt that post-welding heat treatment would not appreciably improve the low-stress rupture life of weldments. The higher joint efficiencies achieved at 1800° F and lower stresses, as-welded, are attributable to an "automatic post-welding heat treatment" occurring during the life of the test specimens.

Of practical significance, a post-welding heat treatment should be given, where possible, for high-stress applications of Inconel weldments.

Summary

Rupture testing of Inconel weldments, plate and weld-metal has shown that:

(1) At 1400° F, 100% joint efficiencies are obtained at all rupture lives.

(2) At 1600° F, 100% joint efficiencies are obtained only up to 500-hr rupture life, and this gradually drops to 80–85% at 10,000-hr rupture life.

(3) At 1800° F, metal-arc joint efficiencies are 75 and 85% at 500 hours rupture life and 85 and 100% at 10,000-hr rupture life for coarse- and fine-grained Inconel plate weldments, respectively.

(4) At 1800° F, joint efficiencies of inert-gas weldments in fine-grained Inconel are 95% at all rupture lives.

(5) Post-welding heat treatment at 2050° F, 2 hr can markedly improve metal-arc weldments rupture life at 1800° F and high-stress levels.

Acknowledgment

The author wishes to thank the various members of the Mines Branch, Department of Mines and Technical Surveys, Ottawa, and in particular H. V. Kinsey, P. Eng., for their cooperation in making this study possible.

A WELD CRACKING SUSCEPTIBILITY TEST FOR SHEET MATERIALS

Quantitative test developed for the determination of the weld cracking properties of sheet materials believed to be a reliable tool for the determination of their weldability

BY JOHN S. BOUDREAU

ABSTRACT. A quantitative test has been developed for the determination of the weld cracking properties of sheet materials. A testing device was designed and built. The test consists of applying a measurable, steady, tensile load to a sample of sheet stock while an inert-arc weld is made normal to the axis of loading, without filler being added. The load at which cracking is initiated is an index of weld cracking susceptibility and may be determined rapidly with a minimum of preparation and examination. Good correlation was obtained between the indices determined and the known weldability of certain materials. Predictions of welding behavior for some new and experimental alloys are made. Photographs of the equipment, specimens and test results are included. Charts showing the comparative index values of several materials are also given.

Introduction

Hot cracking due to welding in many high-temperature alloys, particularly the precipitation-hardening types, has been a major deterrent to their adoption for use in fabricated assemblies. From a welding standpoint, to attempt substitution for an established material, or to evaluate new materials, treatments and alloy modifications usually involve a trial-and-error procedure, incur much expense and are time-consuming as well. Even then, in many cases, successful results cannot be realized. Although many potential material substitutes and improvements exhibit desirable or superior mechanical and physical properties, the lack of information about their behavior when welded, or during welding, precludes their immediate use.

At the present stage of alloy design, theoretical prediction of welding behavior is not possible. Those welding characteristics which are known have been obtained through experience, usually by the evaluation, destructively, of simulated or of actual production assemblies. Furthermore, this procedure is not quantitive, and findings can be applied only to the assemblies under consideration. Repetitive results are infrequent.

The problem of developing weldability tests for various conditions of design and materials has long been a subject of investigation by the General Electric Co. In addition to the standard qualification tests for operators and for joint designs, much work has been done on the evaluation of new and unusual joint configurations and material combinations for the many and varied types of apparatus currently being produced. Most weldability tests, however, are for a specific set of

Fig. 1 Testing machine in operation

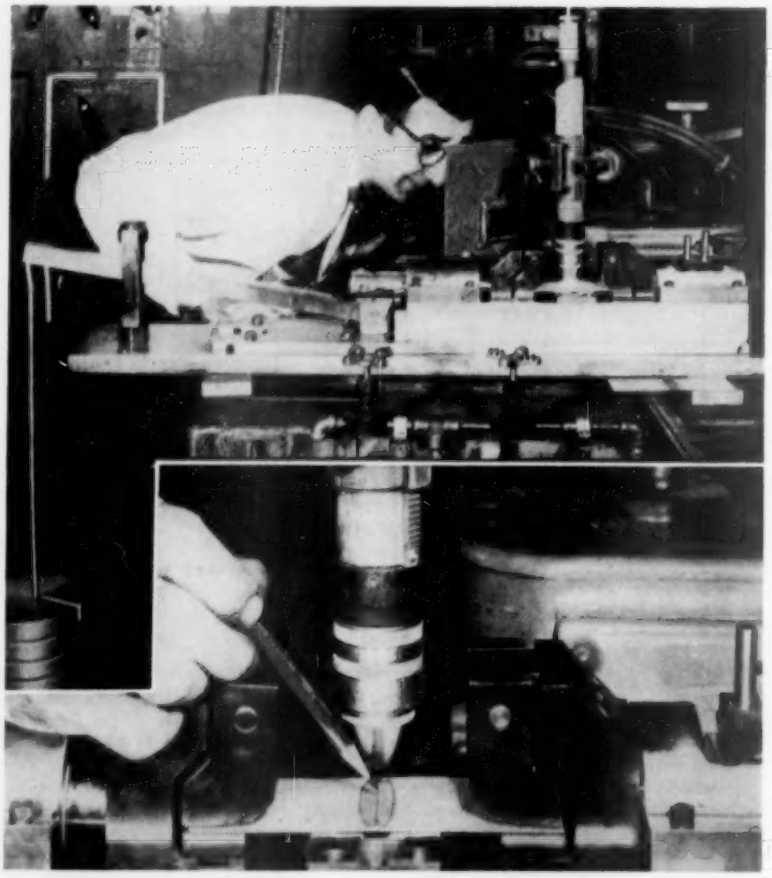

Fig. 2 Tested specimen in place

John S. Boudreau is Welding Engineer in the Thomson Laboratory, Small Aircraft Engine Department, General Electric Co., Lynn, Mass.

Paper to be presented at 1956 AWS National Spring Meeting, Buffalo, N. Y., May 7–11.

conditions. They require much preparation before welding and extensive machining, polishing and visual inspection after welding. They usually involve a "go, no-go," procedure, and results cannot be compared directly to other materials or material combinations. Filler metals are generally required, and this introduces still another variable. At best, these tests are indicative only; quantitative readings are not possible, and any values attached must be assigned arbitrarily. Several of these tests are described by Stout and Doty.[1]

To apply these tests to sheet stock presents a difficult problem. A rigidly held sheet tends to upset when welding stresses and temperature gradients are introduced. Stress levels are not only difficult to control, but are impossible to measure without elaborate equipment. Furthermore, they are never completely reproducible.

The welding properties of sheet metals are of particular importance in the aircraft gas turbine field. In the design of materials to meet the increasing operational temperatures and stresses, the need for a reliable quantitative test for measuring weld cracking susceptibility has long been recognized.

It is a well-established fact that restraint cracking—that is, cracking which occurs when weldments or base metals are unable to withstand the stresses set up in a rigidly held joint—is a major fabrication problem. This effect is accentuated by the fixturing necessary for welding assemblies which must be held to extremely close tolerances. While this property has not been favorable in fabrication, it has been made to work to advantage in testing and is the basis of many weldability tests.

A very promising test employing this principle has been developed. This test consists of applying a definite, steady, tensile load to a sample of sheet stock while an inert-arc weld is made normal to the axis of loading, without filler being added. Thus, a substantially unidirectional, measurable stress is applied to a specimen while it is welded under conditions which simulate the stress due to welding and to the resultant thermal expansion and contraction. The stress level at which cracking is initiated is an index of the weld cracking susceptibility of the material, and rapid determinations can be made with a minimum of preparation and evaluation.

Preliminary Testing

Initial tests along these lines were conducted by S. Weiss.[2] Using a manually operated horizontal tensile testing machine, it was shown rather quickly that cracking occurred at different stress levels for Type 321 material and for A-286 alloy. Since it is well known that Type 321 is readily weldable in production and that A-286 presents a much more difficult fabrication problem, it was felt that these two materials could be used as base points in the development of a weld cracking susceptibility test.

The use of the manually operated testing machine required two men: one to operate the welding equipment, the other to maintain a steady load on the specimen by compensating for the expansion and contraction of the specimen during the welding cycle. Since operator techniques varied, and unattended operation of this equipment resulted in wide variations in load for a given test, it was decided to build a testing device which would automatically compensate for load changes during operation. A static load testing machine was built to accommodate loads up to 2400 lb. Figure 1 is a photograph showing this testing machine in operation. The load is applied to the specimen by means of a lead-weight lever linkage and is indicated on the dial of a force gage. Figure 2 is a close-up of the test specimen in place with the torch in position at the end of a weld pass.

Development of the Test

In order to establish standard specimen size and optimum testing techniques, and to evaluate several materials, the following procedure was employed.

The tests that were made on the original testing machine were limited to specimens whose physical dimensions did not exceed a length of 6 in. and a width of 2 in. A thickness of 0.062 in. was selected, as this size was readily available in the standard alloys and could also be obtained in most experimental materials. The new testing device was also designed to accommodate these sizes, as they appeared to be satisfactory and because considerable data had already been accumulated on several alloys. Final dimensions of the test specimen, however, were dependent on the testing technique evolved. This consisted of initiating a d-c straight-polarity arc, either manually or automatically, between the specimen and a $^1/_{16}$-in. thoriated tungsten electrode with an electrode clearance of 0.062 in. Argon at 10 cfh was employed as a shielding atmosphere. The weld was started at a point far enough from the edge of the specimen to prevent burn-off, but close enough to minimize the influence of the unaffected base metal. Simultaneously, a traveling mechanism was started, and the arc traversed the specimen normal to the axis of loading at a speed of 10 ipm. If the arc was allowed to dwell before the start of travel, a crack was initiated and followed along the weld, indicating an unrealistic index. Too rapid a travel start resulted in a weld bead with inadequate penetration.

As the arc traveled across the specimen, a variable resistance was cut in a short distance from the end of the run. The resultant voltage reduction served to eliminate craters and to cut off the arc completely in a travel distance of $^1/_2$ in. if allowed to run at the testing speed. However, if the arc ran off the specimen, burn-back occurred and the results were not reproducible. Therefore, the arc was interrupted completely during the voltage reduction at a point just before the edge of the specimen was reached.

Having established a suitable welding technique, the optimum specimen width was next determined. Samples of A-286 and Type 321 materials were cut into widths of 2, $1^7/_8$, $1^3/_4$, $1^5/_8$ and $1^1/_2$ in., respectively. Weld cracking susceptibility indices were obtained for

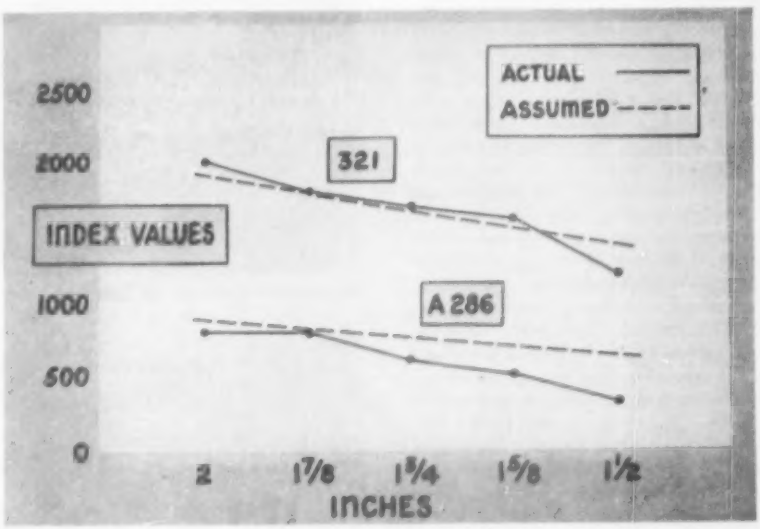

Fig. 3 Index vs. specimen width

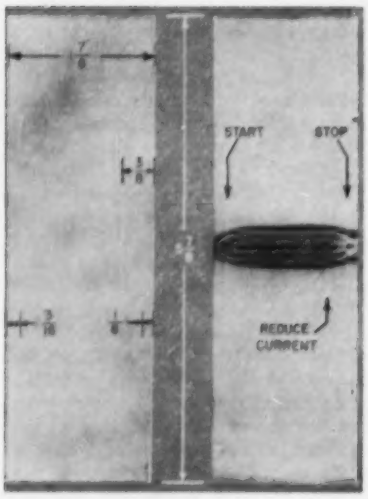

Thickness = 0.062 in.

Fig. 4 Test specimens

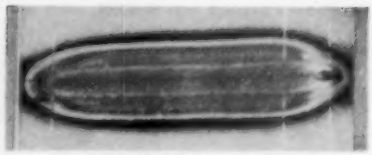

Ideal current, 75 amp; no failure at 1800 lb load (Type 321 index)

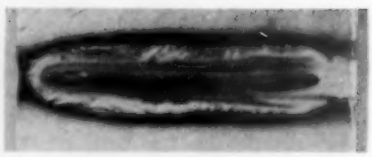

Ideal penetration at 75 amp

Ideal current, 75 amp; failure at 1900 lb load

Enlarged view of cracked specimen

High current, 80 amp; failure at 1700 lb load

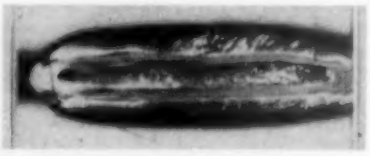

High penetration at 80 amp

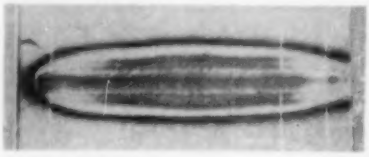

Low current, 70 amp; no failure at 1900 lb load

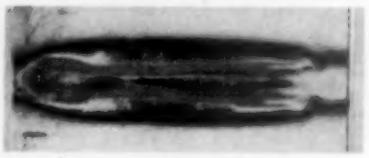

Low penetration at 70 amp

Fig. 5 Testing sequence

each size for the respective alloys. Figure 3 is a plot of the effect of specimen width on the weld cracking susceptibility index. The dotted lines in the figure were drawn by projecting the psi load of the index obtained on a 1 7/8-in. wide specimen, to the other sizes on the assumption that the weldability index is proportional to the cross-sectional areas of the specimens. For Type 321 it will be noted that a fairly good correlation was obtained, while for A-286 the slope is somewhat different. While these relationships might prove useful for evaluating subsize specimens, it was decided to standardize on the 1 7/8 in. width because of conditions imposed by the load capacity of the testing machine and the optimum travel distance of arc. Some tests were made on 0.044-in. stock of standard widths at lower currents, but the indices obtained did not correlate too well with the results on the 0.062 in. thickness on a limited number of materials. However, on a given material the results were reproducible and it is felt that, if necessary, comparative indices could be obtained. A specimen length of 5 7/8 in. was arbitrarily chosen as standard, as it was felt that length is not critical, and this size handled well in the equipment. The dimensions of the standard test specimen and a typical weld pattern are shown in Fig. 4. During the determination of optimum size, it was also found that alignment is quite critical. Extraneous stresses, such as bending or torsion which might be introduced by the testing machine or by the backing fixture, caused erratic results. The jaws of the tensile machine were adjusted for axial alignment, and the backing fixture was held with very light pressure against the specimen. This backing fixture consisted of a copper block 2 x 4 x 3/8 in. with a groove 3/8 in. wide x 1/32 in. deep. Penetration studies indicated that the best condition for duplication of results was achieved by a current setting which would result in a bead penetration with a width of 3/32 to 1/8 in. on the underside of the specimen, while the sag of weld metal did not come in contact with the copper backing. Any penetration below this amount required excessive loading to effect cracking. Penetration in excess of this amount resulted in cracking at lower stress levels and sometimes in the introduction of the chilling

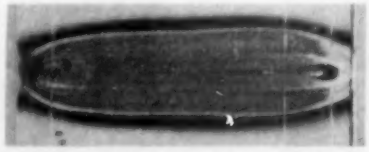

High current, 85 amp; high load 2000 lb

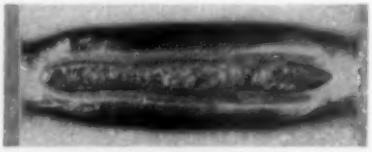

High penetration at 85 amp

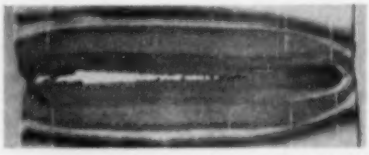

Excessive current, 90 amp; excessive load, 2200 lb

Delay in start of traverse

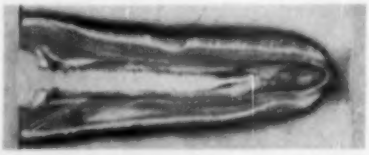

Start too close to edge

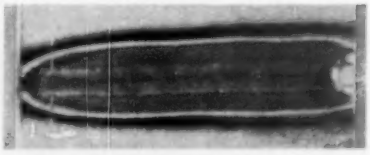

Run-off burn-back

Fig. 6 Improper testing techniques

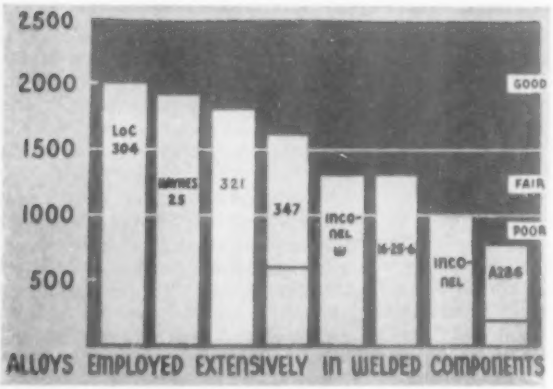

Fig. 7 Weld cracking susceptibility index

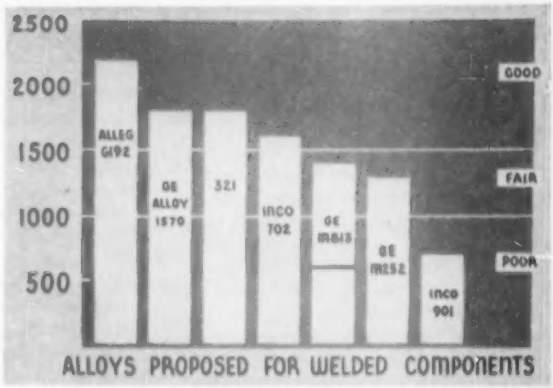

Fig. 8 Weld cracking susceptibility index

effect of the backing against the weldment. Erratic values resulted whenever deviation from this procedure occurred. Because of the differences in arc action of the various materials tested, it was necessary to adjust the current to the material in each case in order to obtain the proper penetration, rather than to maintain a constant current in all cases. Although these adjustments were small, they nevertheless had a profound effect on the index values.

The optimum testing technique, as finally established, is as follows.

The test specimen, scale-free and degreased, is placed in the testing machine, and a load is applied. Generally, the starting point for an unfamiliar alloy would be 1200 lb, but as experience is gained wih a particular family of alloys, a different level might be suggested. A weld is made with a current of approximately 75 amp. The specimen is removed within 30 sec. and examined for penetration and for cracking. If penetration is not correct, adjustments in current are made with each successive test until proper effects are observed. The load is then varied in 100-lb increments until the highest load at which cracking does not occur is determined. This is the weld cracking susceptibility index. Once this is determined, the load is then lowered by 100 lb, the current is increased by 5 amp and the test repeated. This increases penetration, and a crack should occur at the lower load. The load is then raised to a level 100 lb above the index, the current is reduced 5 amp below ideal and the test is repeated. Penetration is low and no cracks should result. These two additional steps serve to bracket the index. Figure 5 illustrates this testing sequence as used on Type 321 alloy and also includes an enlarged view of the type of cracking observed.

Excellent reproducibility of results was possible using this technique. However, misleading observations resulted if the improper techniques previously discussed were employed. The effects of these are illustrated in Fig. 6.

Evaluation of Materials

Along with the development of the testing technique, a program of material evaluation was simultaneously undertaken. Weld cracking susceptibility indices were obtained for several high-temperature alloys and alloy modifications. Good correlation was obtained between the indices determined and the known weldability of certain materials. In the case of new materials or alloys of limited welding experience, predictions of their welding properties were made on the basis of these tests. The indices of alloys which are employed extensively in welded components are given in Fig. 7. The results obtained on alloys proposed for use are shown in Fig. 8. The comparative chemical compositions of these materials are found in Table 1.

It should be noted that many of these results are on the basis of single heats and were made at a time when the test was being developed. For these reasons, the values presented should not be taken as absolute.

The highest index determined was that of Allegheny G-192, an experimental material for which no production welding experience is available. This alloy along with GE alloy 1570 and Inco 702, should prove to be readily weldable if these tests are significant. For the other high index materials—Low Carbon Type 304, Haynes 25 and Type 321—there is excellent correlation between their index level and their ease of welding. In the intermediate range, the Inconels, 16-25-6 and M252, correlate well with experience. At the lower end of the scale may be found A-286 alloy on which many welding problems have been encountered. Also,

Table 1—Nominal Compositions of Materials Evaluated

Material	*Index*	*C*	*Mn*	*Cr*	*Ni*	*Mo*	*Al*	*Ti*	*W*	*Co*	*Fe*	*N*	*Cb*	*V*
Allegheny G192	2200	0.6	8	22	..	..	..	..	..	..	Bal	0.35	..	..
Low C Type 304	2000	0.02	2	19	9	..	..	..	..	..	Bal	..	..	..
Haynes 25	1900	0.10	..	20	10	..	..	..	15	50	2.5	..	..	..
GE Alloy 1570	1800	0.2	..	20	28	..	..	4	7	38	2	..	..	..
Type 321	1800	0.08	2	18	9	..	..	0.4	..	..	Bal	..	..	..
Type 347	600–1600	0.08	2	18	10	..	..	..	..	..	Bal	..	0.8	..
Inco 702	1600	0.02	..	16	80	..	3	0.6	..	..	..	..	..	..
GE M813 (1)	1400	0.03	10	16	17	4	0.75	2	..	..	Bal	..	..	..
GE M813 (2)	600	0.03	..	18	35	2	0.7	2	..	..	Bal	..	..	..
Inconel W	1300	0.04	..	15	74	..	0.6	2.4	..	..	7	..	..	..
16-25-6	1300	0.09	..	16	25	6.5	..	..	..	..	Bal	0.15	..	..
GE M252	1300	0.1	..	19	54	10	0.75	2.5	..	10	2	..	..	..
Inconel	1000	0.05	..	14.5	78	..	..	..	..	..	7	..	..	..
A-286	300–800	0.08	..	15	25	1.25	0.35	2	..	..	Bal	..	..	0.25
Inco 901	700	0.05	0.5	13	43	6	0.15	2.5	..	..	35	..	..	..

it would appear that Inco 901, for which there is no available welding experience, is not a promising material from a fabrication standpoint.

It will also be noted that there is a range of index values for Inconel X, M813, A-286 and Type 347 materials. This is due to variations in composition or treatment and indicates the apparent sensitivity of this test to these factors. There is strong evidence that certain heats of a material, within specification limits, display a difference in weld-cracking properties. The results on Type 347 are an excellent example of this. Of the two heats tested, one exhibited a high index, 1600, while the other gave low results, 600. No significant differences could be noted in their compositions, and both were within specification limits. This is consistent with actual industrial experience.

The results thus far obtained in the evaluation of materials have indicated a certain reliability of this test. However, much more data must be accumulated before a categorical acceptance or rejection of a specific alloy can be made. Many heats and conditions of a given material should be investigated.

In an effort to determine the reliability of this test, a program has been initiated for comparing the results on this test with those made at Rensselaer Polytechnic Institute on the hot ductility apparatus as described by Nippes, *et al.*[3] Several alloys will be tested by both methods, and it is expected that this information will be published at a later date.

Other Observations

In addition to the evaluation of the weldability of specific materials, some miscellaneous tests were conducted. The following observations were made:

Most of the test specimens employed in this investigation were cut to size by flat shearing. On a single heat of A-286, tests indicated no differences in index values on specimens which were machined, ground or sheared to size.

No differences in results were found when welds were made normal or parallel to the direction of rolling on tests which were confined to A-286, Type 321 and Inconel W.

Scale was removed from test specimens either by molten-salt cleaning, grit blasting or by abrasive polishing. The method of scale removal had no measurable effect on the results, but heavily scaled or dirty material gave inconsistent readings. In some cases, materials which had a thin mill or heat-treating scale displayed higher index values than scale-free specimens from these same heats. However, these tests were limited, and no definite conclusions should be drawn without further investigation.

Summary

It is felt that the weld cracking susceptibility test described here is a reliable tool for the determination of the weldability of specific materials. It is also useful for the evaluation of the effects of variations in composition, heat treatment, melting practice and other processes on welding behavior and on hot-tearing properties. Its greatest value, however, may come in furthering a better understanding of the nature of weld cracking as affected by incipient-melting phenomena, precipitation-hardening mechanisms, solidus-liquidus gap and other factors. By correlating the information obtained from this test with metallurgical, chemical, physical and other data, the best avenues of approach to a more effective alloy design program may be delineated, and improved materials and techniques may result. Welding behavior may someday be theoretically predictable.

Acknowledgments

The author wishes to thank the following for permission to publish data on their respective alloys: the International Nickel Co., Allegheny Ludlum Steel Corp., Haynes Stellite Co., the Timken Roller Bearing Co., and General Electric Co.

References

1. Stout, R. D., and Doty, W. D'Orville, "Weldability of Steels," Welding Research Council (1953).

2. Weiss, S., formerly with the Thomson Laboratory, General Electric Co. now with Alco Products.

3. Nippes, E. F., Savage, W. F., Bastian, B. J., Mason, H. E., and Curran, R. M., "An Investigation of the Hot Ductility of High Temperature Alloys," THE WELDING JOURNAL, 34 (4), Research Suppl., 183-s to 196-s (1955).

RESEARCH NEWS

ASTM Publishes Additional X-Ray Diffraction Data

Section 6 of the X-Ray Diffraction Data Card File distributed by the American Society for Testing Materials has recently been completed and published. It is available in plain and keysort cards and covers approximately 600 new powder patterns and 600 revised and improved data patterns previously issued in Sections 1 to 5, inclusive.

The Diffraction Data File is sponsored by the American Crystallographic Association, the American Society for Testing Materials, the British Institute of Physics, and the National Association of Corrosion Engineers.

The file is widely used by research laboratories, geological and research departments of universities, governmental and industrial laboratories in the U. S., Mexico, Canada, Great Britain, France, Italy, Germany, Norway, Sweden, Belgium, Netherlands, Switzerland, Israel, Indonesia, South America, Africa, Australia and Japan.

A revised Cumulative, Alphabetical and Grouped Numerical Index of X-Ray Diffraction Data (STP 48E) including the new Section 6 has also been published.

Section 6 of the X-Ray Diffraction Card File on plain cards (3 x 5 in.) is priced at $135 for the first deck and $50 per deck for additional decks. Section 6 on keysort cards (4 x 6 in.) is priced at $185 for the first deck and $70 per deck for additional decks. A copy of the index book is furnished without charge with each order. The index may also be purchased separately for $10 per copy. Orders or inquiries for additional information should be addressed to the American Society for Testing Materials, X-Ray Dept., 1916 Race St., Philadelphia 3, Pa.

Researches Into Welding of Aluminum

The plan of work to be undertaken by the ADA Welding Research Team at the University of Birmingham, England, under the sponsorship of the Aluminium Development Association, 33, Grosvenor St., London, W.1, was outlined in their Research Report No. 1, and a summary of the work to date was published in their Research Report No. 6 issued at the end of 1949. Over the whole period, from 1944–1950, individual investigations have been reported to learned societies and on occasion in articles in the technical press. The present publication, Research Report No. 27, "Researches Into the Welding of Aluminum and Its Alloys," constitutes a summary of the entire investigation gathered together in a form in which it was thought to be most convenient for other workers in the field, and for the many for whom the results will have practical application.

The Welding Research Team was

(*Continued on page 194-s*)

FRACTURE BEHAVIOR IN THE NOTCH SLOW-BEND TEST

A study of the effect of weld metal, heat-affected zone, and unaffected base plate in the initiation and propagation of the crack leading to brittle failure

BY W. J. MURPHY AND R. D. STOUT

Introduction

The longitudinal-bead-weld notch-bend test has been extensively used to evaluate the notch toughness of welded steels. Of the several designs for specimens of this type, the design proposed by Kinzel and associates[1-3] has become widely accepted. The details of the test specimen as used in the present investigation are shown in Fig. 1.

The purpose of the present investigation in the broad sense was to study the Kinzel type test in order to determine factors which govern brittle behavior in welded steel. In particular, the problem resolved itself into a study of the effect of weld metal, heat-affected zone, and unaffected base plate in the initiation and propagation of the crack leading to brittle failure in the Kinzel test. Questions to be answered included: (1) In what areas do cracks initially form? (2) When and where do such cracks become critical? (3) What are the properties of the various regions in the welded zone and what is the effect of these properties on crack initiation and propagation? (4) How are the preceding factors related to the shape and position of the transition curve? The authors feel that, while the present investigation does not answer all of these questions, it has led to the development of a technique by which such answers can be obtained after more extensive work.

Previous work concerning fracture initiation and propagation leading to brittle failure in the notch slow-bend test is meager. Stout and McGeady[4,5] have demonstrated that initial cracking appears in either prime or welded plate at relatively small angles of bend. When welded with E6010 electrodes in steels containing about 0.18% C and no alloys the first crack was found to appear in the weld metal. In steels of higher alloy or carbon content (0.25% C) the initial crack was found to form in the heated zone of the base plate. Voldrich and co-workers[6] showed that in Kinzel-type specimens of two steels (0.18 and 0.24% C) welded with E6010 electrodes, fractures initiated and propagated first in weld metal. They concluded that the behavior of the welded specimens was controlled primarily by cracking of the weld metal.

Nippes and Savage[7] have investigated the properties of synthetically produced weld heat-affected-zone structures using Charpy V-notch impact specimens. The steel used was a 0.16% Grade A-201 steel and the structures investigated corresponded to those produced in $^1/_2$-in. plate welded with a heat input of 70,000 Jpi. Their results showed that in this steel the structures produced by heating below the lower critical temperature developed the poorest notch toughness. Unfortunately no attempt was made to relate these properties to the behavior of welded specimens.

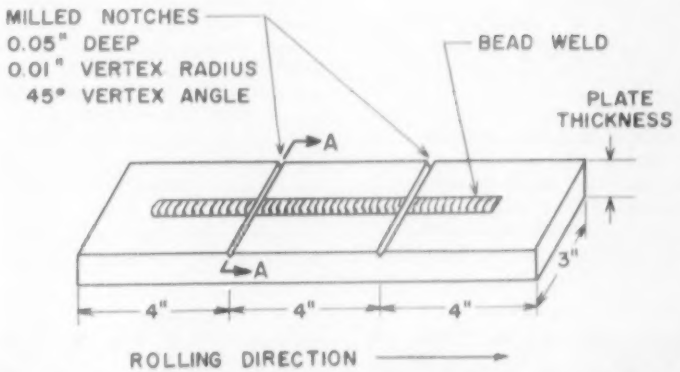

Fig. 1 Details of Kinzel-type longitudinal-bead-weld notch-bend specimen

Granjon and Videau[8] have observed interesting fracture patterns on the fractured surfaces of Kinzel specimens. In certain temperature ranges these specimens showed almost 100% crystalline appearance except for a thin, fibrous semicircle surrounding the heat-affected zone but well below it.

Experimental Procedure

Materials

Steels chosen for this investigation were ordered to ASTM Specifications. Analyses and tensile properties are given in Table 1. Photomicrographs of these steels in the as-received condition are presented in Fig. 2. Test specimens were removed from the as-received plates in a predetermined random pattern.

Electrodes $^5/_{16}$ in. in diam were ordered to AWS specifications. Electrodes used were E6010, E7015, and E9010.

Specimen Preparation and Testing

Kinzel specimens were cut from the as-received plate according to the specifications shown in Fig. 1. The surface

W. J. Murphy and R. D. Stout are associated with Lehigh University, Department of Metallurgical Engineering, Bethlehem, Pa.

To be presented at 1956 AWS National Spring Meeting in Buffalo, N. Y., May 7-11, 1956.

Table 1—Chemical Composition and Properties of Steels

Steel	Thickness, in.	C	Mn	P	S	Si	Mo	Ni	Cr	Yield point, psi	Tensile strength, psi	Elongation, % (2 in.)	Reduction in area, %
A-302	1	0.18	1.12	0.035	0.033	0.23	0.45	0.06	0.03	66,400	91,200	24.6	58.3
A-302	1/2	0.18	1.12	0.035	0.034	0.20	0.41	0.06	0.03	67,300	93,800	25.0	59.2
A-7	1	0.32	0.74	0.013	0.039	0.08	0.02	0.04	0.03	45,500	69,200	26.3	48.3
A-201	1	0.11	0.51	0.020	0.024	0.20	0.01	0.01	0.01	36,600	59,400	45.2	60.9

to be welded was ground to remove all scale. Welding of the single longitudinal bead on plate was accomplished using 180 amp and 28 arc volts for E6010 and E9010 electrodes and 210 amp and 22 arc volts for E7015 electrodes. Except for one series the arc travel was held constant at 6 ipm. If postheating was to be done, this followed welding immediately and was accomplished by holding specimens for 1 hr at 1150° F. All specimens were held 7 days after welding before testing.

Specimens for standard V-notch Charpy impact tests were taken from the plate with the longitudinal axis of the specimen parallel to the rolling direction. The notches in these specimens were located perpendicular to the plate surface. Specimens to be heat treated were machined approximately 0.035 in. oversize in order to allow for oxidation or decarburization of the surface during heating. After heat treatment these specimens were ground to standard dimensions and then notched.

Production of synthetic weld zone microstructures in Charpy specimens was accomplished by heating specimens to carefully chosen temperatures and then cooling in a medium selected to produce a cooling rate approximating that developed in the heat-affected zone of the Kinzel specimens when welded. Heat-treatment temperatures were chosen for each steel after careful metallographic and visual analysis of fracture patterns of Kinzel test specimens. Heating of specimens to 1700° F and below was accomplished in molten lead baths. Total heating time in lead was 2 min. Above 1700° F a high-temperature glo-bar furnace with a gas-air protective atmosphere was employed for heating. Total heating time here was 3 min.

All specimens were still mineral oil quenched after heating. As will be shown later, microstructures produced by cooling in this way were similar to those developed in the heat-affected zones of Kinzel specimens of the various steels. Since the welding heat input was essentially constant for all Kinzel specimens only one cooling rate was needed.

Testing of Kinzel specimens was conducted with a head travel speed of 2 ipm. V-notch Charpy specimens were tested through the transition range in order to obtain the 10 ft-lb transition temperature.

Illustration of Fracture Patterns

Careful examination of the fracture surfaces of all Kinzel specimens was performed after testing. Since these fracture surfaces revealed interesting patterns of fibrous and crystalline appearance which were indicative of specimen behavior during testing, it was decided to record each fracture pattern. Figure 3 is a photograph of a typical Kinzel specimen fracture surface. Areas of fibrous and crystalline fracture are clearly visible in this photograph. Unfortunately it was difficult to show clearly by photographs many of the fracture patterns and for this reason it was decided to use drawings to illustrate fracture appearance.

Figure 4 is a drawing illustrating the fracture pattern of Fig. 3. The root of the notch is represented by the top horizontal line while the fusion line of the weld metal is shown by the semicircular dashed line. Areas of fibrous fracture (ductile behavior) are indicated by cross-hatching, while areas of

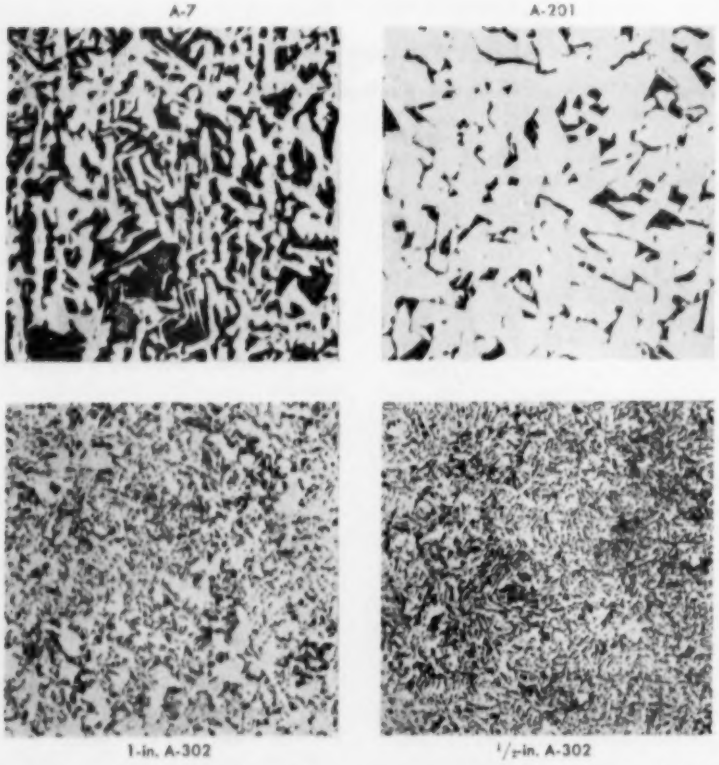

Fig. 2 Photomicrographs of steels in as-received condition; picral etch; X 100

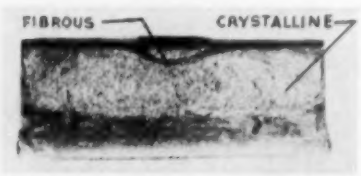

Fig. 3 Photograph of typical Kinzel specimen fracture surface

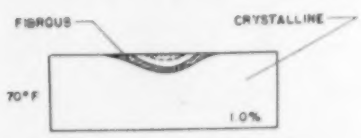

Fig. 4 Drawing illustrating fracture pattern of Fig. 3

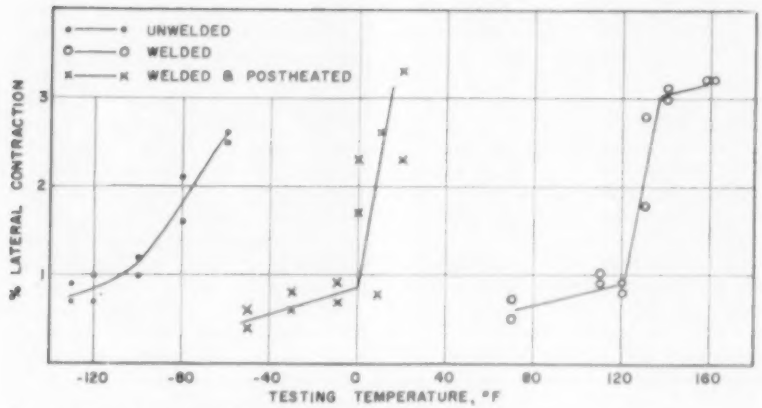

Fig. 5 Kinzel test transition curves for 1-in. A-302 steel

crystalline fracture (brittle behavior) are open. The percentage lateral contraction for each specimen is indicated in the corner. Testing temperature is noted at the side. It will be noticed that the fibrous area in the lower quarter of Fig. 3 has been omitted in Fig. 4. This is done for two reasons. First, the specimens are considered to have failed when the load drops to one-half the maximum load. Failure in the lower quarter of the specimen is therefore usually obtained when separating the two halves of the specimen after the actual testing has been completed. Second, the mode of failure in this region will not affect the percentage lateral contraction, and is sometimes a result of compressive strain during loading.

Results and Discussion—A-302 Steel

1-In. A-302 Steel

The transition curves for the 1-in. thick A-302 steel as-received, as-welded, and as-welded and postheated are presented in Fig. 5. Specimens were welded with E9010 electrodes at 70° F. The 1% lateral contraction transition temperatures taken from these curves are: as-received, −110° F; welded, +120° F; welded and postheated, −10° F. As can be seen, welding severely impaired the notch toughness of the steel, effecting a rise in transition temperature of 250° F. Postheating greatly improved the notch toughness of the welded specimens but the notch toughness is still considerably below that of the unwelded specimens.

Figures 6, 7 and 8 illustrate the variation in fracture pattern through the transition range for the three conditions. The fracture behavior of the unwelded series in Fig. 6 is straightforward. As the temperature rises, a thin shear lip develops over the width of the specimen at the root of the notch. This shear lip increases in depth with increasing temperature. Increasing values of lateral contraction are therefore associated with increasing amounts of shear at the notch root.

The fracture behavior of the welded series as shown in Fig. 7 is relatively complex. With increasing temperature this behavior can be described as follows:

+70° F: The weld metal and a portion of the heat-affected zone have failed by shear. Brittle fracture was initiated somewhere within the heat-affected zone and the remainder of the specimen failed by cleavage.

+110° F: Weld metal and most of

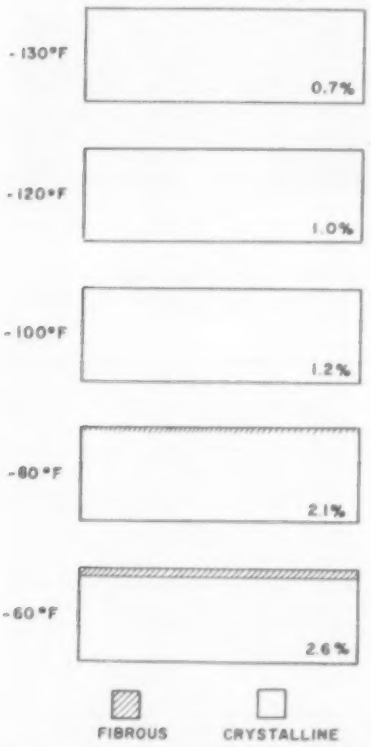

Fig. 6 Fracture behavior of Kinzel specimens of 1-in. A-302 steel, unwelded

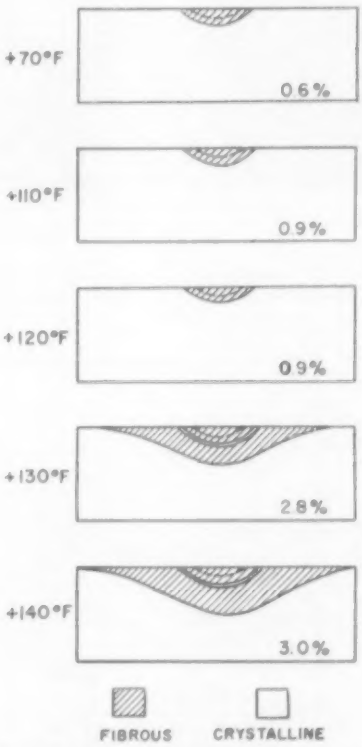

Fig. 7 Fracture behavior of Kinzel specimens of 1-in. A-302 steel, welded

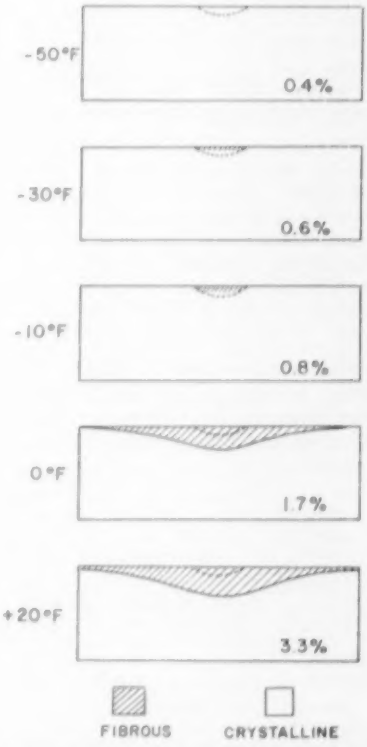

Fig. 8 Fracture behavior of Kinzel specimens of 1-in. A-302 steel, welded and postheated

heat-affected zone have failed by shear. Brittle fracture was initiated within the heat-affected zone.

+120° F: Same as 110° F. Lateral contraction below 1%.

+130° F: Weld metal and most of heat-affected zone have failed by shear. Brittle fracture initiated within the heat-affected zone. Propagation of cleavage crack, however, has been prevented by an apparently tougher microstructure which failed by shear until the crack had been sufficiently resharpened to cause remainder of specimen to fail in a brittle manner. A thin ring of crystalline fracture is visible in the heat-affected zone. A sharp rise in lateral contraction above 1% was observed.

+140° F: Same as 130° F, except for increased base-metal shear due to increased temperature.

The welded and postheated series shows in Fig. 8 the following behavior:

−50° F: Entire specimen failed by cleavage. Point of initiation of failure not possible to detect.

−30° F: Slight shear lip visible in weld metal. Initiation of brittle fracture apparently occurred in weld metal.

−10° F: Same as −30° F, except that the amount of weld metal shear has increased.

0° F: Lateral contraction rose considerably above 1% due to shear failure over width of specimen and considerably below fusion line. Weld metal is 100% shear.

+10 and 20° F: Same as 0° F with increasing extent of base-metal shear.

The behavior of the as-welded series can be summarized as follows: Below 1% lateral contraction the heat-affected zone failed in shear down to a specific point at which cleavage failure was initiated and propagated through the remainder of the specimen. Lateral contraction rose above 1% due to the fact that the initial cleavage crack was stopped and failure by shear once more began. Three areas of the heat-affected zone thus appear to influence the behavior of the specimen: (1) the coarse-grained region which failed in shear, (2) the area which initiated and propagated cleavage failure, and (3) the area which at sufficiently high temperatures stopped propagation of this cleavage crack.

In order to determine microstructurally the location of these areas in the heat-affected zone, the fracture surface of a specimen corresponding to the one tested at +130° F (Fig. 7) was nickel plated and then sectioned at the centerline of the weld. The resulting surface perpendicular to the fracture surface was then polished and etched to allow microexamination of the fracture surface profile. Areas of the heat-affected zone which had failed by shear were characterized by an irregular profile while areas which had failed by cleavage were characterized by sharp well-defined facets. Examination of this specimen revealed that the heat-affected zone could be divided into three distinct areas:

1. The region heated above the upper transformation temperature which was essentially martensitic and which failed by shear.

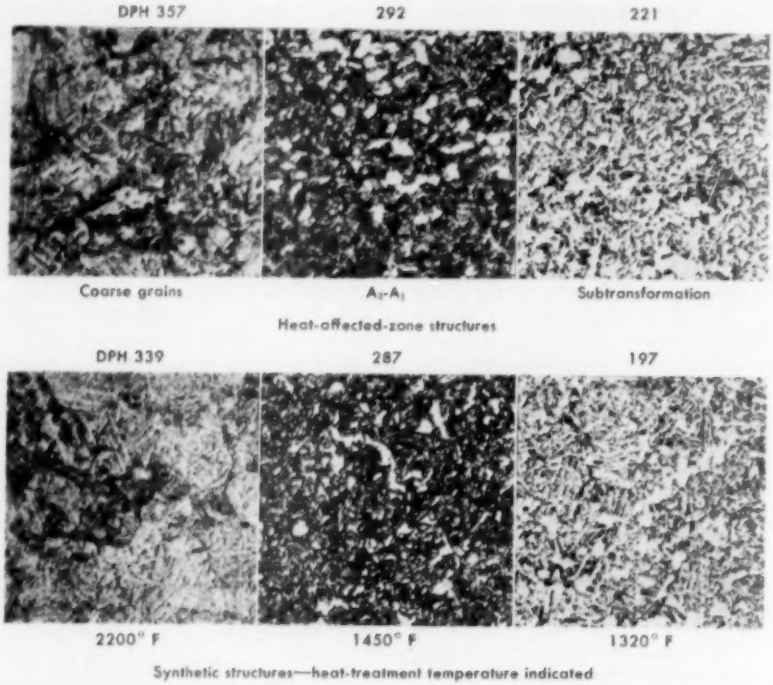

Fig. 9 Comparison of synthetic structures with actual structures from the heat-affected zone of A-302 steel; picral etch; × 100. (10-kg diamond pyramid hardness also shown)

Table 2—Charpy 10 ft-lb Transition Temperatures for Synthetic Heat-Affected Zone Structures of A-302 Steel

Heat treatment	*Microstructure*	*Transition temperature, ° F*
As-received	Ferrite and pearlite	+ 10
1320° F	Ferrite and pearlite	− 10
1450° F	Martensite and ferrite	+130
2200° F	Martensite	− 45
1450° F, postheated	Tempered martensite and ferrite	−120
2200° F, postheated	Tempered martensite	−200

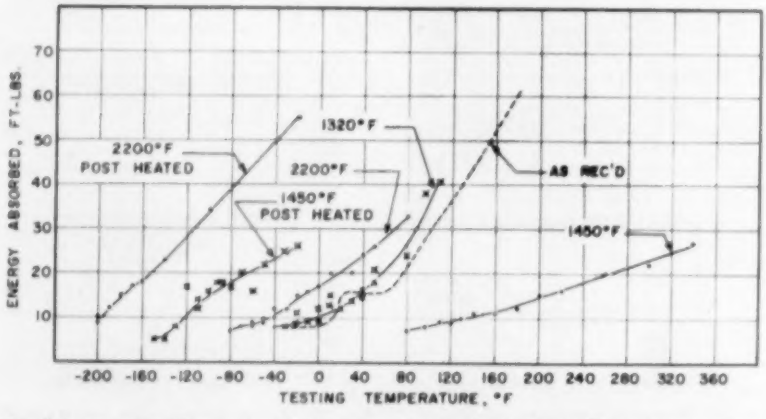

Fig. 10 V-notch Charpy transition curves for synthetic heat-affected zone structures of A-302 steel

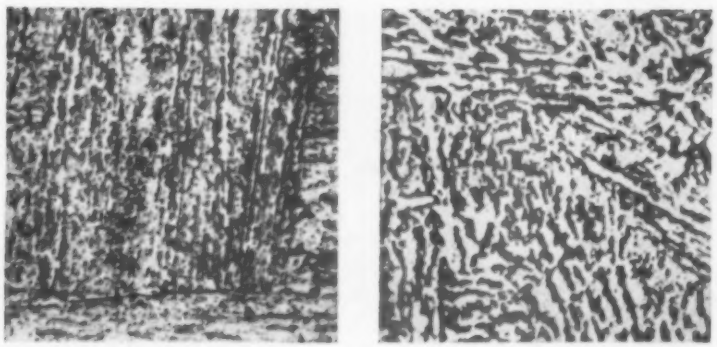

1-in. A-302 $\quad$ $^1/_2$-in. A-302

Fig. 11 Microstructures of coarse grains of heat-affected zone of 1-and $^1/_2$-in. thick A-302 Kinzel specimens welded at 6 ipm; picral etch; X 1000

2. The region heated between the lower and upper transformation temperatures which was mixed martensite and ferrite, and which failed by cleavage.

3. The region heated to temperatures below transformation which was pearlite plus ferrite and which failed by shear.

Initiation of cleavage failure occurred in the region heated just below the upper transformation temperature where a mixture of martensite and ferrite was present. The cleavage crack propagated through this region but was stopped by the apparently tougher region heated below the lower transformation temperature.

V-notch Charpy specimens with microstructures simulating those of the above defined heat-affected zone regions were prepared by heating to 2200, 1450 and 1320° F. These microstructures and their hardnesses are compared in Fig. 9. V-notch Charpy transition curves for these microstructures and as received material are presented in Fig. 10. Curves for specimens heat treated at 1450 and 2200° F and then postheated at 1150° F are also presented. These results are summarized in Table 2, using the 10 ft-lb level as the transition temperature.

It is evident from these data that the martensite and ferrite structure which was most susceptible to cleavage failure in the Kinzel test exhibited the poorest notch toughness in the Charpy V-notch impact test. Furthermore, the martensite structure had notch toughness superior to both the unheated base plate and the material heated to just below the lower transformation temperature. These results are clearly in agreement with observations of the as-welded Kinzel specimen fracture patterns in Fig. 7.

Postheating at 1150° F substantially improved the notch toughness of specimens heat treated at 1450 and 2200° F. This improvement in notch toughness is reflected by an improvement in the Kinzel test transition temperature from +120° F, as-welded, to −10° F welded and postheated. Referring to the fracture behavior of this series in Fig. 8 it is seen that the lateral contraction rose above 1% at 0° F when the heat-affected zone was able to shear instead of cleave as a result of the improvement in notch toughness due to postheating. The drop in lateral contraction below 1% at −10° F was apparently due to the ability of the weld metal to initiate cleavage failure. Once initiated, the cleavage crack was able to propagate through the relatively tough heat-affected zone. These results indicate that although postheating produced structures in the critical areas of the heat-affected zone which have notch toughness superior to that of the base metal a similar improvement in the notch toughness of the weld metal may not result. The properties of the weld metal may, therefore, limit the improvement in Kinzel test transition temperature due to postheating.

$^1/_2$-in. A-302 Steel

An interesting supplement to the fracture study of the 1-in. thick A-302 steel was provided through examination of the fracture behavior of welded Kinzel specimens of $^1/_2$-in. thick A-302 steel. Both the $^1/_2$-in. and 1-in. A-302 plates were rolled from the same heat of steel and as Table 1 indicates their analyses are almost identical. Despite this similarity in analysis, comparison of the fracture behavior of the $^1/_2$-in. and 1-in. specimens when welded with E9010 electrodes showed a surprising difference. As has been shown, initiation of cleavage failure in 1-inch thick specimens occurred most easily in the A_2-A_1 region of the heat-affected zone while the coarse grains of the heat-affected zone failed by shear. In the $^1/_2$-in. thick specimens, however, initiation of cleavage failure occurred most easily in the coarse grains of the heat-affected zone. Metallographic examination of the heat-affected zone of the welded $^1/_2$-in. specimens revealed that the coarse-grained region consisted of pearlite and ferrite. This is in contrast to the martensitic structure of the coarse-grained region in the 1-in. thick specimens. These microstructures are compared in Fig. 11.

The difference in heat-affected zone microstructures is explained if it is realized that the weld zone cooling rates were much faster in the 1-in. thick specimens than in the $^1/_2$-in. thick specimens due to the fact that the heat input per unit volume of metal in the $^1/_2$-in. specimens was twice that in the 1-in. specimens. In order to study further the effect of heat input in fracture behavior, a series of $^1/_2$-in. thick specimens were welded with E9010 electrodes at a travel speed of 12 ipm instead of the standard speed of 6 ipm. This reduced the heat input by one-half, thus

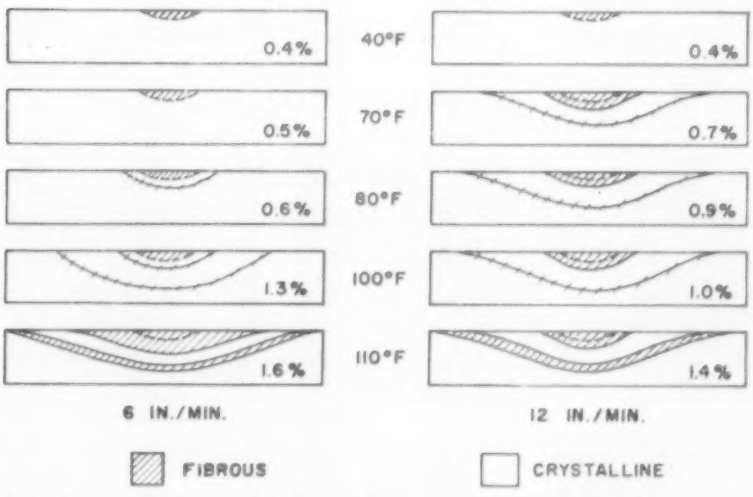

Fig. 12 Fracture behavior of $^1/_2$-in. A-302 steel welded at 6 and 12 ipm

making it comparable to that produced in 1-in. thick specimens welded at 6 ipm. The fracture behavior of the $^1/_2$-in. A-302 steel welded at both 6 and 12 ipm is shown in Fig. 12. Comparison of these two series reveals the following:

1. In the specimens welded at 6 ipm the coarse grains of the heat-affected zone were responsible for initiation of cleavage failure.
2. The specimens welded at 12 ipm behaved like those of the 1-in. plate in Fig. 7 in that at sufficiently high temperatures the coarse grains failed by shear and cleavage was initiated within the A_3-A_1 region of the heat-affected zone.
3. Despite the difference in fracture behavior, the transition temperatures of the two series were approximately the same; +90° F at 6 ipm and +100° F at 12 ipm. The fact that there was little difference in transition temperature was apparently due to the controlling influence of the base material. For both series of specimens the rise in lateral contraction above 1% was due to the ability of the base material to prevent easy propagation of a cleavage crack.

Conclusions—A-302 Steel

1. Welding decreased the notch toughness of Kinzel specimens of A-302 steel by providing a structure within the heat-affected zone which could initiate cleavage failure more readily than can the base material itself. In the 1-in. A-302 steel welded at 6-ipm and the $^1/_2$-in. A-302 steel welded at 12 ipm, this structure consisted of mixed martensite and ferrite, which formed when the base metal was heated within the transformation range. In the $^1/_2$-in. A-302 welded at 6 ipm this structure was ferrite and pearlite in the coarse grained region of the heat-affected zone.
2. The amount of decrease in notch toughness due to welding was limited by the ability of the base material or a subcritically heated portion of the heat-affected zone to resist propagation of a cleavage crack when sufficiently high testing temperatures were reached.
3. Postheating improved the notch toughness of welded specimens by increasing the notch toughness of the structure in the A_3-A_1 region, thus eliminating it as a site for cleavage crack initiation.
4. The extent of improvement in notch toughness due to post-heating was apparently limited by the notch toughness of the weld metal, since in postheated specimens cleavage seemed to initiate within the weld metal.

Results and Discussion, A-7 Steel

The Kinzel test transition curves for the A-7 steel unwelded and in three welded conditions are shown in Fig. 13. It is to be noted that two of these curves exhibit a pronounced plateau over a range of temperatures near the 1% level, making it difficult to choose the transition temperature with any accuracy. If, for these curves, the mid-temperature of the plateau is chosen as the transition temperature, comparative transition temperatures are those listed in Table 3. It is evident that welding severely impaired the notch toughness of the A-7 steel. There was little difference in notch toughness between

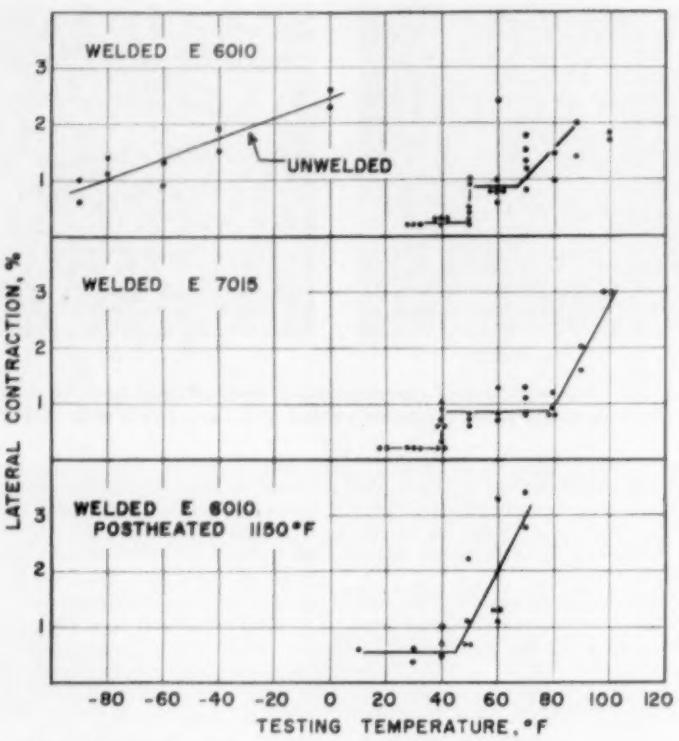

Fig. 13 Kinzel test transition curves for A-7 steel

Table 3—Kinzel Test Transition Temperatures for A-7 Steel

Condition	*Transition temperature, ° F.*
Unwelded	−85
Welded E6010	+60
Welded E7015	+60
Welded E6010 and postheated	+45

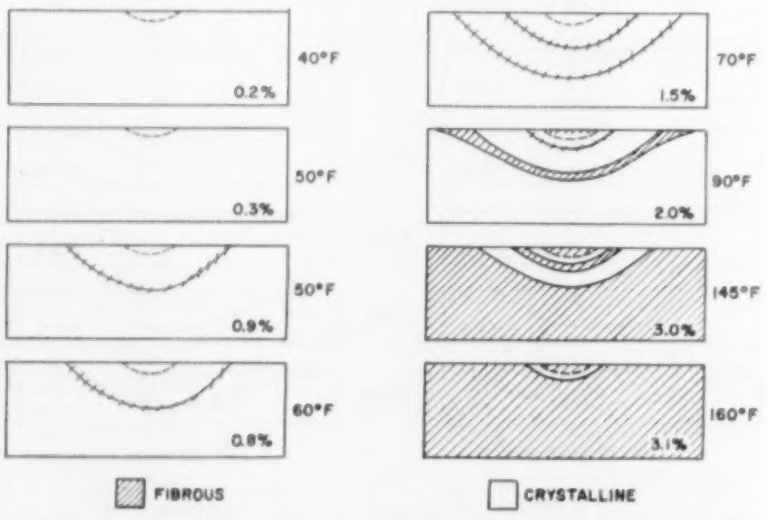

Fig. 14 Fracture behavior of Kinzel specimens of A-7 steel welded with E6010 electrodes

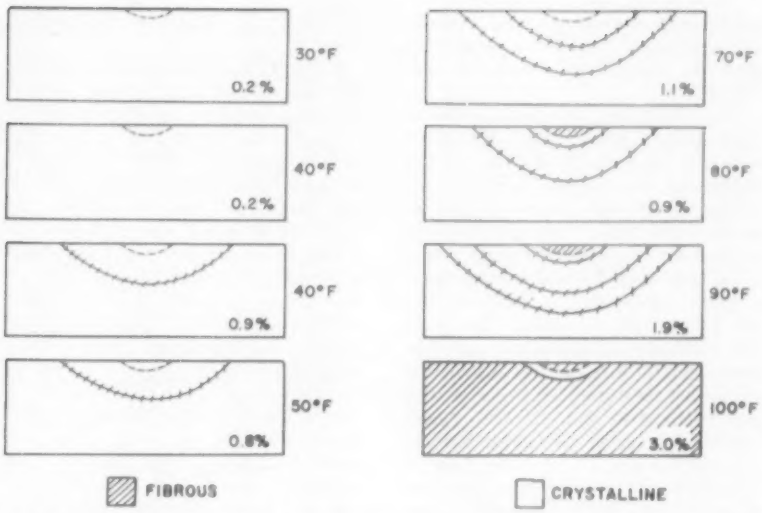

Fig. 15 Fracture behavior of Kinzel specimens of A-7 steel welded with E7015 electrodes

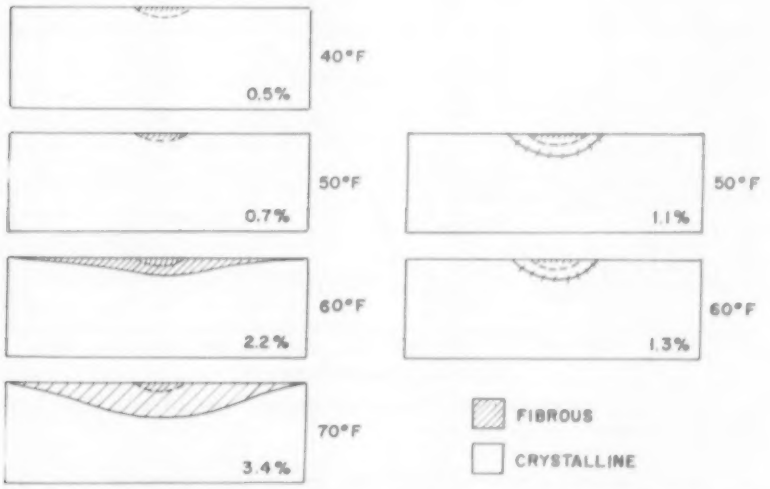

Fig. 16 Fracture behavior of Kinzel specimens of A-7 steel welded with E6010 electrodes and postheated

specimens welded with E6010 and low-hydrogen E7015 electrodes and post-heating the E6010 series effected only a slight improvement in notch toughness.

Fracture behavior of Kinzel specimens, through the transition region, for the three welded series is illustrated in Figs. 14 through 16. The fracture pattern of the unwelded series is similar to that of the A-302 steel shown in Fig. 6. The fracture behavior of the welded E6010 series as shown in Fig. 14 can be described as follows:

40 and 50° F: Entire specimen including weld metal failed by cleavage. Lateral contraction very low. The site of brittle fracture initiation not possible to detect.

50 and 60° F: Weld metal and heat-affected zone failed by cleavage. Initial cleavage crack changed to shear in base material producing a ring of fibrous appearance. Remainder of specimen failed by cleavage when shear crack was resharpened as the load on specimen built up again. Lateral contraction rose sharply to 0.9%.

70° F: Two fibrous rings resulted when base plate increased its resistance to cleavage crack propagation. Lateral contraction rose to 1.5% due to second fibrous ring.

90° F: Weld metal shows slight shear lip. Cleavage initiated either in weld metal or coarse-grained region of heat-affected zone. Fibrous rings have grown in breadth causing rise in lateral contraction to 2.0%.

145° F: Weld metal failed entirely by shear. Brittle fracture initiated in coarse grains of heat-affected zone. Propagation of cleavage crack limited.

160° F: Cleavage initiated in coarse grains of heat-affected zone and propagated through heat-affected zone only. Remainder of specimen fibrous.

The fracture behavior of the E7015 series as shown in Fig. 15 was similar to that of the E6010 series and will not be described in detail. It is to be

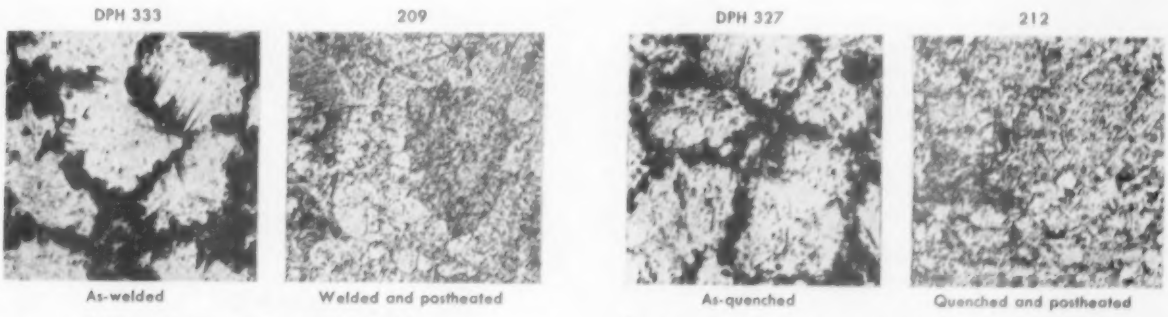

Fig. 17 Comparison of synthetic structures with actual structures from the heat-affected zone of A-7 steel; picral etch; X 100 (10 Kg diamond pyramid hardness also shown)

noted, however, that the E7015 weld metal was somewhat tougher than the E6010, since it was completely fibrous at 80° F, while the E6010 weld metal did not fail completely by shear until temperatures above 90° F were reached.

The fracture behavior of the series welded with E6010 electrodes and then postheated is illustrated in Fig. 16 and can be described as follows:

40° F: Weld metal has slight shear lip. Cleavage failure apparently initiated in weld metal and remainder of specimen failed by cleavage.

50° F: Quantity of weld metal shear increased somewhat but cleavage failure still initiated by weld metal.

50° F: Cleavage failure initiated by weld metal. Thin fibrous ring within or just below heat-affected zone formed when propagation of cleavage crack was interrupted. Shear failure in this region caused a rise in lateral contraction to 1.1%.

60° F: Same as above.

60° F: Weld metal is 100% fibrous. Shear failure includes heat-affected zone. Lateral contraction increased to well above 1%.

70° F: Same as 60° F.

The behavior of the two as-welded series may be summarized as follows: Cleavage failure was initiated by either weld metal or the coarse-grained region of the heat-affected zone. At relatively low temperatures initiation probably occurred in the weld metal, while at higher temperatures the coarse-grained region was responsible. It appears, therefore, that the coarse-grained structure of the heat-affected zone was critical to the behavior of the specimen since it can initiate cleavage failure when the weld metal is unable to do so. Thus even if a tougher weld metal were introduced it is doubtful that much improvement in the Kinzel test transition temperature would be effected. The rise in lateral contraction to 1% was a result of the ability of the base metal to prevent the propagation of a cleavage crack when sufficiently high temperatures were reached and the lateral contraction rose above 1% with increasing amounts of base metal shear. Thus in these series the transition temperature was controlled by the properties of the base material.

As revealed in Fig. 16 postheating improved the toughness of the coarse grains of the heat-affected zone markedly. The fact that only a slight improvement in transition temperature resulted was apparently due to the ability of the weld metal to initiate cleavage failure at sufficiently low temperatures. The rise in lateral contraction to and above 1% occurred either when a structure within the heat-affected zone could prevent propagation of a weld metal initiated cleavage crack or when the weld metal failed completely by shear and thus did not initiate cleavage failure.

Since within the heat-affected zone the coarse-grained structure, i.e., the structure just below the fusion line of the weld metal, was responsible for the initiation of cleavage failure in the as-welded specimens, Charpy V-notch specimens with a microstructure simulating that observed in this region were prepared by heating to 2200° F and still mineral oil quenching. An additional series was postheated after the above treatment to produce a structure simulating that observed in the welded and postheated series. These microstructures together with hardnesses are compared in Fig. 17. V-notch Charpy transition curves for the synthetic structures and for the as-received material are presented in Fig. 18. The 10 ft-lb transition temperatures from these curves are: as-received, +55° F; 2200° F, +180° F; 2200° F, postheated, −50° F.

In Fig. 17 the coarse-grained region of the heat-affected zone of the welded specimens consists of large grains of martensite surrounded by a very fine pearlite associated with the prior austenite grain boundaries. Some ferrite is also visible at these boundaries. As might be expected this structure exhibited extremely poor notch toughness as revealed by synthetic V-notch Charpy specimens. The 10 ft-lb transition temperature is +180° F and examination of the transition curve reveals it to be extremely flat with an energy absorption of less than 15 ft-lb at 360° F despite the fact that at this temperature failure is 100% by shear. The poor notch toughness of this structure is in agreement with the previously discussed fracture behavior of as-welded specimens, since it was shown that the coarse-grained region was responsible for the initiation of cleavage failure even at relatively high temperatures.

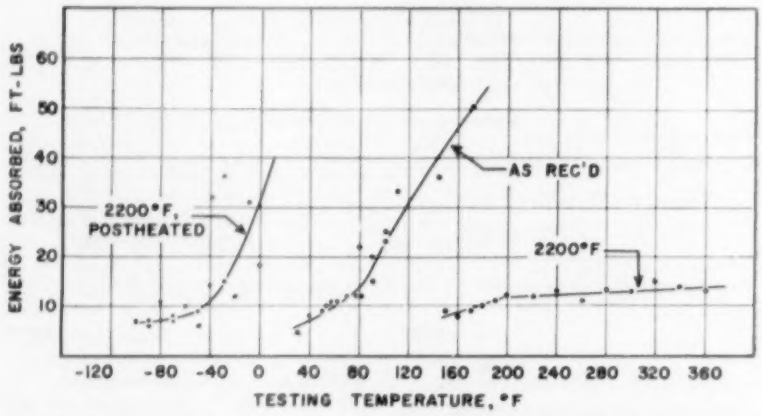

Fig. 18 V-notch Charpy transition curves for synthetic heat-affected zone structures of A-7 steel

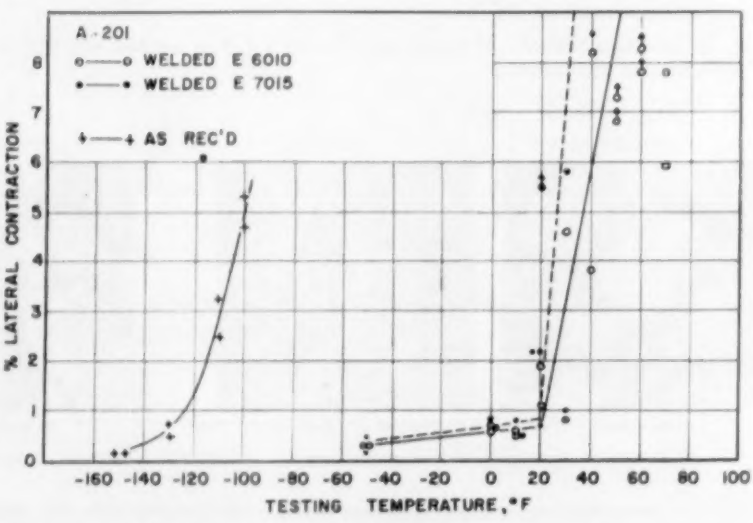

Fig. 19 Kinzel test transition curves for A-201 steel

Postheating of the martensite-pearlite coarse-grained structure produced a marked change in microstructure as revealed in Fig. 17. The martensite is tempered, of course, and now consists of carbide in a ferrite matrix. However, the surprising change is the complete spheroidization of the pearlite. As might be expected this structure had a relatively good transition temperature of −50° F as compared to +180° F for the unpostheated specimens. This improvement in notch toughness supports the observed fracture behavior of welded and postheated Kinzel specimens in Fig. 16 where it was seen that at the test temperatures employed this structure could not initiate cleavage failure. Apparently, however, this structure was capable of propagating a cleavage crack initiated by the weld metal.

Conclusions—A-7 Steel

1. Welding decreased the notch toughness of Kinzel specimens of the A-7 steel by providing a structure within the heat-affected zone which could initiate cleavage more readily than the base material itself. In this steel this structure consisted of mixed martensite and pearlite with some ferrite. This was in the coarse-grained region of the heat-affected zone.

2. The amount of decrease in notch toughness due to welding was limited by the ability of the base material to prevent cleavage crack propagation above a temperature of 60° *F*. Thus the welded transition temperature was controlled by the base material.

3. Welding with E6010 and E7015 low-hydrogen electrodes produced no difference in transition temperature and essentially no difference in fracture behavior. Fracture behavior did, however, reveal that the E7015 weld metal was somewhat tougher than the E6010 weld metal.

4. Postheating produced a slight improvement in notch toughness. The improvement was due to an increase in notch toughness of the coarse grains of the heat-affected zone, i.e., the structure responsible for initiation of cleavage in unpostheated specimens.

5. The fact that the improvement due to postheating was only slight was apparently a result of the ability of the weld metal to initiate cleavage in these specimens. In other words, postheating did not improve the properties of the weld metal as much as those of the heat-affected zone and therefore the weld metal limited the effectiveness of postheating.

Results and Discussion—A-201 Steel

Kinzel test transition curves for the A-201 steel unwelded and in two welded conditions are presented in Fig. 19. The 1% lateral contraction transition temperatures taken from those curves are tabulated in Table 4.

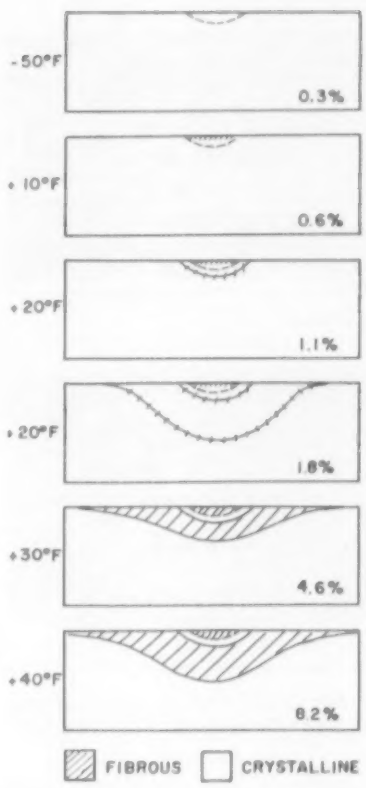

Fig. 20 Fracture behavior of Kinzel specimens of A-201 steel welded with E6010 electrodes

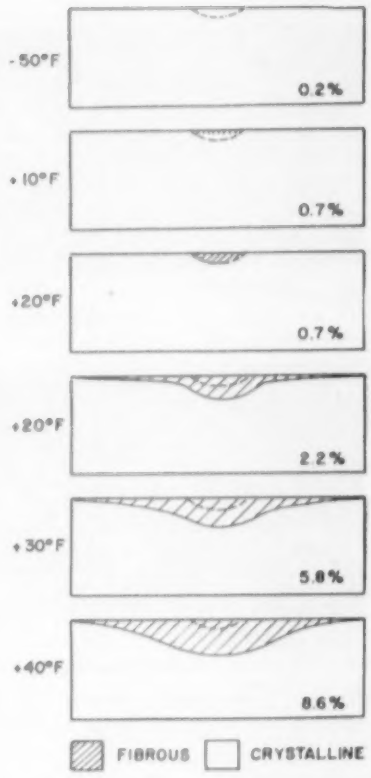

Fig. 21 Fracture behavior of Kinzel specimens of A-201 steel welded with E7015 electrodes

As can be seen, welding severely impaired the notch toughness of the A-201 steel with a rise of the transition temperature from −120° F unwelded to +20° F as-welded. The transition curves for specimens welded with E6010 and E7015 electrodes are almost identical at +20° F.

Fracture behavior of Kinzel test specimens through the transition range for the two welded series is illustrated in Figs. 20 through 22. Fracture behavior of the unwelded specimens is similar to that previously described for the A-302 steel.

The fracture behavior of the E6010 as-welded series as illustrated in Fig. 20 can be described as follows:

−50° F: Entire specimen, including weld metal, failed by cleavage.

+10° F: Slight shear lip visible in weld metal. Remainder of specimen failed by cleavage. Lateral contraction rose from 0.3% at −50 to 0.6% apparently due to partial shear failure of weld metal.

+20° F: Slight shear lip in weld metal. Cleavage crack which was initiated by either the weld metal or coarse grains of the heat-affected zone was changed to shear by a structure within the heat-affected zone. Upon continued loading cleavage was once again initiated. As a result a thin fibrous ring is visible within the heat-affected zone. The shear occurring in this region raised the lateral contraction to 1.1%.

+20° F: Behavior was similar to that described just above except that an additional fibrous ring well down in base metal is now visible. Base metal began to resist propagation of cleavage cracks at this temperature.

+30° F: Although the drawing indicates that the weld metal of this specimen had failed entirely by shear, it is possible that a small portion close to the fusion line failed by cleavage. It is difficult to say, therefore, whether the weld metal or the coarse grains of the

Table 4—Kinzel Test Transition Temperatures for A-201 Steel

Condition	*Transition temperature, ° F*
As-received	−120
Welded E6010	+ 20
Welded E7015	+ 20

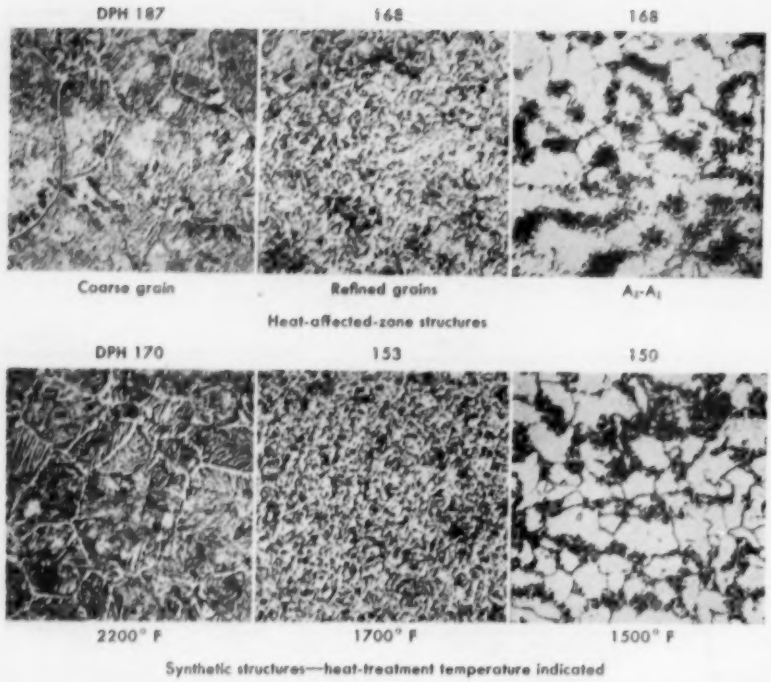

Fig. 22 Comparison of synthetic structures with actual structures from the heat-affected zone of A-201 steel; picral etch; X 100 (10-kg diamond pyramid hardness also shown)

heat-affected zone had initiated cleavage failure. Once initiated, however, the cleavage crack propagated to a structure within the heat-affected zone where it was changed to shear. Extensive shearing then occurred in the base metal of the specimen. This caused a marked rise in lateral contraction.

+40° F: Same as +30° F, except for increased base metal shear.

+50° F: (Not shown) Entire specimen, including heat-affected zone failed by shear.

The fracture behavior of specimens welded with E7015 electrodes is shown in Fig. 21 and can be described as follows:

−50° F: Same as E6010 specimen.

+10° F: Same as E6010 specimen.

+20° F: Weld metal appeared to be 100% shear. However, as was observed previously it was difficult to determine whether or not cleavage did occur in the weld metal near the fusion line. The site of initiation of the cleavage failure was therefore in doubt and could possibly have been in the weld metal, or in the coarse grains of the heat-affected zone. Cleavage, once initiated, propagated through entire specimen.

+30° F: In this specimen the weld metal failed completely by shear. The shear crack grew through the heat-affected zone and over the width of the specimen until well within the base plate where cleavage failure began. The lateral contraction rose from 0.7% in the previous specimen to 2.2% in this specimen.

+30° F: Same as +20 with increasing base metal shear.

+40° F: Same as +30° F.

Although the transition temperatures of the A-201 steel welded with E6010 and E7015 electrodes were identical at +20° F, a comparison of Figs. 20 and 21 reveals a difference in their fracture behaviors. In Fig. 20 it is seen that the E6010 weld zone can initiate a cleavage crack up to +40° F but that at temperatures of +20° F or above both the base material and an area within the heat-affected zone can prevent easy propagation of this crack. In Fig. 21, the E7015 weld zone can initiate cleavage only up to +20° F which is coincidently the temperature at which the base material will not propagate a cleavage crack readily. Thus the transition temperature of both series was controlled by the ability of the base plate or fine-grained heated zone to interrupt cleavage cracks initiated in the weld zone.

It could not be established from the examination of fracture surfaces whether the weld metal or coarse grains of the heat-affected zone were responsible for the initiation of cleavage failure in either series of welded specimens.

The fibrous ring caused by shearing within the heat-affected zone for the E6010 specimens is shown clearly in the +20° F specimens in Fig. 20. The position of this ring was determined by nickel plating the fracture surface of a specimen containing this ring, sectioning it at the weld centerline, and examining the fracture profile metallographically. This examination revealed that the initial cleavage crack was stopped by the region heated only slightly above the upper transformation temperature during welding and which, therefore, possessed a refined microstructure. Cleavage was once again initiated when the shear crack, after propagating through this refined structure entered the structure formed due to heating just below the upper transformation temperature. V-notch Charpy specimens with structures simulating those of three zones, the coarse grained region, the refined structure and the A_3-A_1 structure, were prepared by heating to 2200, 1700 and 1500° F, respectively, and then still mineral oil quenching. In Fig. 22 the synthetically produced structures are compared with the appropriate weld heat-affected zone structures. V-notch Charpy impact curves for these structures are presented in Fig. 23. The 10 ft-lb transition temperatures from these curves are presented in Table 5.

These data confirm the above observations concerning the origin of the fibrous ring in the heat-affected zone of

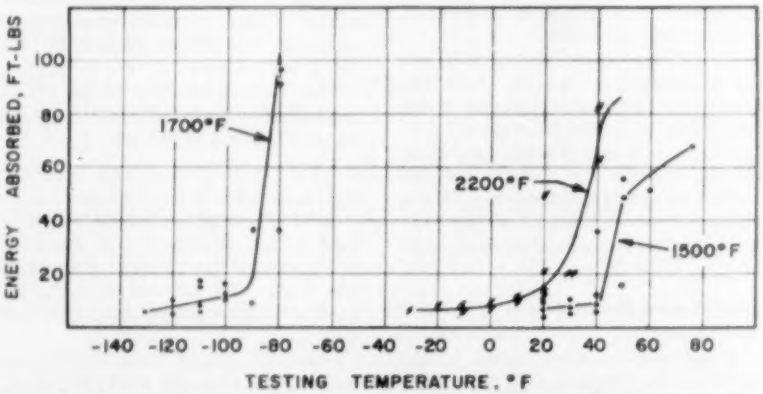

Fig. 23 V-notch Charpy transition curves for synthetic heat-affected zone structures of A-201 steel

specimens welded with E6010 electrode and tested at +20° F. The refined structure in which shearing occurred was definitely tougher than the structures on either side of it which at +20° F failed by cleavage. In addition Table 5 shows that the coarse ground region of the heat-affected zone has notch toughness equal to that of the base plate. This should be true at least for the E7015 series in which the effect of hydrogen is minimized. Thus it appears reasonable to assign to the weld metal tentative responsibility for initiating cleavage failure.

Conclusions—A-201 Steel

1. Welding decreased the notch toughness of Kinzel's specimens of the A-201 steel by producing a structure in the weld zone which could initiate cleavage more readily than the base material itself. It has been tentatively established that the weld metal was responsible for the initiation of cleavage failure in these specimens.

2. The amount of decrease in notch toughness due to welding was limited by the ability of the base material to interrupt a cleavage crack initiated in the weld zone. Thus the transition temperature was controlled by the base material.

3. A tough structure within the heat-affected zone also contributed to the effect noted in (2) above. Thus the refined region of the heat-affected zone was able, at sufficiently high testing temperatures, to stop a cleavage crack initiated above it.

General Discussion

Although only three steels have been included in this investigation, it is believed that the general conclusions concerning fracture behavior are applicable to other steels and that a technique has been developed which can be used to explain the effect of welding on Kinzel specimen behavior. This technique is based on two of the basic concepts of brittle fracture: (1) initiation of cleavage failure, and (2) propagation of cleavage failure.

The ductility transition temperature of a steel as determined by unwelded Kinzel specimens is associated primarily with the ease or difficulty with which a cleavage crack can be initiated in that steel and not with the cleavage crack propagating properties of the steel. That this is true is apparent when two experimental observations are considered. First, in unwelded specimens when a cleavage crack is initiated at relatively low values of deflection, it always propagates throughout essentially the entire specimen; i.e., propagation of the crack is not prevented by the base material. As a matter of fact this is true at even higher temperatures when the cleavage crack is initiated by structures other than that base material, e.g., the heat-affected zone due to welding. Second, in specimens which are tested at the ductility transition temperature (about 1% lateral contraction) there is almost a complete absence of a shear lip at the sides indicating that propagation is easy even where the complexity of the stress system is reduced. It is convenient to call the transition temperature at 1% lateral contraction for unwelded specimens T_i, i.e., the temperature at which initiation of cleavage occurs relatively easily in the base material.

Table 5—Charpy 10 Ft-Lb. Transition Temperatures for Synthetic Heat-Affected Zone Structures of A-201 Steel

Structure	*Heat treatment temperature, ° F*	*Transition temperature, ° F*
Coarse grains	2200	+ 5
Refined grains	1700	−105
A_R-A_1 region	1500	+ 40
As-received	...	+ 5

The welding of a Kinzel specimen often introduces into that specimen a material or structure which can initiate cleavage failure more readily than the base material itself. If a cleavage crack is initiated by the weld zone, as the temperature of testing is raised a temperature can be reached such that this crack will no longer propagate easily through the base material. At this temperature, as has been observed, thin rings of fibrous appearance will be developed in the base material and the measured lateral contraction will rise abruptly. As testing temperature is raised further, the cleavage crack will encounter increasing resistance to propagation, the amount of base metal shear will increase, and the lateral contraction will rise further, usually well above 1%. It is convenient to define as the T_p temperature above which a cleavage crack cannot propagate easily but is interrupted in the base material, thus resulting in a rise of lateral contraction to 1%. Both T_i and T_p are properties of the base material as determined by the Kinzel test under standard testing conditions. Changing any of the test conditions such as rate of loading, notch geometry, etc., may change the position of T_i or T_p on the temperature scale.

In the Kinzel test T_p becomes the highest possible temperature to which the 1% lateral contraction transition temperature can rise as a result of welding. Even though welding produces a structure which can initiate cleavage failure above T_p, the lateral contraction will rise to 1% at T_p. For any one steel, therefore, the welded transition temperature must be between T_i and T_p, both temperatures being properties of the base material itself. When the welded transition temperature falls between T_i and T_p, its location depends primarily upon the notch toughness of the heat-affected zone and weld metal. It will be the highest temperature at which either of them can initiate cleavage failure in the Kinzel test. This characteristic temperature of the weld zone will be designated T_{wz}. The notch toughness of the weld metal and the various heat-affected zone regions depends ultimately, of course, upon the welding conditions, the electrode type and composition, and the composition and response to welding of the base material. Thus the weld zone controls the transition temperature of welded Kinzel specimens by determining the temperature T_{wz} between T_i and T_p at which brittle failure can be initiated. If T_{wz} is greater than T_p, then T_p will be the transition temperature of the test.

In a few cases, the influence of the weld zone on the transition temperature has been found to be altered by an additional factor. If, by the heat of welding, a structure is produced in the heat affected zone which can prevent propagation of a cleavage crack initiated in a structure above it, then shearing within this region may raise the lateral contraction above 1%. This mechanism is not common, but can occur when a brittle coarse-grained region is enveloped by a tougher fine-grained region.

The foregoing discussion may be summarized and perhaps clarified with the aid of the schematic diagrams in Fig. 24, which show the effect of a variety of welding conditions on the transition temperature of any one steel. In these diagrams the symbols are defined as follows:

T_i = temperature at which cleavage is *initiated* easily in unwelded specimens. Defined here at 1% lateral contraction

T_p = lowest temperature at which the *base* material can prevent easy *propagation* of a cleavage crack and thus raise the lateral contraction to 1%

T_{wz} = highest temperature at which any area in the *weld zone* can *initiate* cleavage failure

In Fig. 24 the horizontal axis represents the temperature scale. The heavy arrow indicates where the 1% lateral contraction transition temperature is located. Figure 24*A* represents the situation for unwelded Kinzel specimens of any one steel. Here the transition temperature is determined by T_i. Since T_i and T_p are properties of the base material, their position on the temperature scale will remain constant for welded specimens. Figure 24*B* represents the situation when the above steel is welded under a particular set of welding conditions. The transition temperature here is determined by T_{wz}.

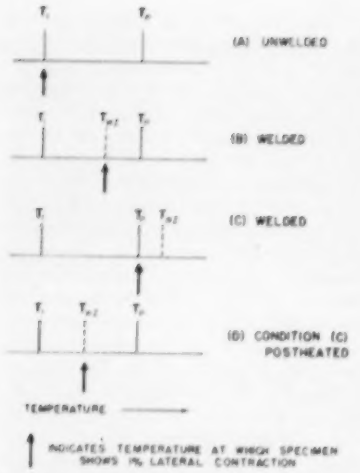

Fig. 24 Schematic diagram showing the factors which control the Kinzel test transition temperature

If the welding conditions are made more severe so that T_{ws} rises above T_p, then, as Fig. 24*C* shows, the transition temperature is determined by T_p. An additional increase in T_{ws} due to still more severe welding conditions will not affect the transition temperature. Figure 24*D* shows how postheating reduces T_{ws}, thus lowering the transition temperature. Here the assumption is made that postheating does not change T_t or T_p appreciably. This is, of course, not true for all steels, since postheating has been found to improve the toughness of some steels and to embrittle others.

Additional variations of the diagrams in Fig. 24 are possible. The important thing, however, is the fact that two factors must be considered in attempting to understand how welding influences the Kinzel test transition temperature. These two factors are:

1. The tendency of the weld zone to initiate cleavage failure.
2. The ability of the base material to prevent propagation of cleavage failure.

It should be noted that under some conditions the properties of the base material itself may be all important in determining the welded transition temperature. This fact is important since it may explain, among other things, the beneficial effect of prenormalizing on welded transition temperature. Perhaps prenormalizing is beneficial mainly because it imparts increased notch toughness to the base-plate material. The influence of the base material may also have to be considered when attempting to study the effect of other variables on weldability. For example, the beneficial effects of preheating may not be evident if the welded transition temperature is being controlled by the base material instead of the weld zone.

It has been stated that the temperature T_p is that temperature at which the base material can interrupt a running cleavage crack originating in the weld zone. The drop-weight test used at the Naval Research Laboratory employs a brittle weld deposit to induce a cleavage crack at the inception of plastic deformation of the testpiece. Since the transition temperature of the drop-weight test is taken as that minimum temperature at which the plate can resist cleavage failure from the crack of the weld, it appears that the T_p defined here for the Kinzel test should be a measure of the same characteristics of the plate as the nil-ductility transition temperature of the drop weight test. The differences that may exist between these transition temperatures as a result of unlike testing conditions between the two test methods will be determined quantitatively by work now under way.

General Conclusions

1. The examination and analysis of fracture patterns on Kinzel test specimens is a valuable method of determining the influence of weld metal, heat-affected zone and base material on the welded transition temperature.

2. Welding decreased the notch toughness of Kinzel specimens by providing a structure either in the weld metal or in the heat-affected zone which was able to initiate cleavage failure more readily than the base material itself.

3. The loss in toughness due to welding can be limited by the properties of the base material itself. Thus the base material can control the welded transition temperatures by interrupting the propagation of a cleavage crack initiated by the weld zone.

4. When postheating improved the notch toughness of welded specimens, it did so by increasing the notch toughness of the structures responsible for cleavage crack initiation thus reducing the temperature at which they became effective. The improvement in notch toughness due to postheating may be limited by the degree of improvement that the weld metal undergoes when postheated.

5. The heat-affected zone may also influence the welded transition temperature if there is present in this zone a fine tough structure which is capable of interrupting a cleavage crack initiated above it before this crack can enter the base material.

Bibliography

1. Jackson, C. E., and Goodwin, W. J., "Effect of Variations in Welding Technique on the Transition Behavior of Welded Specimens," THE WELDING JOURNAL **27** (5), Research Suppl., 253-s to 266-s (1948).

2. Kinzel, A. B., "Ductility of Steels for Welded Structures," *Ibid.*, **27** (5), Research Suppl., 217-s to 234-s (1948).

3. Offenhauer, C. M., and Koopman, K. H., "Factors Affecting the Weldability of Carbon and Alloy Steels," *Ibid.*, **27** (4), Research Suppl., 234-s to 252-s (1948).

4. Stout, R. D., and McGeady, L. J., "Notch Sensitivity of Welded Steel Plate," *Ibid.*, **28** (1), Research Suppl., 1-s to 9-s (1949).

5. Stout, R. D., and McGeady, L. J., "Metallurgical Factors in the Embrittlement of Welded Plate," *Ibid.*, **26** (1), Research Suppl., 683-s to 692-s (1947).

6. Rieppel, P. J., and Voldrich, C. B., "Fracture Initiation and Propagation in Welded Ship Steels," *Ibid.*, **28** (4), Research Suppl., 188-s to 197-s (1952).

7. Nippes, E. F., and Savage, W. F., "Tests of Specimens Simulating Weld Heat-Affected Zones," *Ibid.*, **28** (12), Research Suppl., 599-s to 616-s (1949).

8. Granjon, H., and Videau, J. P., "Remarques sur la compaison et la signification des essais," *Soudure et Techniques Connexes*, **32** (3 and 4) pamphlet (1953).

Weldability of Steels

Copies of the monograph entitled "WELDABILITY OF STEELS" by Robert D. Stout and W. D'O. Doty, who were commissioned by the Weldability Committee of the WELDING RESEARCH COUNCIL to prepare this book, are still available for distribution. This monograph consists of 381 pages, handsomely bound and copiously illustrated. A limited edition of this book has been published. The list price is $6.50. Special arrangements with the American Welding Society are such that Members of the Council and the American Welding Society receive a 20% discount from the list price. The distribution of four or more copies will be handled by the WELDING RESEARCH COUNCIL. Less than four copies may be ordered from the American Welding Society, 33 West 39th Street, New York 18, N. Y.

THE ARC WELDING OF 2.25% CR–1.0% MO ALLOY STEEL PIPE

Investigation shows the extent to which thermal treatments are required in order to obtain satisfactory properties in welded pipe

BY JAY BLAND

ABSTRACT. The arc welding of 2.25% Cr – 1.0% Mo alloy steel pipe, using 2.25% Cr – 1.0% Mo and 1.25% Cr – 0.5% Mo low-hydrogen electrodes, has been investigated.

A significant correlation was found to exist between hardness and ductility and between hardness and tensile strength, for heat-treated 2.25% Cr – 1.0% Mo alloy steel pipe material and for 2.25% Cr – 1.0% Mo alloy weld deposits. On these bases the properties of the various zones in the welds have been more realistically evaluated. Longitudinal bend tests have provided confirming evidence for weld metal and heat-affected zone ductilities which are not apparent from results of the usual reduced section tensile tests of butt-welded specimens.

The results of this investigation indicate that a minimum postheat treatment of 1250° F for one hour is required in order to develop satisfactory ductility of the 2.25% Cr – 1.0% Mo alloy weld deposit. Satisfactory static and impact physical properties are obtained for unrestrained welds made in 2.25% Cr – 1.0 Mo alloy steel pipe using 1.25% Cr – 0.5% Mo low-hydrogen electrodes, welded without preheat or postheat treatment. The as-welded properties of the heat-affected zone in the 2.25% Cr – 1.0% Mo alloy pipe appeared to be satisfactory.

For welding under conditions of restraint and in the absence of data reflecting restrain vs. preheat, it is suggested that a nominal preheat of 300° F be used in order to minimize the possibility of cracking of root passes.

Jay Bland is Head, Metals Section, Engineering Research Department, Standard Oil Co. (Ind.), Whiting, Ind.

To be presented at AWS 1956 Spring Meeting in Buffalo, N. Y., May 7–11.

Introduction

The low chromium-molybdenum steels are becoming increasingly important in the steam power industry and in process equipment for the petroleum refining industry. Previous papers by the author,[1,2] have summarized the various considerations which have led to the use of these alloy steels. Particular reference was made to the resistance to graphitization and to high-temperature hydrogen embrittlement phenomena, exhibited by the low chromium-molybdenum steels.

There is relatively little information on the weldability characteristics of 2.25% Cr – 1.0% Mo alloy steel. Manufacturer's literature[3] recommends a welding procedure involving a preheat temperature of a minimum of 300° F for material under $^3/_4$ in. thickness; heavier sections or assemblies welded under restraint should be preheated up to 400° F or higher. This procedure also recommends a postheat treatment at 1350° F, noting that the material should be heated immediately after the weld has been made and before it has cooled below the minimum preheating temperature. The tentative rules for welding ferritic alloy steel piping in marine construction, issued by the AMERICAN WELDING SOCIETY,[4] recommend a minimum preheat for material under $^3/_4$ in. in thickness of 300° F, a preliminary postheat treatment at 1350° F and a stress-relief treatment at 1350° F.

The Pipe Fabrication Institute[5] recommends a 250° F minimum preheat temperature before tack welding, and a 400 to 700° F preheat and interpass temperature or a partial stress relief at 1200° F minimum for $^1/_2$ hr or more, if welding is interrupted. Postheat treatment of 1300 to 1400° F for 1 hr per in. of thickness, but not less than 1 hr, also is recommended by the Institute. The new AWS Standard for Interruption of Heat Treatment[6] states that the heating cycle may be safely interrupted for the 2.25% Cr – 1.0% Mo pipe in wall thicknesses 1 in. and below provided it is welded under controlled procedures using low-hydrogen electrodes. It is noted, in this connection, that the weld deposit prior to interruption should never be less than one-third the wall thickness or two layers, whichever is greater.

The investigation reported herein is part of a continuing program which is intended to evaluate the properties of weldments made using low-hydrogen alloy electrodes on low and intermediate chromium-molybdenum alloy steels. As indicated in the previous papers, one of the major aspects of this work is to determine the extent to which thermal treatments are required in order to obtain satisfactory properties of the weldments.

It was noted in a previous paper[2] that the usual studies of the weldability characteristics of low-alloy steels had

Table 1—Chemical Composition of Deposited Weld Metals and Alloy Pipe Material

Electrode designation	*AWS class*	*Covering type*	*Chemical composition, %*							*Nominal Cr – Mo*
			C	*Mn*	*P*	*S*	*Si*	*Cr*	*Mo*	
Code A	E9015-B3	Low-hydrogen sodium	0.07	0.74	0.014	0.028	0.24	2.57	1.40	$2^1/_4$ – 1
Code B	E9015-B3	Low-hydrogen sodium	0.08	0.48	0.020	0.015	0.15	2.32	1.07	$2^1/_4$ – 1
Code C	E9016-B3	Low-hydrogen potassium	0.10	0.52	0.026	0.017	0.47	2.43	1.06	$2^1/_4$ – 1
Code D	E9016-B3	Low-hydrogen potassium	0.10	0.53	0.017	0.039	0.44	2.17	1.02	$2^1/_4$ – 1
Code E	E8015-B2	Low-hydrogen sodium	0.08	0.67	0.018	0.022	0.36	1.14	0.70	$1^1/_4$ – $^1/_2$
Pipe material	A335-52T	Gr. P22	0.13	0.37	0.013	0.024	0.21	2.25	1.06	$2^1/_4$ – 1

indicated a lack of correlation between survey hardness measurements of the welds and heat-affected zones and the ductility exhibited by butt-weld tensile and bend-test specimens. This lack of correlation was emphasized in particular when electrodes depositing high-strength weld metals were used, since deformation in these specimens under load was forced to take place preferentially in the lower strength parent metal.

The previous investigation included the determination of the ductility-hardness relationships for a 1.25% Cr – 0.5% Mo steel, heat treated to hardness levels encompassing those found in the several unaffected and heat-affected zones of the material when welded under various preheat and postheat conditions, and also the ductility-hardness relationships for similar alloy weld metals deposited under similar conditions. The usefulness of the ductility-hardness relationships for the evaluation of the weldability characteristics of the 1.25% Cr – 0.5% Mo alloy steel demanded a similar approach in this study of the weldability of 2.25% Cr – 1.0% Mo alloy steel pipe.

In the test that follows, the designation "1¼ Cr Mo" will be used for the 1.25% Cr – 0.5% Mo alloy and "2¼ Cr Mo" will be used for the 2.25% Cr – 1.0% Mo alloy, as a matter of convenience. The abbreviation "HAZ" used in some of the tables and illustrations refers to the "heat-affected zones" in the base metal.

Experimental Procedure

Side-bend, notched-bend, hardness-metallographic and Charpy V-notch impact specimens were prepared from full thickness multipass butt welds made between 6-in. long sections of 2¼ CrMo alloy steel pipe. Longitudinal-bend specimens were prepared from full-thickness multipass longitudinal-butt welds made between 8-in. long quarter sections of the pipe. The weld joints were 60° included angle single vees, with a 1/32 to 1/16-in. root face and 3/32 to 1/8-in. root opening. No backing rings were employed in order to duplicate, as closely as possible, procedures typical of refinery piping fabrication. The various welding conditions used are described in several tables included hereafter with results. All welds were made in the flat position (pipe horizontal rolled) and welding currents in the range recommended by the manufacturer for the particular electrode brand were used.

The determination of the ductility-hardness relationships for the 2¼CrMo alloy steel pipe was made from oversized button-head 0.505-in. diam tensile specimens which were machined from 5.5-in. long sections of the pipe and given the thermal treatments indicated in Table 2. The heat treatments were designed to cover the range of hardness levels found in the heat-affected zones of weldments welded under various preheat and postheat conditions. After heat treatment the specimens were machined or ground to final dimensions and tested to failure in an hydraulic testing machine.

Test plates for all-weld-metal specimens were made in accordance with AWS specifications using the brands of low-hydrogen alloy electrodes given in Table 1. The various preheat and postheat conditions used are included in Table 3. Two button-head 0.505-in. diam specimens were machined from the weld metal of each test plate and tested to failure in the hydraulic testing machine.

After testing, the button-heads of all tensile specimens were cut off and used for hardness measurements and metallographic examinations.

Table 2—Physical Properties of Heat-Treated 2¼ CrMo Steel Pipe

Specimen No.	*Thermal treatment*	*Hardness, Bhn**	*Yield strength, psi†*	*Ultimate strength, psi*	*Elongation, % in 2 in.*	*Reduction of area, %*
1	As-received	132	33,500	67,000	38.5	72.0
2	300° F—1 hr	130	33,000	67,000	38.5	72.0
3	500° F—1 hr	130	32,000	65,500	39.0	72.0
4	1350° F—1 hr	132	44,500	68,000	38.0	71.0
5	300° F, 1350° F—1 hr	130	39,500	65,500	38.0	72.0
6	Normalized—1700° F	279	81,250	131,750	19.0	56.5
7	1700° F, H_2O	371	140,000	187,000	16.5	57.0
8	1700° F, H_2O, 1050° F—1/2 hr	348	149,000	167,000	18.5	63.5
9	1700° F, H_2O, 1050° F—1 hr	348	148,000	165,250	18.0	64.5
10	1700° F, H_2O, 1050° F—4 hr	340	143,000	155,000	16.0	66.5
11	1700° F, H_2O, 1200° F—1/2 hr	250	105,000	117,750	22.0	72.5
12	1700° F, H_2O, 1200° F—1 hr	250	104,750	117,250	23.0	74.0
13	1700° F, H_2O, 1200° F—4 hr	230	94,250	107,750	23.5	76.0
14	1700° F, H_2O, 1350° F—1/2 hr	220	76,750	91,000	22.5	79.0
15	1700° F, H_2O, 1350° F—1 hr	200	72,500	87,250	26.0	77.5
16	1700° F, H_2O, 1350° F—4 hr	178	65,000	81,500	29.5	77.5
17	Normalized—1900° F	286	96,500	142,750	19.5	58.5
18	1900° F, H_2O	371	136,500	184,500	15.5	56.5
19	1900° F, H_2O, 1050° F—1/2 hr	344	147,000	164,000	20.0	65.0
20	1900° F, H_2O, 1050° F—1 hr	344	147,500	164,000	18.5	66.0
21	1900° F, H_2O, 1050° F—4 hr	336	141,750	153,250	16.5	65.5
22	1900° F, H_2O, 1200° F—1/2 hr	264	108,750	122,500	21.0	72.5
23	1900° F, H_2O, 1200° F—1 hr	250	105,000	119,500	22.5	73.5
24	1900° F, H_2O, 1200° F—4 hr	234	93,250	107,570	23.0	78.5
25	1900° F, H_2O, 1350° F—1/2 hr	230	80,250	94,500	22.0	77.0
26	1900° F, H_2O, 1350° F—1 hr	213	75,500	89,750	24.0	77.5
27	1900° F, H_2O, 1350° F—4 hr	180	67,000	84,250	28.5	79.0

* Converted from Rockwell hardness measurements.
† 0.2% permanent set.

Table 3—Physical Properties of Deposited Weld Metal and Alloy Pipe Material

Weld metal	*Preheat, ° F*	*Postheat, ° F*	*Hardness, Bhn**	*Yield strength, psi†*	*Ultimate strength, psi*	*Elongation, % in 2 in.*	*Reduction of area, %*
Code A	None	None	275	107,750	131,000	13.0	31.5
	300	None	240	92,000	118,000	18.5	34.5
	500	None	255	83,250	119,750	15.5	25.0
	None	1350	205	79,000	93,750	22.0	59.0
	300	1350	200	74,700	91,850	22.5	53.5
Code B	None	None	271	110,500	123,000	13.0	26.0
	300	None	245	101,250	120,500	17.5	50.5
	500	None	237	92,250	116,250	17.0	52.0
	None	1350	188	73,000	86,000	24.0	66.0
	300	1350	195	74,000	87,000	23.0	66.0
Code C	None	None	258	107,750	127,725	9.5	14.5
	300	1350	202	76,500	91,250	25.0	63.5
Code D	None	None	286	121,250	133,750	6.0	13.0
	None	1350	222	87,500	98,750	20.0	55.0
	300	1350	210	80,500	94,000	23.5	56.5
Code E	None	None	210	82,500	95,000	23.5	62.0
	300	1300	178	64,750	80,500	26.5	68.0
Pipe	None	None	132	33,500	67,000	38.5	72.0
	300	1350	130	39,500	65,500	38.0	72.0

* Converted from Rockwell hardness measurements.
† 0.2% permanent set.

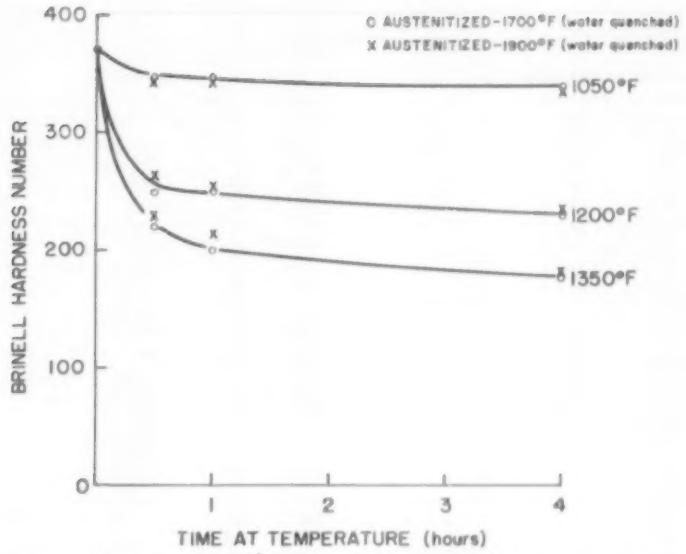

Fig. 1 Effect of temperature and time of tempering on hardness of $2^1/_4$ CrMo steel, water quenched from 1700° F and from 1900° F

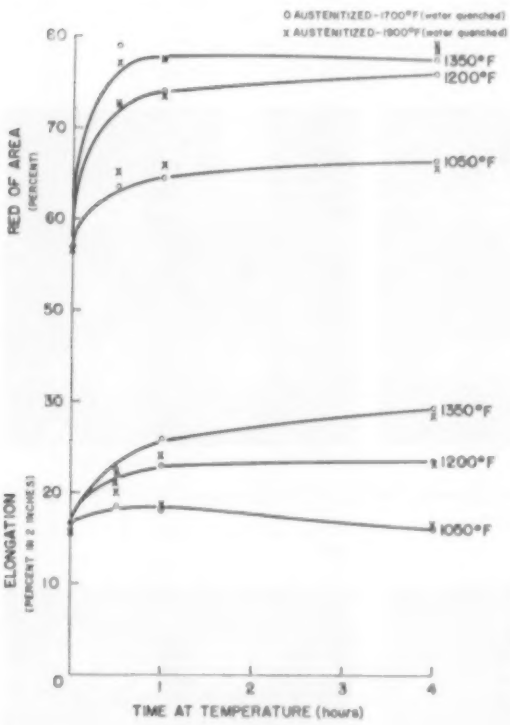

Fig. 2 Effect of temperature and time of tempering on ductility of $2^1/_4$ CrMo steel, water quenched from 1700° F and from 1900° F

An additional series of welds was made in the $2^1/_4$ CrMo pipe using $1^1/_4$ CrMo alloy electrodes; these are described in Part B.

All specimens were tested at room temperature, except where otherwise noted.

Materials

The material employed for this investigation was nominal $2^1/_4$ CrMo steel pipe, 5-in. nominal schedule 160, conforming to the requirements of ASTM Specifications A335-52T, Grade P22. The chemical composition of this alloy is included in Table 1.

The welding electrodes used were designed to deposit weld metals with nominal compositions of $1^1/_4$ CrMo and $2^1/_4$ CrMo. The chemical compositions of the weld metal deposits also are listed in Table 1. All of the electrodes employed were of the low-hydrogen type.

Part A—$2^1/_4$ CrMo Welds in $2^1/_4$ CrMo Pipe

Results

Heat-Treated $2^1/_4$ CrMo Steel Pipe. The results of hardness measurements and tensile tests of heat-treated $2^1/_4$ CrMo steel pipe material are presented in Table 2 and in Figs. 1 and 2. Plots of the data indicated that a definite correlation existed between hardness and ductility (elongation) as well as between hardness and tensile strength regardless of the type of metallurgical structure for $2^1/_4$ CrMo steel. Computation of the limits of precision of the regression for tensile strength, ultimate strength, elongation and reduction of area as functions of Brinell hardness, at 95% significance level, and within the range of 371 Bhn (water-quenched from 1700° F) to 178 Bhn (water-quenched from 1700° F and tempered 4 hr at 1350° F) gave the following equations:

$$\text{Yield strength, psi} = 449.90\ \text{Bhn} - 15{,}935\ (\pm 20{,}800\ \text{psi}) \quad (1)$$

$$\text{Ultimate strength, psi} = 530.33\ \text{Bhn} - 17{,}351\ (\pm 10{,}850\ \text{psi}) \quad (2)$$

$$\%\ \text{Elongation} = 36.55 - 0.0558\ \text{Bhn}\ (\pm 2.88\%) \quad (3)$$

$$\%\ \text{Reduction of area} = 98.92 - 0.1059\ \text{Bhn}\ (\pm 8.74\%) \quad (4)$$

The above equations cover the range of hardnesses found in the heat-affected zones of welds made with or without preheat or postheat.

Heat-Treated $2^1/_4$ CrMo Weld Metal. Results of hardness measurements and tensile tests of $2^1/_4$ CrMo weld metals made using various preheating and postheating conditions are presented in Table 3. As with the base metal, the data when plotted indicated that a definite correlation existed between hardness and ductility (elongation) as well as between hardness and tensile strength. Computation of the limits of precision of the regression for yield strength, ultimate strength, elongation and reduction of area as functions of Brinell hardness, at 95% significance level, and within the range of 286 Bhn (as-deposited) to 188 Bhn (1350° F postheat) gave the following equations:

$$\text{Yield strength, psi} = 454.2\ \text{Bhn} - 14{,}906\ (\pm 12{,}440\ \text{psi}) \quad (5)$$

$$\text{Ultimate strength, psi} = 530.1\ \text{Bhn} - 14{,}472\ (\pm 8{,}345\ \text{psi}) \quad (6)$$

$$\%\ \text{Elongation in 2 in.} = 57.0 - 0.168\ \text{Bhn}\ (\pm 4.35\%) \quad (7)$$

$$\%\ \text{Reduction of area} = 167.1 - 0.527\ \text{Bhn}\ (\pm 17.30\%) \quad (8)$$

The results of tensile tests of all-weld-metal specimens, Table 3, indicate that the physical properties of postheat-treated weld deposits made with the four brands of $2^1/_4$ CrMo electrodes essentially are comparable. A high-tem-

Table 4—Bend Tests of Welds in $2^1/_4$ CrMo Steel Pipe

Welding electrode	Specimen code	Thermal treatment—Preheat, °F	Thermal treatment—Postheat, °F†	Longitudinal bend*—Bend angle, deg	Longitudinal bend*—Elongation, %‡	Longitudinal bend*—Remarks	Side bend—Bend angle, deg	Side bend—Pass or fail§	Side bend—Remarks
Code A	A-0-0	None	None	180	20.6	.....	180	3P	Unfused root—1
	A-3-0	300	None	180	20.3	.....	180	3P	OK
	A-5-0	500	None	180	20.0	.....	180	3P	OK
	A-0-13	None	1300	180	20.0	.....	180	3P	Unfused root—1
	A-3-13	300	1300	180	19.7	.....	180	2P—1F	Root tear—1
Code B	B-0-0	None	None	180	20.6	.....	180	3P	Unfused root—1
	B-3-0	300	None	180	20.0	.....	180	3P	Unfused root—1
	B-5-0	500	None	180	...	One failed at 90°	180	3P	Tear at toe of weld—1
	B-0-13	None	1300	180	19.8	.....	180	3P	OK
	B-3-13	300	1300	180	20.2	.....	180	3P	OK
Code C	C-0-0	None	None	180	20.3	.....	180	3P	Unfused root—1
	C-3-13	300	1300	180	20.5	.....	180	3P	Unfused root—3
Code D	D-0-0	None	None	180	19.5	One failed at 65°	180	3P	OK
	D-3-13	300	1300	180	19.9	One failed at 95°	180	1P—2F	Root tear—1
									1 spec. 90° bend
Code E	E-0-0	None	None	180	...	OK	180	3P	1 unfused root
	E-3-0	300	None	180	...	OK	180	3P	2 unfused roots
	E-5-0	500	None	180	...	OK	180	3P	.....
	E-0-13	None	1300	180	...	OK	180	3P	.....
	E-3-13	300	1300	180	...	OK	180	3P	1 tear in toe of weld

* Averages of duplicate specimens.
† Postheat treatment for 1 hr at temperature.
‡ Elongation in outer fiber, % in 2 in.
§ Cracks or tears longer than $^1/_8$ in. constitute failure.

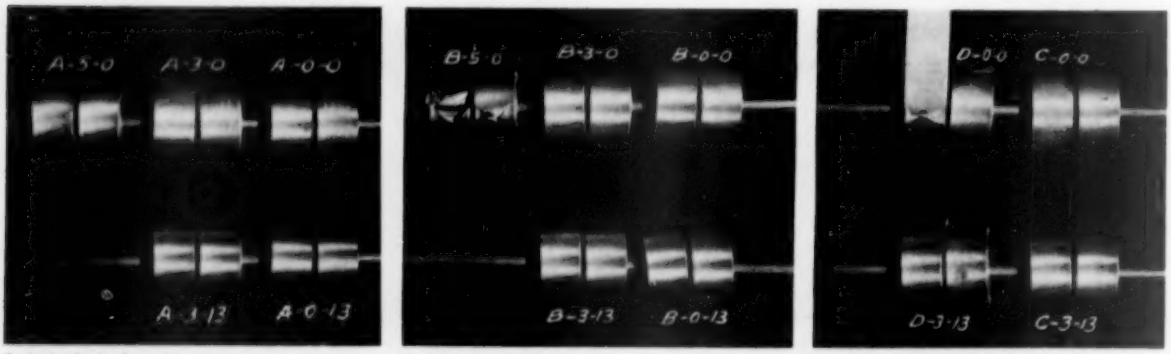

Code A electrode welds | Code B electrode welds | Code D and Code C electrode welds

Fig. 3 Longitudinal bend specimens after testing. See Table 4 for code identifications and corresponding thermal treatments

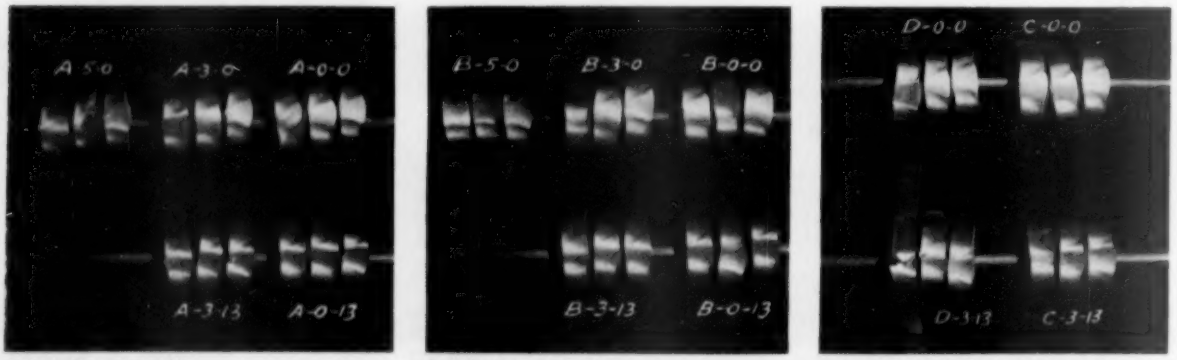

Code A electrode welds | Code B electrode welds | Code D and Code C electrode welds

Fig. 4 Side bend specimens after testing. See Table 4 for code identifications and corresponding thermal treatments. (Each group of three specimens obtained from a single pipe weld)

perature postheat treatment appears to be required in order to provide adequate tensile ductility of the weld metal.

No tensile tests of reduced-section butt-welded 2¼ CrMo pipe specimens were made, in view of the noted difference in tensile strength between the weld metals and the pipe base metal. Such specimens obviously would fail in the base metal even if abnormally large defects were present in the weld deposits.

Bend Tests of Flat Position Butt Welds

Longitudinal bend tests were made for each of the four brands of 2¼ CrMo electrodes with various conditions of preheat and postheat treatments. The results of the longitudinal bend tests, Table 4, and Fig. 3, indicate that the 2¼ CrMo weld metal, even in the as-welded condition, has remarkably good ductility. Except for one specimen (Code D electrode; D-0-0) all of the as-welded specimens bent 180° with about 20% elongation in the outer fibers. Specimens of Code B electrode welds made using 500° F preheat, with no postheat, failed to pass the longitudinal bend test. No attempt was made to determine the reason for this result; other specimens made using lower or no preheat and/or postheat treatments passed the longitudinal bend test without difficulty.

Side Bend Test Results

The results of side bend tests of specimens cut from butt welds in the 2¼ CrMo pipe also are listed in Table 4, and the appearance of the test specimens is shown in Fig. 4. In general, the various electrode welds exhibited satisfactory side bend test results in the as-welded condition as well as in the various preheat and/or postheat-treated conditions.

Most of the failures in the side bend tests, particularly for the Code D electrode weld, were due to tears which initiated at unfused roots. In only one instance (center specimen in B-5-0 group, Fig. 4) did a tear develop at the toe of the face of the weld.

It may be noted that, because of the higher hardness and strength of the weld metal, most of the elongation and bending in the side bend test takes place in the base metal. The specimens, Fig. 4, exhibit, at the sides of the weld deposit, severe necking-down which accompanies the localization of the deformation in the base metal. The effect of the high-temperature postheat treatment is to reduce the hardness and strength of the weld metal, whereby appreciable deformation of the weld then can take place. This deformation of the softer postheat-treated weld metal may account, in part for the greater frequency of root tears in the side bend test specimens in that condition compared with those not postheat treated.

Table 5—Effect of Preheat and Postheat on Hardness-Ductility of 2¼ CrMo Steel Pipe Welds

	—Thermal treatment—		—Brinell hardness*—			—Ductility†—	
	Preheat,	Postheat,	Weld	HAZ§	Pipe	Weld	HAZ§
Weld metal	° F	° F‡	Avg	Avg	Avg	Avg	Avg
Code A	None	None	235	245	144	14.2	22.9
	300	None	235	213	139	14.2	24.7
	500	None	231	210	135	15.8	24.8
	None	1300	190	210	135	25.8	24.8
	300	1300	200	213	135	23.4	24.7
Code B	None	None	265	228	147	7.3	23.8
	300	None	245	216	137	12.3	24.5
	500	None	240	222	135	13.5	24.2
	None	1300	185	200	135	27.1	25.4
	300	1300	190	208	135	25.9	24.9
Code C	None	None	250	245	147	11.1	22.9
	300	1300	210	200	130	20.9	25.4
Code D	None	None	270	250	144	6.1	22.6
	300	1300	210	188	125	20.9	26.1
Code E	None	None	222	230	141	21.6	23.8
	300	None	213	234	143	22.8	23.5
	500	None	220	250	143	21.9	22.7
	None	1300	172	180	137	28.0	26.5
	300	1300	178	175	137	27.2	26.8

* Converted from Rockwell hardness values.

† Elongation, % in 2 in. Data calculated from eqs 3 and 7. (±2.9% for base metal and ±4.4% for weld metal.) Data for 1¼ CrMo weld metal calculated from equations in ref. 2 (±2.0%).

‡ Postheat treatment for 1 hr at temperature.

§ HAZ = heat-affected zone.

Evaluation of Preheat and Postheat Treatments by Hardness Measurements

The effects of preheat and postheat treatments on the hardness and ductility of welds in 2¼% CrMo steel are shown in Table 5. Table 6 shows the effects of time and temperature of postheat treatments on the hardness and ductility of various specimens welded with and without preheat, for the Code A electrode, as typical of the four brands of 2¼ CrMo electrodes. In all of these tables the ductility values have been calculated from the equations of correlation previously determined for the 2¼ CrMo alloy pipe material and weld metals (eqs 3 and 7). The effect of temperature of postheat treatment is shown in Fig. 5.

The results indicate that postheat treatment of the 2¼ CrMo weld metals at 1050° F for times up to 16 hr, or at

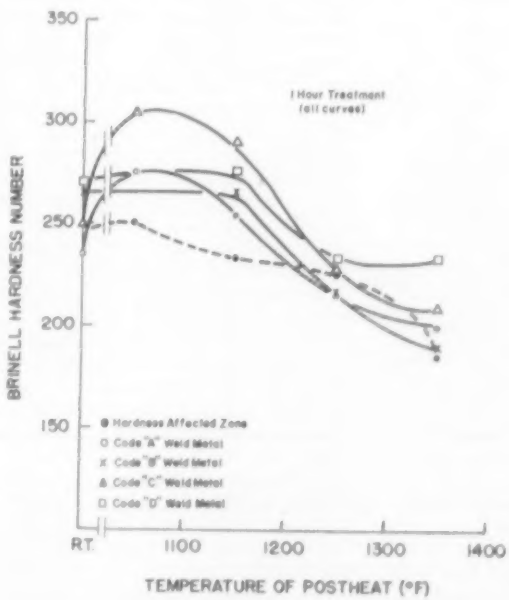

Fig. 5 Effect of postheat treatment on hardness of 2¼ CrMo weld deposits and base metal heat-affected zone

Table 6—Effect of Time and Temperature on Hardness-Ductility of Welds Made in 2¼ CrMo Steel Pipe Using Various Electrodes

Electrode brand	Thermal treatment: Preheat, °F	Postheat, °F	Postheat, Hours	Brinell hardness*: Weld avg	Brinell hardness*: HAZ‡ avg	Brinell hardness*: Pipe avg	Ductility†: Weld avg	Ductility†: HAZ‡ avg
Code A	None	As-welded	...	235	245	144	14.2	22.9
		1050	1	276	255	139	4.7	22.3
			4	276	255	139	4.7	22.3
			16	276	255	139	4.7	22.3
		1150	1	255	228	135	9.7	23.8
			2	265	216	135	7.3	24.5
			4	245	216	135	12.3	24.5
			8	216	210	135	19.4	24.8
		1250	1	216	200	135	19.4	25.4
			2	200	180	130	23.4	26.5
			4	200	176	135	23.4	26.7
		1350	½	200	190	135	23.4	25.9
			1	200	176	135	23.4	26.7
			2	190	180	135	25.9	26.5
	300	As-welded	...	235	213	139	14.2	24.7
		1050	1	265	235	139	7.3	23.4
			4	265	235	139	7.3	23.4
			16	255	245	135	9.7	22.9
		1150	1	255	235	135	9.7	23.4
			2	245	210	135	12.3	24.8
			4	235	210	130	14.2	24.8
			8	216	200	130	19.4	25.4
		1250	1	210	180	130	20.9	26.5
			2	200	180	130	23.4	26.5
			4	200	190	135	23.4	25.9
		1350	½	190	176	130	25.9	26.7
			1	190	180	135	25.9	26.5
			2	180	169	135	28.3	27.1
	500	As-welded	...	231	210	135	15.8	24.8
		1150	1	255	235	135	9.7	23.4
			2	245	235	135	12.3	23.4
			4	245	216	130	12.3	24.5
			8	228	200	135	16.5	25.4
		1250	1	210	210	135	20.9	24.8
			2	210	200	130	20.9	25.4
			4	190	169	130	25.9	27.1
		1350	1	190	180	135	25.9	26.5
			2	190	176	135	25.9	26.7
Code E	None	As-welded	...	222	230	141	21.6	23.8
		1150	½	216	238	136	22.4	23.3
			1	228	231	138	20.9	23.7
			2	207	220	138	23.5	24.3
			4	200	200	137	24.4	25.4
		1250	½	207	207	141	23.5	25.2
			1	198	198	141	24.6	25.1
			2	185	185	137	25.3	26.3
	300	As-welded	...	213	234	143	22.8	23.5
		1150	½	216	220	137	22.4	24.3
			1	224	243	137	21.3	23.0
			2	207	210	136	23.5	24.9
			4	207	204	136	23.5	25.2
		1250	½	204	207	141	23.9	25.1
			1	198	185	138	24.6	26.3
			2	198	188	136	25.9	26.1
	500	As-welded	...	220	250	143	21.9	22.6
		1150	½	221	234	138	21.9	23.5
			1	216	238	140	22.4	23.3
			2	210	192	136	23.1	25.9
			4	198	210	137	24.6	24.9
		1250	½	200	195	138	24.4	25.7
			1	192	195	141	25.4	25.7
			2	180	192	137	26.9	25.9

* Converted from Rockwell hardness values.

† Elongation, % in 2 in. Data calculated from eqs 3 and 7. (±2.9% for parent metal and ±4.4% for weld metal.) Data for 1¼ CrMo weld metal calculated from equations in ref. 2. (±2.0%.)

‡ HAZ = heat-affected zone.

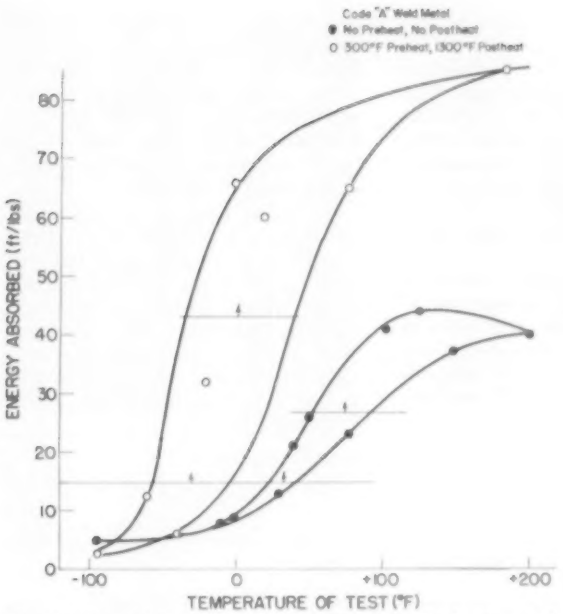

Fig. 6 Transition temperature curves for Code A weld metal deposited under various preheat and postheat conditions

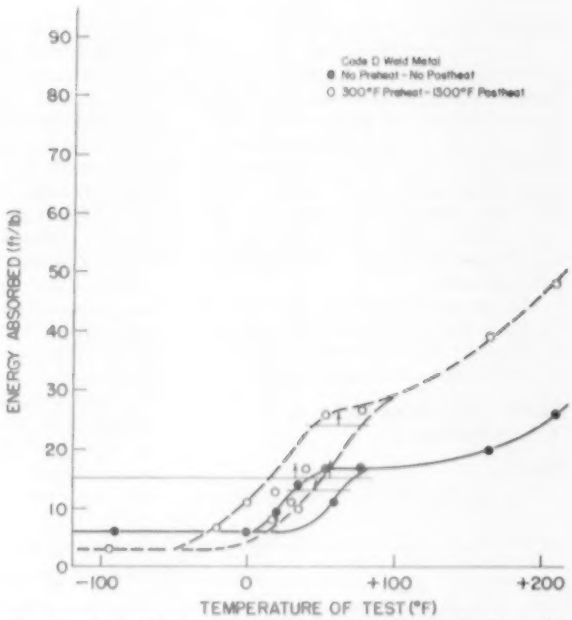

Fig. 7 Transition temperature curves for Code D weld metal in the no preheat, no postheat and 300° F preheat, 1300° F postheat conditions

1150° F for times up to 2 hr, produces an undesirable increase in hardness and corresponding decrease in ductility. The base metal heat-affected zone is affected adversely, though only slightly, by these treatments; the base metal actually is softened somewhat by these treatments.

Initial significant reductions in hardness from the as-welded condition require postheat treatments for a minimum of about 8 hr at 1150° F or about 1 hr at 1250° F. It would appear, therefore, that a minimum temperature of 1250° F should be specified for postheat treatments of 2¼ CrMo alloy weldments, based on the criterion of hardness reduction (and improved ductility).

It may be noted also that preheat treatments at temperatures up to 500° F produce, both in the weld metal and in the heat-affected zone, a lower hardness when postheated at 1050 and 1150° F. When postheat temperatures of 1250° F or over are used, the final hardnesses of all zones in the weld appear to be about the same regardless of any preheat treatment.

Based on the criterion of hardness and the requirement of a 1250° F minimum postheat treatment temperature, it would appear that preheat treatment is unnecessary for 2¼ CrMo alloy steel welds. However, it is recognized that preheat is of significant value where weldments are made under conditions of restraint. No data have been derived as yet relative to the amount of preheat required for specific restraints; in the absence of such information the use of a 300° F minimum temperature for preheat of these alloy welds appears to be reasonable.

Evaluation of Preheat and Postheat Treatments by Notch Bend Tests

Notch bend specimens were prepared from butt welds made using the four brands of 2¼ CrMo electrodes, and from the base metal. Information on the preheat and postheat treatments used, and data obtained from the notch bend tests are presented in Table 7.

The results indicate that all of the weld metals and the base metal heat-affected zones could sustain maximum loads greater than those for the base metal itself, regardless of whether or not preheat and/or postheat treatments were used. Furthermore, although deflections at maximum load were less, the weld metals and heat-affected zones in the as-welded or preheated conditions absorbed more energy to maximum load than did the base metal, except for the Code D electrode weld, as-welded.

The absence of measurable deflection or energy absorption after maximum load indicates fracture of the specimen at maximum load. This condition of notch brittleness generally is undesirable in view of the lack of any warning which might precede catastrophic failures. Therefore, the advantage of the higher load-carrying capacity of the as-welded or preheated weld metals is offset in their notch brittleness disadvantage. On these bases, therefore, postheat treatment of the weld metal at 1300° F (or as previously determined, 1250° F or over) is required.

Data for the two brands of electrodes for which no preheat, and 300° F preheat, 1300° F postheat treatments were used indicate no consistent effect on notch bend properties attributable to the 300° F preheat.

In practically all cases, the base metal heat-affected zone absorbed energies to maximum load and after maximum load which equalled or exceeded that absorbed by the base metal. The ductility of the heat-affected zone as evidenced by deflection after maximum load was greater in all instances than that of the base metal.

The notch bend test results indicate that thermal treatments are not required in order to obtain satisfactory properties of the base metal heat-affected zone. However, a postheat treatment at 1250° F or over is necessary for the 2¼ CrMo weld metals.

Impact Test Results

Transition temperature curves were determined for the four weld metals, the base metal and the heat-affected zone, under various conditions of preheat and postheat treatments. The impact energy data, together with welding conditions, are presented in Table 8. Representative transition temperature curves are presented in Figs. 6 and 7, for weld metal, and in Fig. 8 for the 2¼ CrMo base metal.

The use of preheat up to 500° F increases slightly the impact energy absorbed at room temperature of the 2¼ CrMo weld metal, and also decreases slightly the transition temperature. Preheat, however, is not as effective as postheat with respect to increase in energy absorbed in impact and to lower-

ing of the transition temperature.

The impact properties of the as-deposited 2¼ CrMo weld metals are definitely inferior to both the 2¼ CrMo base metal and the base metal heat-affected zone. Postheat treatment for 1 hr at 1300° F improves the impact properties of all zones of the welds; however, the improved properties of the weld metals are still inferior even to the impact properties of the as-welded heat-affected zones.

The impact properties of the Code A electrode deposit appears to be superior to those of the other three brands of 2¼ CrMo alloy steel weld metals.

Part B—1¼ CrMo Welds in 2¼ CrMo Pipe

Results

Tensile Test Results. The data in Table 3 indicate that the room temperature yield and tensile strengths of the 1¼ CrMo weld deposit are higher than those of the 2¼ CrMo alloy pipe. The as-welded ductility of the 1¼ CrMo weld metal is comparable to that of the heat-treated 2¼ CrMo weld metal. Although both of these ductilities are lower than that of the pipe material, they are considered to be entirely satisfactory and adequate.

Table 9 and Fig. 9 show some short-time evaluated temperature tensile properties of the alloy pipe and the two CrMo weld deposits. It will be noted that the short-time elevated temperature tensile strengths of both weld deposits exceed those of the 2¼ CrMo alloy pipe throughout the range of temperature cited. Although no data for the yield strengths of the base metal were available, it is reasonable to assume that these would also be lower than those of either weld deposit. The ductilities of the weld metals at the elevated temperatures of test are lower than those of the pipe; however, the former are considered to be entirely satisfactory and adequate.

No tensile tests of reduced section specimens of butt welds of 2¼ CrMo pipe using 1¼ CrMo electrodes were made, in view of the noted differences in tensile strength between the weld metal and the base metal pipe. As previously indicated, such specimens obviously would fail in the base metal even if abnormally large defects were present in the weld deposits.

Bend Test Results

The results of longitudinal and side

Table 7—Notch Bend Tests of Welds in 2¼ CrMo Steel Pipe*

	Thermal treatment			Bend	Max	Deflection		Energy	
Electrode brand	Preheat, °F	Postheat, °F†	Notch location‡	angle, deg	load, lb	At max load, in.	After max load, in.	To max load, ft-lb	After max load, ft-lb
Base metal	None	None	Base	74	2400	0.75	0.36	120.5	65.2
	300	None	Base	90	2400	0.74	0.39	120.6	73.2
	500	None	Base	71	2420	0.74	0.36	122.1	63.9
	None	1300	Base	70	2400	0.71	0.29	118.2	48.2
	300	1300	Base	79	2420	0.71	0.52	122.4	85.8
Code A	None	None	Weld	44	4150	0.54	0	159.2	0
	300	None	Weld	38	3940	0.46	0	127.0	0
	500	None	Weld	45	3990	0.48	0	128.4	0
	None	1300	Weld	77	2920	0.40	0.75	90.7	82.2
	300	1300	Weld	90	2960	0.50	0.72	112.6	79.8
	None	None	HAZ	103	3000	0.43	1.33	95.8	198.9
	300	None	HAZ	109	3000	0.52	1.20	108.6	179.4
	500	None	HAZ	115	3500	0.69	1.03	173.8	197.4
	None	1300	HAZ	103	2700	0.54	1.08	104.9	147.2
	300	1300	HAZ	88	2660	0.60	0.73	119.0	123.5
Code B	None	None	Weld	48	3960	0.49	0	134.0	0
	300	None	Weld	49	3950	0.49	0	141.9	0
	500	None	Weld	46	3900	0.48	0	131.1	0
	None	1300	Weld	92	3110	0.50	0.90	111.0	83.5
	300	1300	Weld	91	2980	0.41	1.00	90.7	91.4
	None	None	HAZ	90	2940	0.51	0.89	99.3	164.1
	300	None	HAZ	89	3390	0.55	0.87	134.4	167.5
	500	None	HAZ	88	3010	0.51	0.90	106.3	154.7
	None	1300	HAZ	87	2800	0.61	0.81	125.0	139.6
	300	1300	HAZ	88	2830	0.65	0.76	133.7	139.0
Code C	None	None	Weld	54	4370	0.66	0	196.9	0
	300	1300	Weld	51	2920	0.35	0.33	73.4	41.6
	None	None	HAZ	100	3160	0.43	1.28	104.5	151.5
	300	1300	HAZ	113	2880	0.62	1.14	129.9	175.0
Code D	None	None	Weld	33	3960	0.38	0	104.7	0
	300	1300	Weld	49	3200	0.45	0.04	110.1	10.5
	None	None	HAZ	110	3060	0.42	1.32	91.9	197.4
	300	1300	HAZ	124	2840	0.66	1.07	114.5	182.5
Code E	None	None	Weld§	..	2720	0.80	0.20	153.0	23.6
	300	None	Weld	..	2605	0.69	0.44	126.7	26.3
	500	None	Weld	..	2550	0.69	0.49	118.8	46.3
	None	1300	Weld	..	2195	0.95	1.13	151.8	119.8
	300	1300	Weld	..	2160	0.96	1.05	145.5	101.7
	None	None	HAZ	..	2685	0.80	1.24	154.1	118.1
	300	None	HAZ	..	2650	0.96	0.95	176.6	149.8
	500	None	HAZ	..	2495	0.94	1.14	163.6	166.0
	None	1300	HAZ	..	2075	0.91	1.03	133.9	142.6
	300	1300	HAZ	..	2285	0.93	1.11	133.7	158.9

* Averages of duplicate specimens.
† Postheat treatment for 1 hr at temperature.
‡ HAZ refers to base metal heat-affected zone.
§ Single specimen.

bend tests of welds made in the 2¼ CrMo pipe, using 1¼ CrMo electrodes, are shown in Table 4. Photographs of the bends after tests are shown in Fig. 10 for the longitudinal bend specimens, and in Fig. 11 for the side bend specimens.

All of the bend test specimens bent 180° in the guided bent test jig without failure, regardless of whether or not preheat and/or postheat was used. In the group of side bend specimens, one in the as-welded condition and two in the 300° F preheat-no postheat condition exhibited lack of penetration at the root, due to an excessively wide root face at these locations. However, even with the notch effect at the root, no cracks were propagated through the weld metal, thus demonstrating further the toughness of the 1¼ CrMo weld metal in the as-welded condition.

The comparison results for the 2¼ CrMo weld in similar alloy pipe also indicate satisfactory bend properties for all conditions of thermal treatment. It will be noted, in Fig. 11, that a considerable part of the deformation takes place in the base metal and heat-affected zone, at which location some local necking-down is shown. This condition is observed mostly in the specimens without postheat treatment and is due primarily to the difference in properties between the high-strength weld metal and the lower-strength base metal. However, the extent of this localization of deformation is less for these specimens than that previously found for 2¼ CrMo welds in the same alloy pipe (see Fig. 4) in view of the even higher strength of this alloy weld metal deposit.

Evaluation of Thermal Treatments by Hardness Measurements

The effects of preheat and postheat treatments on the hardness and ductility of 1¼ CrMo welds in 2¼ CrMo pipe are shown in Table 5. Comparison data for 2¼ CrMo welds are included in this table. Table 6 shows the effect of time and temperature on the hardness and ductility of various specimens of 1¼ CrMo welds in 2¼ CrMo pipe, welded with and without preheat. In both of these tables the ductility values have been calculated from the equations of correlation previously determined for the alloy materials.

The results indicate that although postheat treatments soften the various zones of the weld, adequate ductilities are exhibited by the 1¼ CrMo weld in 2¼ CrMo pipe in the no preheat-no postheat condition. This is not true of 2¼ CrMo welds, which previously were found to require a 1250° F minimum temperature postheat in order to obtain at least 20% ductility of the weld metal. In both cases, however, the heat-affected zone ductilities appear to be adequate in the no preheat–no postheat condition.

Table 8—Impact Properties of Welds in 2¼ CrMo Steel Pipe*

	—Thermal treatment—		—Transition temperature and energy ranges—			
			—½ Energy level—		15 ft-lb level,	Room temp.
Electrode code	*Preheat, ° F*	*Postheat, ° F†*	*Ft-lb*	*Temp., ° F*	*Temp., ° F*	*energy, ft-lb*
Code A	None	None	22	+56 ± 16	+34 ± 9	31 ± 7
	300	None	27	+75 ± 37	+34 ± 22	29 ± 9
	500	None	25	+37 ± 23	+12 ± 20	38 ± 5
	None	1300	41	+24 ± 28	−15 ± 22	69 ± 8
	300	1300	43	+ 3 ± 37	−30 ± 26	73 ± 6
Code B	None	None	19	+61 ± 29	+47 ± 30	22 ± 6
	300	None	20	+73 ± 4	+53 ± 8	22 ± 1
	500	None	21	+55 ± 32	+42 ± 31	25 ± 7
	None	1300	40	+30 ± 14	− 7 ± 14	70 ± 5
	300	1300	37	+51 ± 8	+12 ± 9	54 ± 4
Code C	None	None	14	+56 ± 14	+59 ± 14	22 ± 5
	300	1300	31	+85 ± 27	+46 ± 24	29 ± 11
Code D	None	None	13	+47 ± 16	+56 ± 15	17 ± 1
	300	1300	24	+61 ± 16	+33 ± 19	26 ± 1
Code E	None	None	33	− 5 ± 30	−30 ± 15	65 ± 7
	300	None	32	−20 ± 20	−25 ± 20	51 ± 9
	500	None	38	+15 ± 15	−10 ± 12	63 ± 12
Base metal	None	None	63	0 ± 6	−11 ± 6	125 ± 14
	300	1300	84	+10 ± 5	−38 ± 4	168 ± 18
Heat-affected zone	None	None	>120	−15 ± 80	−61 ± 45	>200 ± 40
	300	1300	>120	−16 ± 80	−82 ± 16	>200 ± 40

* Averages of duplicate or triplicate specimens.
† Postheat treatment for 1 hr at temperature.

Table 9—Short-Time Elevated Temperature Tensile Properties of Low-Alloy Weld Deposits and Steel Pipe

Material	*Conditions*	*Temp. of test, ° F*	*Yield strength, psi‡*	*Ultimate strength, psi*	*Elongation, % in 2 in.*	*Reduction of area, %*
Code A deposit	As-welded*	80	107,800	131,000	13	32
	Str. rel.*, ‖	80	74,700	91,850	23	54
	Str. rel.¶	850	59,000	70,000	20	64
	Str. rel.¶	950	56,500	61,700	24	68
	Str. rel.¶	1050	47,500	55,700	25	73
	Str. rel.¶	1150	33,900	47,500	29	72
Code E deposit	As-welded*	80	82,500	95,000	23.5	62
	Str. rel.*, §	80	65,000	81,500	26	68
	As-welded	850	58,000	87,100	33	54
	As-welded	950	54,800	78,700	29	59
	As-welded	1050	52,500	65,400	30	71
	As-welded	1150	35,000	48,900	39	82
Pipe†	Annealed	80	45,000	70,000	49	...
	Annealed	850	...	65,250	31	69
	Annealed	950	...	56,750	34	77
	Annealed	1050	...	44,500	45	86
	Annealed	1150	...	35,200	56	91

* Data from Table 3.
† Data interpolated from information in Babcock & Wilcox Co. Tech. Bull. 6F.
‡ 0.2% permanent set.
§ Postheat treatment for 1 hr at 1300° F.
‖ Postheat treatment for 1 hr at 1350° F.
¶ Postheat treatment for 1 hr at 1250° F.

It will be noted that postheat treatments of at least 2 hr at 1150° F or ½ hr at 1250° F are required in order to produce significant reductions in the hardness of the 1¼ CrMo weld metal or the 2¼ CrMo base metal heat-affected zone. Therefore, the usual 1 hr at 1150° F postheat treatment would result in relatively little change, except insofar as certain restraint stresses might be reduced.

The hardness-ductility results indicate also that preheat treatment is not required for 1¼ CrMo welds in 2¼ CrMo pipe, regardless of whether or not postheat treatment is applied. However, it is recognized that preheat is of significant value where weldments are made under conditions of restraint, particularly if no postheat treating is done. No data have been derived as yet relative to the amount of preheat required for specific restraints; in the absence of such information, the use of a 300° F minimum temperature for preheat of restrained 1¼ CrMo welds in 2¼ CrMo

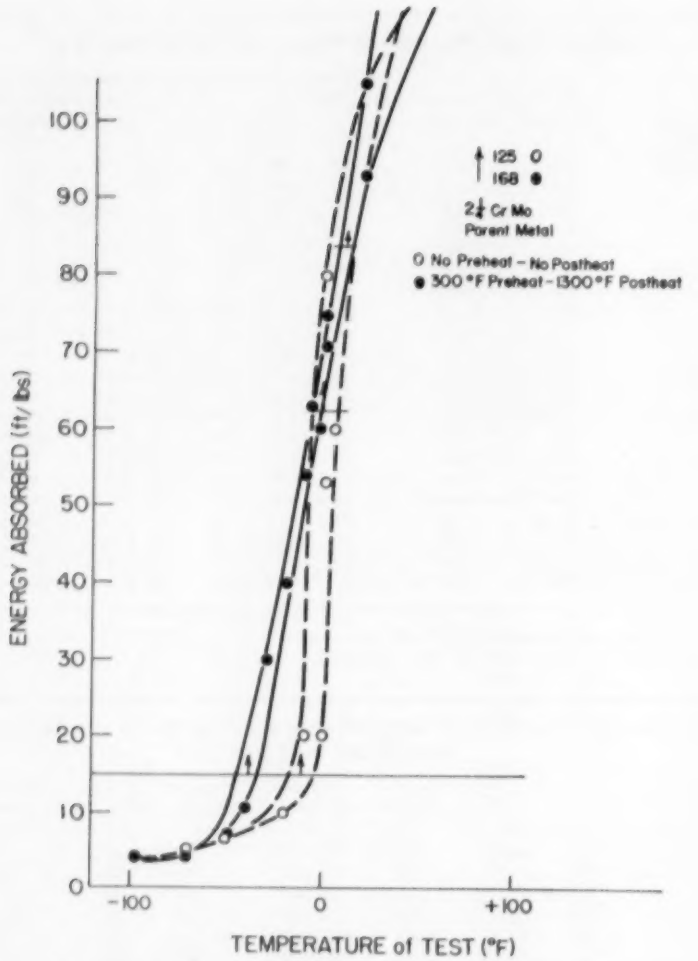

Fig. 8 Transition temperature curves for 2¼ CrMo base metal as-received and after heat treatment

alloy pipe appears to be reasonable.

Evaluation of Thermal Treatments by Notch-Bend Tests

The data in Table 7 indicate that in the no preheat-no postheat or preheat-no postheat conditions, the 1¼ CrMo weld metal and heat-affected zone could sustain maximum loads greater than those for the base metal. Postheat treatment reduces the strength of these zones, so that somewhat lower maximum loads, compared with the base metal, can be sustained. The higher maximum loads sustained by the 2¼ CrMo weld can be accounted for by its greater strength compared with the 1¼ CrMo weld metal. The deflections of the notch bend specimens under loading are indications of ductility, and for the 1¼ CrMo weld and heat-affected zone, these values are equal or superior to those for the base metal. Of particular significance is the fact that the 2¼ CrMo weld exhibits zero deflection after maximum load, in the no postheat condition, whereas the 1¼ CrMo deposit shows appreciable deflection.

Similarly, the energy absorbed values for the 1¼ CrMo weld are superior in general, to those of the 2¼ CrMo weld, especially after maximum load has been applied. The absence of measurable deflection or energy absorbed after maximum load indicates fracture of the specimen at maximum load. As noted previously, this condition of notch brittleness is undesirable in view of the lack of any warning which might precede catastrophic failures. The energies absorbed after maximum load for the 1¼ CrMo weld, in the no postheat condition, are lower than those for the base metal or heat-affected zone; however, the values indicate some significant toughness, especially compared with the 2¼ CrMo weld in a similar condition.

The results for the heat-affected zone of 1¼ CrMo welds indicate that thermal treatments are not required in order to obtain satisfactory properties. This conclusion also was reached previously for the heat-affected zone of 2¼ CrMo welds; however, in this case the weld metal requires postheat in order to develop adequate ductility. These results are not unexpected, since for comparable energy inputs (jpi based on average arc voltage, average current and speed in ipm) the base metal heat-affected zone will respond similarly for either electrode. However, it must be noted that, of the three zones tested, the heat-affected zone will exhibit the widest variation in test results. This is due to the difficulty in locating the notch in the same metallurgical structure of different specimens. This structure varies considerably across the width of the heat-affected zone, from the unaffected base metal to the fusion zone at the weld metal.

Impact Test Results

The results of impact tests of 1¼ CrMo welds in 2¼ CrMo pipe are shown in Table 8 and Fig. 12. Comparison data for 2¼ CrMo weld metal and base metal are included in Table 8.

The room temperature energy absorption of the 1¼ CrMo weld metal, in the no postheat condition is comparable to that of postheat-treated 2¼ CrMo weld metal; both are considerably lower than that for the base metal. The transition temperatures for the 1¼ CrMo weld metal, based either on 15 ft-lb energy absorption level or ½ maximum energy absorption level, are of the same order of magnitude as those for the base metal. The transition temperatures for the 2¼ CrMo weld metal also are comparable, but only when postheat treatment has been applied.

Table 10—Stress-Rupture Properties of Low-Alloy Weld Deposit and Steel Pipe*

Material	*Condition*	*Test temp., °F*	*Load, psi*	*Time to rupture, hr*	*Elongation, % in 2 in.*	*Reduction of area, %*
1¼ CrMo weld deposit	As-welded	1100	20,000	279	14.5	29.2
			16,000	376	14.0	25.8
	Postheated†	1100	20,000	308	14.5	24.1
			16,000	645	10.0	19.2
2¼ CrMo steel pipe	Annealed	1100	20,000	75	...	...
			16,000	500	...	...

* Data from Babcock & Wilcox Co.

† Postheat treatment for 1 hr at 1150° F. This postheat treatment is inadequate for significant reductions in hardness.

Data for the impact properties of these materials at elevated temperatures have been plotted as shown in Fig. 13. It will be noted that the 1¼ CrMo weld metal has somewhat superior impact properties over the range of temperatures shown compared with those for the 2¼ CrMo weld deposit, both being in the as-welded condition. The base metal and the heat-affected zone impact properties are superior to those of either weld metal; however, the values for the welds are not unacceptably low.

Stress-Rupture Properties

Table 10 shows some limited data obtained from the Babcock and Wilcox Co. for 1¼ CrMo weld deposits and for 2¼ CrMo pipe. These data are included here for the purpose of discussion.

It will be noted that at 1100° F, the time-to-rupture of 1¼ CrMo deposits, as-welded, exceeds that for the 2¼ CrMo pipe, at the 20,000 psi load. At 16,000 psi load, the 2¼ CrMo pipe requires more time-to-rupture than the 1¼ CrMo deposit; however, the difference, proportionately, is not as great as at 20,000 psi. In the absence of additional data, it is not known whether the trend shown by the lower load would continue at still lower loads. However, it is apparent that the 1¼ CrMo deposit, in the as-welded condition, exhibits fairly good stress-rupture properties. Thus, it would be expected that sudden overloads of 1¼ CrMo welds in 2¼ CrMo pipe, in the no postheat condition, would not result in sudden catastrophic ruptures or failures.

Discussion

The calculated ductility values for the 2¼ CrMo and 1¼ CrMo weld deposits and the 2¼ CrMo heat-affected zone, based on hardness-ductility correlations previously reported, have recognized limitations for interpretation. It has been noted previously[2] that the heating and cooling rates, as well as time at temperature, for the base metal heat-affected zone are different from those used to determine the hardness-ductility correlations, and that the resultant metallurgical structures are dissimilar. However, the cooling rates of the heat-affected zone are intermediate between air-cooling (normalizing) and water-quenching, as were used for the hardness-ductility relationships, so that these extremes should encompass cooling rates experienced in these zones. The ductilities of the alloy weld deposits probably are more correct than for the 2¼ CrMo heat-affected zone as the former were correlated from similarly-treated weld deposits.

In any event, it is believed that the estimate of both weld metal and heat-affected zone ductilities, based on the hardness-ductility correlations, provides

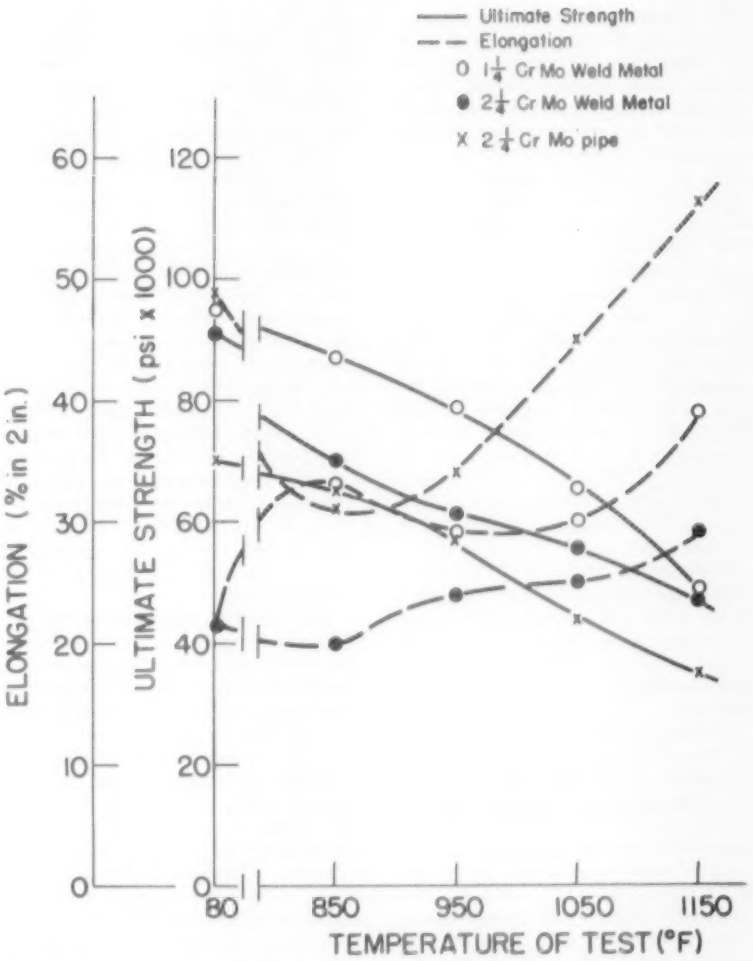

Fig. 9 Short-time elevated temperature tensile properties of low-alloy weld deposits and steel pipe

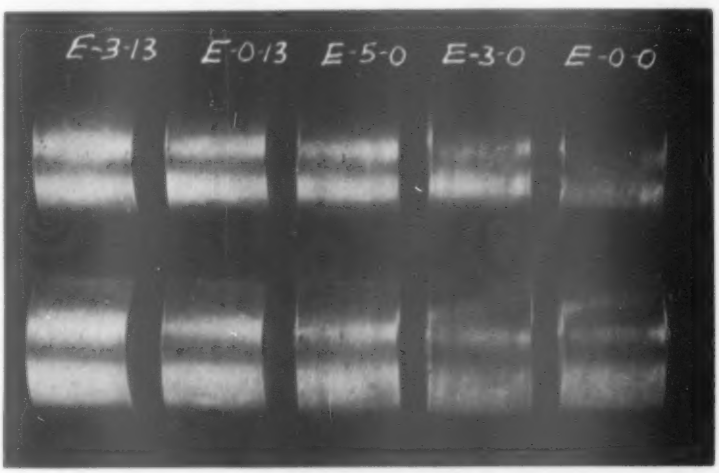

Fig. 10 Photograph of longitudinal bend specimens of 1¼ CrMo welds in 2¼ CrMo pipe after testing. See Table 4 for code identifications and corresponding thermal treatments. Approx. X ½

a more reasonable basis for evaluation of weldment properties than would be the results obtained from reduced-section tensile specimen tests, where nonuniform straining of high-strength weld metal and of lower strength base metal has been observed.

The results of tests reported herein indicate that a postheat treatment for at least 1 hr (per in. of thickness) at 1250° F is necessary in order to obtain required ductility of the 2¼ CrMo weld metals. The as-welded ductility of the 2¼ CrMo alloy steel pipe heat-affected zone is adequate, and postheat treatment for the purpose of compensating for the increase in hardness of the base metal resulting from the welding operation is unwarranted. Preheat treatment may be of value in the case of highly restrained joints; in the absence of data relative to the effect of restraint, a preheat temperature of 300° F is recommended.

It should be emphasized that weldments made using 2¼ CrMo alloy electrodes should not be postheat treated in the temperature range of 1050 to 1150° F, in view of the embrittlement (loss of ductility) which is produced by this treatment.

The results of tests also indicate that the as-welded properties of 1¼ CrMo welds in 2¼ CrMo alloy pipe, tested at room and at lower temperatures, are satisfactory and adequate. The data included herein for the elevated temperature short-time tensile tests and stress-rupture tests indicate that these properties of the 1¼ CrMo weld metal, in the as-welded condition, are equal or superior to those of the 2¼ CrMo alloy pipe. Similar data for the impact properties at elevated temperatures indicate that those of the 1¼ CrMo weld metal are superior to those of the 2¼ CrMo weld metal, both being in the as-welded condition. Both of these alloy weld deposits have elevated temperature impact properties which are inferior to those of the 2¼ CrMo alloy pipe; however, the impact values are not unacceptably low.

Low-alloy CrMo pipes are used for several reasons. These include resistance to graphitization and to elevated-temperature hydrogen embrittlement, adequate strengths at operating temperatures and pressures, and some measure of resistance to corrosion and scaling. Both the 1¼ CrMo and 2¼ CrMo alloys have adequate resistance to graphitization, and within the normally expected maximums of temperatures and hydrogen pressures for refinery processes the 1¼ CrMo alloy would be adequate (up to 1000 psi partial pressure of hydrogen at 1150° F, according to G. A. Nelson's data).

The strength properties of the 1¼ CrMo weld metal exceed those of the 2¼ CrMo pipe, and it is reasonable to assume that the elevated temperature creep properties of 1¼ CrMo weld metal would be equal, if not superior to those of the 2¼ CrMo alloy pipe material. Although the ductility of the 2¼ CrMo pipe exceeds that of the 1¼ CrMo weld metal, the ductility of the latter is considered to be entirely adequate. Published data[7] indicate that the corrosion resistance of the 2¼ CrMo alloy toward various refinery media is somewhat better than that of the 1¼ CrMo alloy. This also is the situation with respect to scaling. However, the differences noted are not great, and it is quite probable that these properties of the 1¼ CrMo alloy would be entirely satisfactory.

The selection of the 2¼ CrMo alloy pipe in lieu of the 1¼ CrMo pipe generally is made on the basis of creep properties, upon which allowable unit stresses for elevated temperature service, for design purposes, are based. The ASME Code for Unfired Pressure Vessels for example, specifies equal allowable unit stresses for both the 1¼ CrMo and 2¼ CrMo wrought alloys at 1000° F. At 1050° F the respective allowable unit stresses are 5500 and 5800 psi; at 1100° F these stresses are 4000 and 4200 psi; and at 1100° F these stresses are 2500 and 3000 psi. These differences are significant, to some extent, but they apply only to wrought alloys. It is believed that similar data for the 1¼ CrMo weld metal and the 2¼ CrMo wrought alloy would show very little, if any, difference in stresses based on creep properties.

It is recognized, of course, that present Code requirements will not permit the welding of 2¼ CrMo piping without postheat treatment. Many similar requirements have been relaxed in recent years based on investigations, similar to this one, which have demonstrated conclusively the practicability of welding certain materials without necessarily requiring postheat treatments. These postheat treatments always are expensive, and in many instances, they cannot be applied adequately in the field.

Under the present requirements which specify postheat treatment of the 2¼ CrMo alloy, there still are several reasons for considering the use of 1¼ CrMo welds for this material. The superior as-deposited ductility of 1¼ CrMo welds, compared with 2¼ CrMo welds, would decrease the possibility of cracking under conditions of low or inadequate preheat and/or high restraint. Also, the satisfactory as-welded properties of the 1¼ CrMo weld in 2¼ CrMo alloy material suggests the possibility of using 1¼ CrMo electrodes for seal beads or fillet welds, as for furnace tubes in headers, where adequate postheat treatments are difficult to apply. Further, 1¼ CrMo welds in 2¼ CrMo pipe, which have satisfactory properties in the as-welded condition, would exhibit even higher ductilities and still adequate strengths were the weldments to be postheat treated, thereby providing an extra margin of safety, compared with 2¼ CrMo welds in similar alloy pipe.

It has been the usual practice in the past, to specify the use of electrodes depositing weld metals having chemical compositions comparable with those of the alloy being welded. In the case of dissimilar metals, the deposit analysis

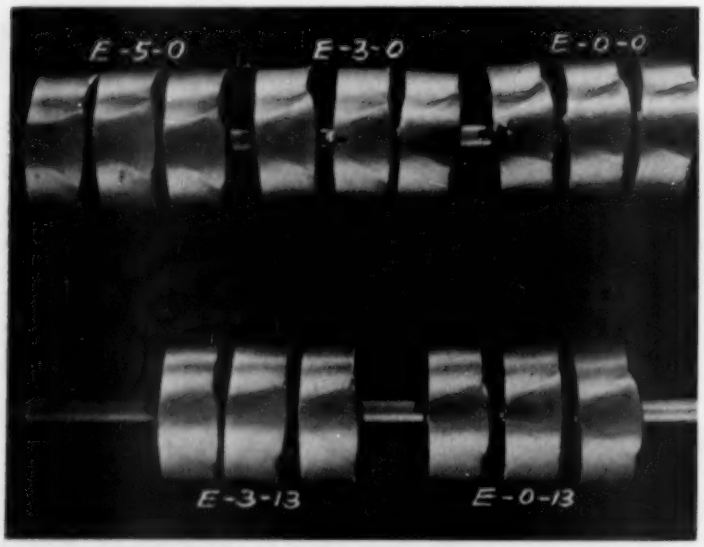

Fig. 11 Photograph of side bend specimens of 1¼ CrMo welds in 2¼ CrMo pipe after testing. See Table 4 for code identifications and corresponding thermal treatments. (Each group of three specimens represents a single pipe weld.) Approx. × ½

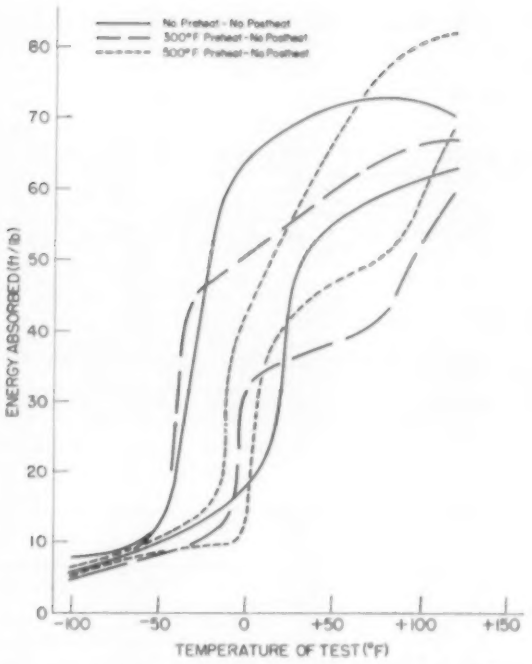

Fig. 12 Transition temperature curves for Code E weld deposits in $2^1/_4$ CrMo steel pipe, under various preheat and postheat conditions

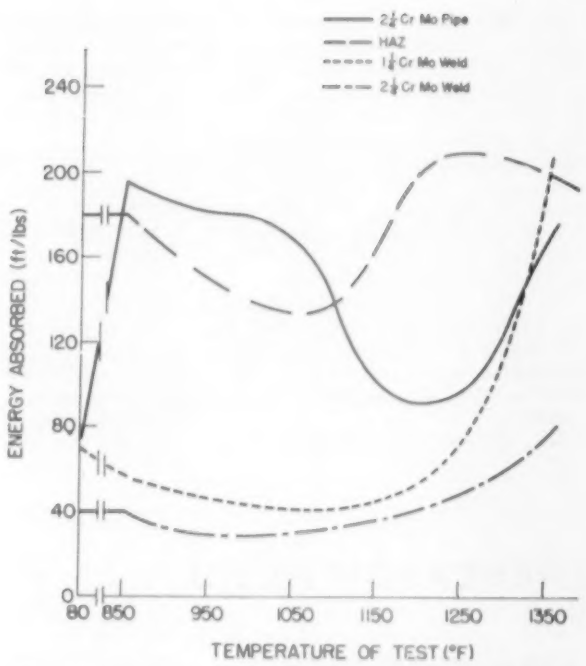

Fig. 13 Charpy vee-notch impact test results for welds in $2^1/_4$ CrMo pipe (as-welded condition)

normally would match that of the higher alloyed material. Unless notable differences exist with respect to other conditions of service, as discussed previously, it is believed preferable to match physical properties of the weld metal and base metal rather than to match chemical compositions. Weldments made according to the strength concept should exhibit improved serviceability, since they would not contain welds having excessively high strength and consequently which would tend to show nonuniform yielding under transient overloading conditions. The use of $1^1/_4$ CrMo welds in the $2^1/_4$ CrMo pipe is a step in this direction, and the results of this investigation appear to justify this concept.

Summary

The results of this investigation of the arc welding of $2^1/_4$ CrMo alloy steel pipe appear to warrant the following conclusions:

1. A significant correlation exists between hardness and ductility, and between hardness and tensile strength, for heat-treated $2^1/_4$ CrMo alloy steel pipe material and for $2^1/_4$ CrMo weld deposits.

2. The use of preheat temperatures up to 500° F has little or no effect on the strength, ductility and impact properties of weld metal deposited from $2^1/_4$ CrMo low-hydrogen electrodes or of base metal heat-affected zone.

3. Postheating welds deposited from $2^1/_4$ CrMo alloy low-hydrogen electrodes at temperatures below 1050° F produces no significant changes in properties. Postheating in the range of 1050° F (for 16 hr) to 1150° F (for 2 hr) produces an undesirable increase in hardness and decrease in ductility of the $2^1/_4$ CrMo weld metals. The base metal heat-affected zone is relatively unaffected by these treatments.

4. The ductility of $2^1/_4$ CrMo alloy weld deposits is increased to over 17% (minimum required by AWS specification A316-54T for E9015-16-B3 electrodes) by a minimum postheat treatment of 1250° F for 1 hr.

5. Unrestrained welds in $2^1/_4$ CrMo alloy pipe made without preheat and/or postheat were found to be sound and free from cracks.

6. The room temperature yield and tensile strengths of $1^1/_4$ CrMo weld metal are higher than those of the $2^1/_4$ CrMo pipe. The ductility of the as-welded $1^1/_4$ CrMo deposit is higher than that of $2^1/_4$ CrMo weld metal in the preheated-postheated conditions.

7. The short time elevated temperature tensile strengths of $1^1/_4$ CrMo weld metal, within the range of 850 to 1150° F, exceed those of the $2^1/_4$ CrMo pipe. No creep data for the $1^1/_4$ CrMo weld metal are available: however, it is reasonable to assume that the creep strength of this material will not be below that of the $2^1/_4$ CrMo pipe, in view of the above results.

8. The ductility of $1^1/_4$ CrMo welds in $2^1/_4$ CrMo pipe, in the no preheat-no postheat condition, is entirely satisfactory and adequate, as evidenced by the results of side bend and longitudinal bend tests.

9. Previously determined hardness-ductility correlations for $1^1/_4$ CrMo weld metal and $2^1/_4$ CrMo base metal were applied to hardness measurements made on these welds. The calculated ductilities of the $1^1/_4$ CrMo weld metal and $2^1/_4$ CrMo heat-affected zone in the no preheat-no postheat condition, appear to be entirely satisfactory and adequate.

10. Postheat treatments of at least 2 hr at 1150° F or $^1/_2$ hr at 1250° F are required in order to produce significant reductions in the hardness of $1^1/_4$ CrMo weld metal or $2^1/_4$ CrMo pipe heat-affected zone.

11. Notch-bend test results indicate that the as-deposited $1^1/_4$ CrMo weld metal can sustain somewhat higher loads than those for the $2^1/_4$ CrMo base metal. Although the energy absorbed after maximum load was lower for the $1^1/_4$ CrMo weld, in the no preheat-no postheat condition, than for the $2^1/_4$ CrMo pipe, it was not unacceptably low.

12. The notch-bend properties of the $2^1/_4$ CrMo heat-affected zone, in the no preheat-no postheat conditions, are superior to those either of the base metal or of the $1^1/_4$ CrMo and $2^1/_4$ CrMo weld deposits in any thermally treated condition. Although the $2^1/_4$ CrMo pipe alloy is considered to be air hardening, the results of tests indicate no adverse effects from the observed hardness increase.

13. The impact properties of as-deposited 1¼ CrMo welds are superior to those of 2¼ CrMo welds in the no preheat-no postheat conditions. The 1¼ CrMo weld impact properties, in the no preheat-no postheat condition, are comparable to those of 2¼ CrMo weld metal in the preheated-postheated condition. Both alloy weld deposits exhibit impact properties substantially lower than those of the 2¼ CrMo base metal, but not unacceptably low.

14. The transition temperature of 1¼ CrMo weld metal, as deposited, is comparable to that of the 2¼ CrMo base metal, and to that of 2¼ CrMo weld metal in the thermally treated condition.

15. The results reported herein were obtained on pipe with a wall thickness of ⅝ in. It is believed that the above conclusions are warranted for comparable analysis plate and pipe up to at least one in. in thickness.

Acknowledgments

The author wishes to acknowledge the assistance of C. F. Braun, J. M. Backus and other personnel of the Engineering Research Department for the preparation of the welds and test specimens and in securing the data.

The permission of the Standard Oil Co. (Ind.) to publish this paper is greatly appreciated, as are the advice and encouragement given through this investigation by Dr. C. H. Samans, Associate Director, Materials Division, and G. W. Watts, Director of Engineering and Engineering Research.

References

1. Bland, J., Privosnik, L. F., and Windsor, F. J., "The Arc Welding of Low Chromium-Molybdenum Steel," The Welding Journal, 31 (9), 783–791 (1952).

2. Bland, J., "Arc Welding of Low Chromium-Molybdenum Steel Pipe," *Ibid.*, 32 (9), 803–814 (1953).

3. *Methods of Working Seamless Tubes and Pipe of the Intermediate B & W Crolays*, Babcock & Wilcox Tube Co. Tech. Bull. No. 9C (1954).

4. "Rules for Welding Piping in Marine Construction-Ferritic Alloy Steels," AWS Std. D3.4-52 (tent.).

5. "Recommended Preheat and Postheat Welding Practices for Low Chromium-Molybdenum Steel Pipe," Pipe Fabrication Institute Standard FS(M)8-1955.

6. "Recommended Practices for Interruption of Heat Treatment Cycles for Low Chromium-Molybdenum Steel Pipe Materials," AWS Std. D-10.3-55 (tent.).

7. Babcock & Wilcox Technical Bulletin 6F.

RESEARCH NEWS

(*Continued from page 168-s*)

constituted to obtain basic data on the factors influencing the welding of aluminum alloys in order to improve the welding of existing alloys, and to develop new alloys with good welding characteristics and other satisfactory properties.

The Report is divided into the following main sections: cracking at temperatures above the solidus; cracking at temperatures below the solidus; factors affecting weldability; temperature distribution during the welding of aluminum alloys; the development of alloys having good welding and mechanical properties; cracking diagrams for aluminum alloys. Appendices describe (I) the cracking tests used, i.e. ring casting tests and restrained weld tests, and (II) the complete list of Papers published by the Welding Research Team. Price 7*s*, 6*d*.

Develop Impact Guillotine for Testing Shock Resistance

To a metallurgist, the Charpy notch impact test is as familiar as the chemical symbols Fe, C, and O. Although long used as a method for determining the transition point between ductile and brittle zones of metals, the method has some major disadvantages. For example, sample preparation takes considerable time and a V-shaped notch must be accurately machined 79 mils deep into one side of the small sample. A pendulum-type apparatus breaks the sample by swinging a weight against it. Final data are in the form of a graph with impact energy for rupture plotted against the temperature of the sample. Even after elaborate preparations and careful technique, the exact temperature of the transition is not clearly defined.

A new method now being used by materials engineers at the Westinghouse Electric Corp. uses an impact guillotine and a much larger sample, 14 in. long by 3½ in. wide, by 1 in. thick. Instead of the notch, a weld bead is put on the bottom side of the sample and an artificial crack put into

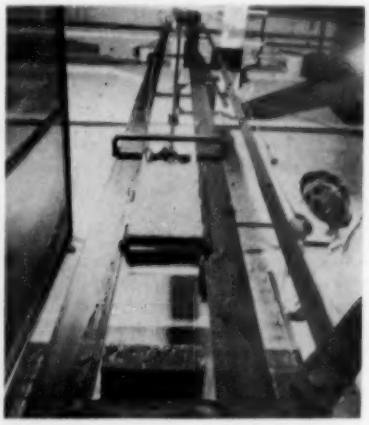

this weld by means of an abrasive cutting wheel. A standard weight is dropped on samples at various temperatures and the transition temperature readily bracketed within a narrow range. For example, if trials at −20° F show breakage each time, and trials at +20° F produce no breakage, the transition point is clearly defined within useful limits.

Results are reproducible by the guillotine method and sample preparation has been cut to one third that of the Charpy method. Another laboratory step that's making the metallurgist's job a little easier.

New Spectrographic Standard Samples of Stainless Steel Now Available

The National Bureau of Standards, U. S. Department of Commerce, Washington 25, D. C., has announced the availability of six new standard samples of stainless steel. The samples, carefully analyzed and certified for composition, are designed for calibrating and checking spectrochemical methods of analysis. Together with a set of three spectrographic standards issued earlier, NBS standards now provide certified concentration values for determining most of the elements encountered in the analysis of stainless steels.

The new stainless steel standards are certified for concentrations of six major and minor elements: manganese, silicon, copper, nickel, chromium, and molybdenum. Samples are available in two forms: rods 7/32 in. in diam and 4 in. long, and rods ½ in. in diam and 2 in. long. Both forms serve as electrodes for spark excitation in spectrochemical analysis. The three stainless steel standards issued previously are

(*Continued on page 216-s*)

EFFECT OF COLD WORK ON THE MECHANICAL PROPERTIES OF PRESSURE VESSEL STEELS

PVRC interpretive report reviews and appraises the present state of knowledge regarding the effects of cold work on the mechanical properties of steels and indicates areas where further research is needed

By W. T. LANKFORD

SUMMARY. The mechanical properties of steel plate measured prior to fabrication into pressure vessels give no assurance of corresponding properties in the completed vessel because cold forming, or cold working of any kind, considerably alters the properties of the plate. In general, these changes include an increase in yield strength, decreased ductility with less ability to flow plastically, and decreased toughness as reflected by an increase in the transition temperature from tough to brittle behavior. Basically, these alterations in properties are a result of strain hardening, and the aging which occurs with time after cold working and which proceeds more rapidly at moderately elevated temperatures. The rate of work hardening is high at low strains and decreases as the magnitude of strain increases.

The effects of heating cold-worked steels in the range of temperatures commonly used in stress relieving are different for different types of steel. Carbon steels appear to undergo little if any improvement in ductility and notch toughness when heated in the range 900–1200° F after moderate amounts of cold work. Almost complete recovery of notch toughness has been observed in certain alloy steels, on the other hand, when heated at about 1050° F after cold working. The need for further work in this field is indicated. At a sufficiently high temperature recrystallization occurs, which completely removes the effects of cold work. The temperature required for recovery and recrystallization depends upon the amount of cold work previously imposed.

Materials Division
Pressure Vessel Research Committee
Welding Research Council

Introduction

In the manufacture of pressure vessels, cold-forming operations are used extensively in shaping initially flat plate material into desired vessel contours. The resulting plastic deformation plays an important role in establishing the mechanical properties of the material in the completed vessel. Local plastic deformation occurring at points of high stress concentration in a vessel when subjected to service loads may also result in significant changes in properties. It is the purpose of this interpretive report to review and appraise the present state of knowledge regarding the effects of cold work on the mechanical properties of steels, and to indicate areas where further research is needed. Emphasis has been placed wherever possible on data pertaining specifically to those carbon and constructional alloy steels that can be utilized in pressure vessel construction. Data on similar grades of carbon and constructional alloy steels are also presented, however, in order to provide a more general background of information.

If the practical significance of the effects of cold work on the properties of steel is to be appraised properly, it is essential at the outset that the inherently unstable nature of cold-worked steels be clearly recognized. While cold work, *per se*, produces pronounced changes in mechanical properties, further changes in the cold-worked material that result from secondary effects may also be quite significant. In general, the properties existing immediately following a cold-forming operation will have been modified, in varying degrees, by the time the material is placed in service and may continue to change during service. The nature and extent of the changes in properties that actually occur will depend on the type of steel involved as well as on the specific thermal history experienced by the cold-formed material during subsequent fabrication operations.

As has been discussed in another Materials Division interpretive report,[1] many steels that have been plastically deformed are subject to the phenomenon known as strain aging and undergo progressive changes in properties as a result of such aging. While strain aging can proceed at atmospheric temperatures, it is greatly accelerated even at moderately elevated temperatures. At still higher temperatures, the processes of recovery and recrystallization may become operative, thus providing still another source of modification of the properties of a cold-worked steel. Cold working, therefore, can in a sense be regarded as "conditioning" the material for the development of the properties that exist as the material is placed in service.

Since it is obviously important to understand all of the stages in the development of the final properties, the changes produced by cold work as such, as well as changes induced by subsequent fabrication operations and by exposure to service temperatures, will be considered in the following discussion. Strain aging will not be discussed in detail, however, inasmuch as it has been treated in another report.[1]

In most of the experimental work that has been carried out for the purpose of evaluating the effects of cold work on properties, methods of straining have been employed that produce essentially uniform strains through the cross section of the specimen. The objective of such experiments has been primarily to establish trends and to reveal differences in materials under closely controlled conditions of cold working. The problem of relating results of tests on uniformly strained specimens to the property changes that would occur in plates formed into pressure vessel components, in which the strains would generally not be uniform, has received relatively little attention. Emphasis has been placed in this report, therefore, on outlining basic trends and indicating the nature of the changes in properties resulting from cold work. As a rough guide in considering the effects of various amounts of cold work, it may be noted

W. T. Lankford is Chief Research Engineer, Specialty Products; Applied Research and Development; United States Steel Corp.

that forming of 1-in.-thick plate into cylinders ranging in diameter from 20 in. to 120 in. results in outer fiber strains ranging from about 5% for a diam of 20 in. to about 0.8% for a diam of 120 in. It is also of interest to note that Paragraph UCS-56(a)(5) of Section VIII of the ASME Boiler and Pressure Vessel Code limits the thickness, and thereby the strain, permissible without stress relieving for a given diameter of vessel. The maximum thickness is given by $(D + 50)/120$ in. where D is the ID of the vessel, or 20 in., whichever is greater. It happens that the greatest strain permitted on the basis of this formula is slightly less than 3%, corresponding to a D value of 20 in.

Before the various changes in properties resulting from cold work are considered in detail, the following circumstances may be cited to indicate the various conditions that can lead to changes in the mechanical properties of cold-worked steels:

1. Exposure to atmospheric temperatures
2. Exposure to preheating or postheating in connection with welding
3. Exposure to the heat of welding
4. Exposure to the heat of stress-relief annealing

It is readily apparent that the thermal conditions that can be encountered, as well as the volumes of material affected thereby, are subject to wide variation. Consequently, wide variations in the properties of a previously cold-formed steel can be expected in a completed pressure vessel.

Effect of Cold Work on Strength Properties

When steel is plastically deformed at ordinary or moderately elevated temperatures, its resistance to continued deformation progressively increases. This increase in strength or flow resistance is known as "strain hardening" or "work hardening" and is one of the most important effects of cold working. Strain hardening can be described most simply by considering the so-called "true" stress-strain curve determined in a uniaxial tension test. In the true stress-strain relationship, stress is based on the actual area of the specimen at any instant, rather than on the original area, i.e., stress is corrected for the changing cross section of the specimen. Likewise, strain is based on the instantaneous gage length of the specimen, rather than on the original gage length. With stress and strain defined in this manner, the stress-strain relationship appears as shown in Fig. 1. It is evident that the stress required to cause further deformation increases continuously as the strain increases. The slope of the stress-strain curve at any point is a measure of the rate of work hardening, i.e., the rate at which the stress required to produce further deformation is increasing. It can be seen that the rate of work hardening decreases with increasing strain. This behavior results in the occurrence of a maximum load and the familiar phenomenon of necking down. At low strains the rate of work hardening is sufficiently high that, even though the cross-sectional area of the specimen is decreasing, the specimen can carry a larger load as the strain increases. Finally, however, the rate of work hardening decreases to such an extent that the loss of cross section is no longer compensated and the net load-carrying capacity of the specimen decreases.

When plastic deformation occurs under complex stress conditions, special stress and strain functions sometimes referred to as "effective stress" and "effective strain" can be employed to describe work hardening. These functions, which take into account all the principal stresses and strains, were developed on the basis that a single stress-strain curve should describe the plastic deformation of a given material under any state of stress. Considerable experimental evidence supports the validity of this theory for isotropic materials.[3] Similar relationships have been developed[4] for materials having certain types of simply defined directionality, but the introduction of parameters to correct for directionality is required. Hot-rolled, annealed, normalized, or quenched-and-tempered plate steels can be expected to be sufficiently isotropic that the strain-hardening characteristics can be described by the unmodified effective stress-strain relationship. It should be noted that the constants involved in the definitions of effective stress and effective strain can be chosen so that the stress-strain curve determined in simple tension is actually the effective stress-strain curve.*

L. R. Jackson[5] has suggested that the effective stress-strain relationship can sometimes be used to estimate the amount of work hardening produced by deformation under conditions for which the actual state of stress may not be known. If the strains are substantially uniform, the principal strains can be measured and the effective strain can be computed. A true stress-strain curve can be quickly determined on the virgin material by a simple tension test, thus establishing the effective stress-strain relationship. By then referring the effective strain determined after straining under the unknown state of stress to the effective stress-strain curve, the corresponding effective stress value can be ascertained. This value represents the effective stress that would be required for further flow, or can be considered as equivalent to the yield stress for material that has the measured amount of prior strain. In Fig. 2, the application of this method to the analysis of strain hardening produced by reduction by cold rolling is illustrated.[2,5] It can be seen that points determined by measuring yield stresses in simple tension after various amounts of cold rolling lie along the same curve established by straining entirely in tension. For large and substantially uniform strains, therefore, it appears that work-hardening effects can be predicted from a knowledge of the principal strains and the flow curve determined in simple tension.

It is of interest to note in Fig. 2 that the stress-strain values lie on a straight line on a double logarithmic plot. For most ferritic steels, it has been found that the true stress-strain curve can be approximated very closely, at least up to maximum load, by the empirical relationship, stress $= k \times \text{strain}^n$ where k and n are material constants usually referred to as the strength coefficient and the strain-hardening exponent, respectively.[6] These two parameters provide a convenient and widely used method for describing the stress-strain curve. The strain-hardening exponent n is intimately related to the amount of uniform elongation that the material is capable of undergoing, i.e., elongation prior to necking down. Larger n values correspond to larger uniform elongations.

It has been shown that for large uniform strains, the analysis of the response of the material with respect to strain hardening is rather straightforward. For small amounts of prior strain, however, the behavior of most steels is unfortunately not so simple. When in the hot-rolled, normalized, or annealed condition, most ferritic steels of the types used in pressure-vessel construction exhibit an abrupt type of yielding which is quite different from the gradual type of yielding observed in nonferrous metals and austenitic steels. Although the abrupt yielding behavior is very familiar, its general features will be briefly reviewed. The stress at which strain rapidly increases with no further increase in stress is known as the yield point. In some instances a drop in load occurs upon initial yielding, and flow continues at a somewhat lower load. The stress at which yielding first begins is then usually referred to as the upper yield point, while the lower stress level at which flow continues is known as the lower yield point. The amount of elongation occurring before the stress-strain curve begins to rise uniformly is known as the yield-

* Effective stress: $\bar{s} = [1/2[(s_1 - s_2)^2 + (s_2 - s_3)^2 + (s_3 - s_1)^2]]^{1/2}$. Effective strain: $\bar{e} = [2/3(e_1^2 + e_2^2 + e_3^2)]^{1/2}$, where s_1, s_2, s_3, and e_1, e_2, e_3 are the principal stresses and strains, respectively.

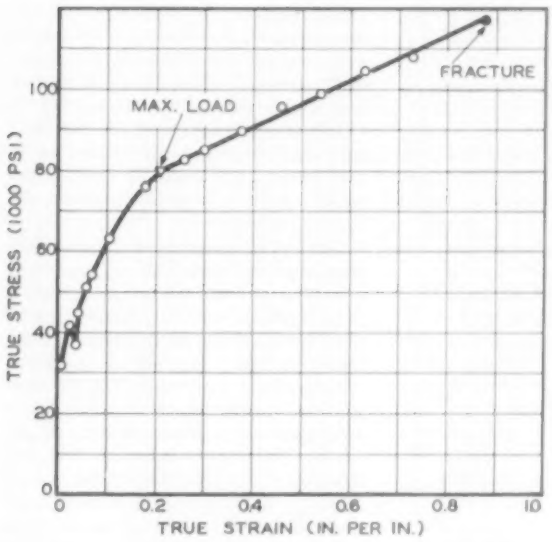

Fig. 1. True stress-strain curve for annealed 0.19% C, 0.85% Mn steel (MacGregor[2])

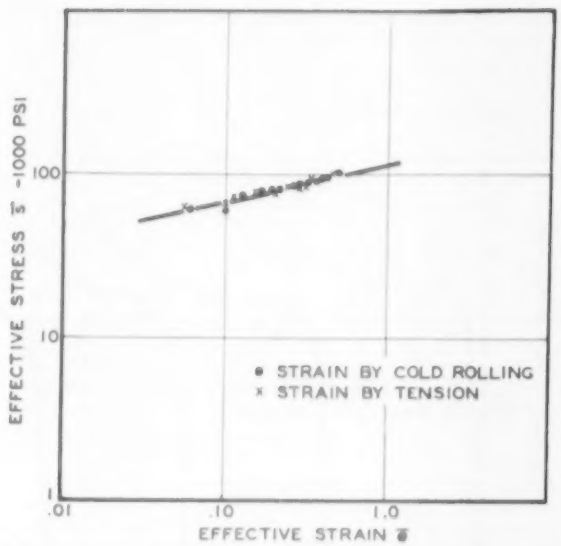

Fig. 2. Comparison of work hardening by cold rolling and by simple tension for annealed 0.19% C, 0.85% Mn steel (Jackson[3])

point elongation. The yield-point elongation may vary from a slightly perceptible jog in the stress-strain curve for steels quenched and tempered to high hardness levels to values of elongation approaching 10% for box-annealed deep-drawing steels. The yield-point elongation for structural carbon-steel plate material is usually in the neighborhood of 1 to 2%. During the yield-point elongation, the specimen does not strain uniformly, but rather by the progressive formation of localized strain bands, known as Lüder's lines or bands. Only one or a very few Lüder's bands form on initial yielding, and the remainder of the specimen remains unyielded. As straining proceeds, Lüder's lines continue to form and propagate until the end of the yield-point elongation range is reached.

Steel that has been cold worked prior to testing may exhibit gradual yielding rather than a definite yield point, and under certain circumstances may yield at a somewhat lower stress than that observed prior to cold working. The effect of cold work introduced by bending and straightening of $^1/_2$-in.-thick standard ASTM plate specimens of a semikilled carbon steel (0.23 C, 0.40 Mn)[7] is illustrated in Fig. 3. The specimens were bent to the indicated permanent deflections by a uniform bending moment acting over a 10-in. span and were then straightened by reverse bending. The outer fiber strains in the bent conditions amounted to approximately 0.38% for the $^1/_8$-in. bend, 0.63% for the $^1/_4$-in. bend, 0.87% for the $^3/_8$-in. bend and about 1.11% for the $^1/_2$-in. bend. It can be seen that after the bend of $^3/_8$ in. and straightening, the yield point disappeared. The stress at 0.2% offset dropped from 34,600 psi for the hot-rolled material to 31,300 psi for that bent $^1/_2$ in. and straightened. The yield-point elongation for the hot-rolled material was about 1.5%. It appears likely that residual stresses produced by the flexing operation are responsible for lower initial yield stresses.

Osborn, Scotchbrook, Stout, and Johnston[8] conducted an extensive series of tests on $1^1/_4$-in.-thick plates of rimmed A-285 (formerly A-70) and silicon-aluminum killed A-201 steels to determine the effect of cold work on the tensile properties. Axial tensile strains of 1, 5, and 10% were applied, as well as an axial compressive strain of 1%. In addition, some specimens were strained 1% in tension in the direction perpendicular to the direction of subsequent testing. Tests were conducted after a standard elapsed time of five days with the objective of minimizing differences arising from aging. The present discussion of the results will be confined to tests of longitudinal specimens, i.e., those parallel to the rolling direction of the plate. The larger tensile prestrains raised the yield points of both materials very markedly. The prestrain of 5% resulted in an increase of about 27,000 psi, while the prestrain of 10% produced an increase of about 37,000 psi. A tensile strain of 1% in the rolling direction had practically no effect on the yield point of the A-201 steel but raised the yield point of the A-285 steel about 8000 psi. The compressive prestrain or the transverse tensile prestrain tended to lower the stress required to produce yielding in tension. This phenomenon, wherein a prior strain in one direction lowers the stress required to produce yielding under subsequent loading in the opposite direction, is known as the Bauschinger effect.

It can be seen, therefore, that no simple rules can be advanced for predicting the quantitative effects of small amounts of prior strain on initial yielding. The response varies with the manner in which the prior strain is produced, and also undoubtedly varies considerably with the extent of the yield-point elongation present in the original material. Qualitatively, it can be said that a tensile strain less than the yield-point elongation will have little effect on the lower yield point but may eliminate the upper yield point. If a prior tensile strain is greater than the yield-point elongation, the yield stress should be higher than that of the virgin material, and abrupt yielding may be replaced by gradual yielding. Small prior strains produced by compression, or by tension applied in a direction perpendicular to the direction of testing, tend to lower slightly the stress required for yielding (the Bauschinger effect). If compressive prestraining is continued to sufficiently high values, the tensile yield stress will rise above that of the original material as a result of strain hardening.[15] If the prior strain is produced by bending, so that residual stresses are set up, relatively small prior strains may result in gradual yielding and a lowering of the apparent stress at which yielding is initiated.

Stout and co-workers[8] state that with the exception of the 1% prestrain on the A-201 steel, all plastic prestrains raised the nominal maximum stress (tensile

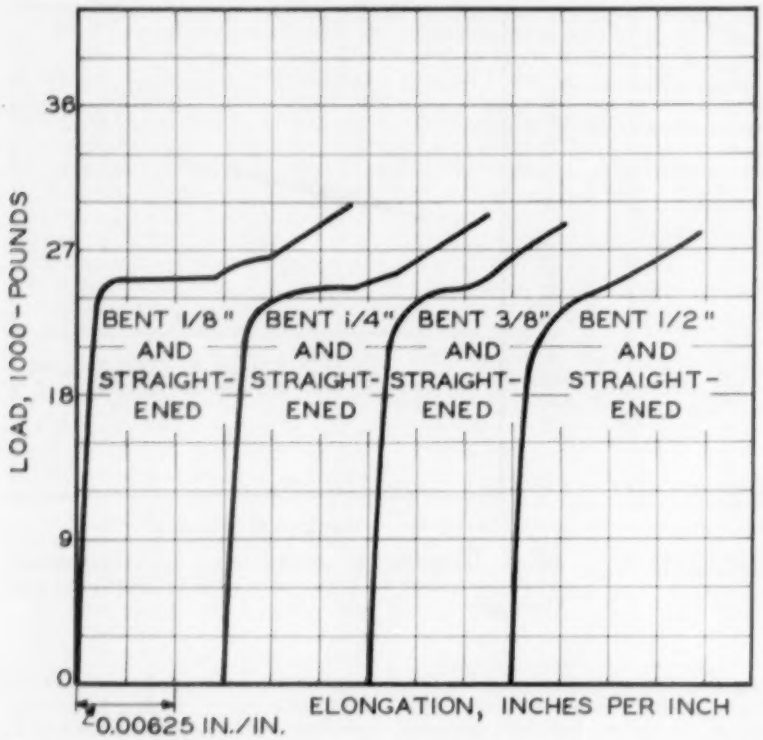

Fig. 3. Effect of bending and straightening on the initial yielding characteristics of 1/2-in. thick carbon-steel plate material

strength) in the tension test. The magnitude of the effect increased with increasing prestrain and amounted to about 8000 psi for prestrains of 10%. It appears that a large part of the reported increases in tensile strength can be accounted for by the fact that the tensile strength of the cold-worked material is computed on the basis of the new area after straining. Thus, an increase in tensile strength would be reported even though the maximum loads for specimens with and without prior cold work were identical. Strain aging between prestraining and final testing may have contributed slightly to the observed increases in tensile strength.

Effect of Cold Work on Ductility and Fracture Stress in the Tension Test

A. *Ductility.* Extensive investigations of the effects of prior straining on the ductility of steels in tension tests have been carried out. One type of experiment frequently conducted involves prestraining at a temperature above the range of temperature in which the transition from ductile to brittle behavior occurs, and then measuring the remaining ductility at some lower temperature. The simplest type of behavior can be illustrated as shown in Fig. 4*a*. The strain to fracture at Temperature 2 after prior straining at Temperature 1 decreases linearly with increasing prior strain. For example, if a strain is applied at Temperature 1 corresponding to 75% of the fracture strain at that temperature, then the additional strain at Temperature 2 before fracture will be 25% of the ductility that would have been observed at that temperature if there had been no prior strain at Temperature 1.

Under certain circumstances, however, quite complex effects resulting in the type of behavior illustrated in Fig. 4*b* may occur. For small prestrains, the ductility at Temperature 2 drops rather rapidly, but at somewhat higher prestrains begins to rise, passes through a maximum that may be considerably in excess of the value for no prestrain, and then decreases in a regular manner. The relative magnitudes of the changes in ductility that are observed as the prestrain is increased may vary considerably, and in some instances the initial drop in ductility at low prestrains may be hardly detectable. Since the deficiency of ductility at the lower prestrains can be partially eliminated by prior plastic flow, the behavior has been termed "rheotropic" embrittlement by Baldwin and co-workers.[9] While this type of behavior had been observed by other investigators,[10] the phenomenon has been subjected to extensive systematic study by Baldwin. An understanding of the mechanism of rheotropic effects on low-temperature behavior should be of value in developing a better understanding of the general problem of low-temperature embrittlement of ferritic steels. The practical implications of rheotropic embrittlement, however, are not as yet clear. Only a limited amount of work has been reported in which notched specimens have been used, and whether small amounts of cold work might under some circumstances actually improve notch toughness is problematical.

Geil and Carwile[11] have reported that rheotropic embrittlement of ingot iron is dependent upon the initial condition of the material. Prior straining in tension at room temperature improved the low-temperature ductility of hot-rolled or normalized ingot iron, whereas with annealed ingot iron, the opposite effect was observed. Recent work carried out by Gensamer[12] indicates that the rheotropic embrittlement behavior is related to the effect of prior strain upon the initial yielding behavior at the testing temperature. Small amounts of prestrain may eliminate the upper yield point at the subsequent testing temperature, thus causing yielding to occur at a lower stress and permitting a larger amount of plastic flow prior to fracture. At larger prestrains, the effect of strain hardening becomes predominant and the ductility decreases in a regular manner.

Another aspect of the effect of prior strain on ductility is illustrated by Bridgman's work on prior straining under high hydrostatic pressure.[13] Bridgman found that if a specimen was elongated in the presence of a high hydrostatic pressure, the ductility was very much greater than at atmospheric pressure. Furthermore, after prestraining under hydrostatic pressure, considerable ductility remained at atmospheric pressure even though the prior strain exceeded the original fracture strain at atmospheric pressure. Sachs[10] also discusses the different effects on ductility obtained by prestraining in tension, in

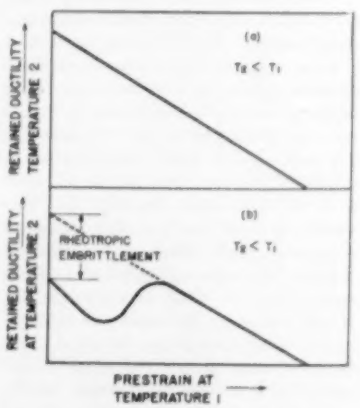

Fig. 4. Schematic illustration of rheotropic embrittlement

wire drawing, or in extrusion. The compressive stresses prevailing in the latter methods of deformation result in greater remaining ductility after a given amount of extension. These observations are mentioned only as a matter of general interest, inasmuch as it is believed that the variations in hydrostatic compression that would be encountered in plate-forming operations would be too small to result in significant effects of this type. Under some conditions, small amounts of prior compressive strain may tend to lower ductility because of a tendency to lower the fracture stress, as discussed in the following section.

B. *Fracture Stress.* In general, the breaking stress or fracture stress is affected by prior strain in much the same manner as yield stress. Fracture stress is quite difficult to study because it is a function of so many different variables. Perhaps the most straightforward studies of the effect of cold work on fracture stress have been those in which a prior strain is applied at room temperature and the final testing carried out at a low temperature at which very little ductility remains. Thus, strain at the low temperature does not tend to mask the effects of the prior strain at a higher temperature. It has been observed that under these conditions, increasing amounts of prior tensile strain result in an increasing fracture stress.[14] For prior straining in compression, McAdam has shown that the fracture stress at first decreases and then increases continuously with increasing compressive strain.[15] With regard to the effect of prior compressive straining, McAdam states: "The effect on the tensile fracture stress is similar to the effect on the tensile flow stress. The effect is the resultant of two factors, namely, a shift of the elastic range and a work-hardening effect." The shift of the elastic range referred to is the Bauschinger effect, described previously in this report. This observation is in accord with Zener's hypothesis,[16] also held by many others, that fracture in metals is always preceded by plastic flow at least on a microscopic scale, even though there may be very little, if any, outward evidence of ductility. Furthermore, it is presumed that so-called "brittle" fractures of steel are nucleated by stress concentrations resulting from the first microscopic traces of plastic flow. According to this view, therefore, prior straining in compression would be expected to at first lower the fracture stress, because plastic flow would be initiated at a lower stress as a result of the Bauschinger effect.

Effect of Cold Work on Notch Toughness

It is generally recognized that cold working impairs the ability of ferritic steels to resist the initiation of brittle fracture. In actual practice, the effects of strain aging are superimposed on the effects of the cold work. While the final toughness is of primary interest from the point of view of the suitability of the material for service, it is important to know the relative contributions of straining and of aging to the impairment of toughness, if steps are to be taken to design steels of improved overall resistance to the effects of cold work.

A number of different procedures have been employed in evaluating the effects of cold work on toughness. Not only has a variety of methods of introducing cold work into the material been employed, but also numerous types of test specimens have been employed. The significance of notch toughness tests and methods of evaluation of results of various tests have been discussed at length elsewhere[17–19, 37] and will not be reviewed in this report. It is now generally recognized that for the most information and least ambiguous results, tests to evaluate the effects of cold work on toughness must be conducted over a range of temperatures so that the transition temperatures for each condition to be studied can be determined. Tests conducted only at room temperature have been subject to misinterpretation in the past, even though a range of degrees of cold work was used. Unless otherwise indicated, attention will be directed herein primarily at the change in the so-called "ductility" transition temperature, which is considered to be intimately associated with crack initiation. It has been pointed out elsewhere[19] that the fracture transition temperature, or transition temperature based on fracture appearance, is usually not greatly affected by cold work, especially if the ductility transition temperature for the test under consideration is well below the fracture transition temperature for the virgin material. If the ductility transition temperature is about the same as the fracture transition temperature, then increasing amounts of cold work will tend to increase both transition temperatures at the same rate.

Straining in tension has been the most commonly employed method of introducing cold work for the purpose of evaluating the effects of cold work on notch toughness. This procedure has the advantage that a relatively large area of material can be strained at one time, thus providing a number of specimens with only one straining operation. Straining has also been carried out prior to testing for notch toughness by reduction as a result of rolling and by axial compression. The latter methods have the advantage that, with the exception of notching, individual impact specimens can be completely machined to final dimensions prior to straining. In this manner, the time interval between straining and testing can be kept to a minimum. Another method of straining involves the drawing of a tapered bar through a die, thus producing a continuous variation of cold work along the bar, the range of strain being determined by the taper.

Stout and co-workers[8] studied the effects of cold work on the notch toughness of 1¼-in.-thick plate material of A-285 steel and A-201 steel (the same two heats previously mentioned). The Charpy V-notch impact test and the Lehigh slow notch-bend test were used. Transition temperatures were evaluated on the basis of energy absorption, fracture appearance, and lateral contraction measured 1/32 in. below the base of the notch. For the evaluations of transition temperature based on energy absorption, the criterion used was the temperature at which the energy value was midway between minimum and maximum values. Similarly, for the evaluation based on lateral contraction, the criterion selected was the temperature at which the value of lateral contraction was midway between the minimum and maximum values. The fracture-appearance transition temperature was selected as the temperature corresponding to 50% fibrous fracture. A standard elapsed time of seven days after final treatment was employed for the Lehigh slow notch-bend test, while a period of ten days was used for the Charpy V-notch impact tests.

The increases in transition temperature resulting from the various straining treatments are summarized in Table 1. On the basis of energy absorption in the Charpy V-notch impact test, the A-285 steel exhibited a somewhat greater shift than did the A-201 steel. It was also observed that while the transition temperature of the A-201 steel was shifted progressively to higher temperatures with increasing amounts of tensile strain, that of the A-285 steel was shifted almost as much by 1% tensile strain as by 10%. The shifts observed after 10% strain were about 50° F for the A-201 steel and about 75° F for the A-285 steel. If a criterion of lateral contraction is used, the data appear somewhat inconsistent, but the shifts in transition temperature resulting from 5 and from 10% cold work were not greatly different for the two steels. In the Lehigh slow notch-bend test, the A-285 steel exhibited a considerably greater shift in transition temperature after 5% strain than did the A-201 steel, but after 10% strain the shifts were very similar for the two steels, amounting to about 80–90° F. Lehigh slow notch-bend tests were also conducted on 5/8-in.-thick plate material that had been strained 20% in tension from each of these two heats.[39] Again the two steels exhibited very similar

Table 1—Effects of Cold Work on Transition Temperatures of A-285 and A-201 Steels (1 1/4-in.-Thick Plates) in Charpy V-Notch Impact Tests and Lehigh Slow Notch-Bend Tests (Stout, et al)

	Increase in transition temperature (° F)			
	A-201		A-285	
Strain	Energy	Lateral contraction	Energy	Lateral contraction
Charpy V-notch impact test				
1% Compression	32	7	30	18
1% Tension	28	2	63	48
5% Tension	38	44	66	57
10% Tension	48	50	77	32
Lehigh slow notch-bend test				
1% Compression	...	45	...	43
1% Tension	...	27	...	10
5% Tension	...	38	...	90
10% Tension	...	81	...	90

shifts of transition temperature. An increase of about 81° F was observed for the A-201 steel, while that for the A-285 was about 89° F.

Compressive strains of 1% caused a shift in transition temperature in the Lehigh slow notch-bend test of about 45° F for both steels as compared with shifts resulting from 1% tensile strain of about 10° for the A-285 steel and 25° for the A-201 steel. In the Charpy V-notch impact test, on the other hand, the two methods of straining produced about the same shift in transition temperature for the A-201 steel, but tensile straining produced a larger shift than did compressive straining for the A-285 steel. Some of the seeming inconsistencies in the results for the material strained 1% may possibly be attributable to the difficulty of obtaining uniform deformation at such a low average strain level.

With regard to the over-all interpretation of the results, it is interesting to note that in the final summary of the five-year program at Lehigh University, Tör and Stout[21] state: "One simplification can be made at the outset of this discussion. The aluminum-killed A-201 and the rimmed A-285 steel responded to all of the simulated fabrication operations in essentially the same manner. The notch toughness of the A-285 was inherently lower than that of the A-201, but prestraining or welding or heat treatment altered both steels in the same direction and to about the same extent."

Klier, Wagner, and Gensamer[22] reported results of tests on a series of ship-plate steels in which the effects of axial tensile strains of 2, 5 and 10% on transition temperatures in the Charpy keyhole-notch impact test were determined. Average curves were drawn through the data and transition temperatures were selected at 25 and 50% of maximum energy absorption. In the following discussion, the values selected at 25% of maximum energy will be used inasmuch as this criterion is believed to correspond more closely than those selected at 50% to the ductility transition temperature as usually defined for the Charpy keyhole-notch impact test. The results are summarized in Table 2. For 2% strain, the reported shifts in transition temperature ranged from −10 to 45° F. (The two values of negative shift reported are not considered sufficiently great to be significant.) For 5% strain the shifts ranged from 25 to 55° F, and for 10% strain from 40 to 75° F. No consistent trends with steelmaking practice were discernible. One steel with higher than normal nitrogen (0.010%) exhibited a shift that was on the high side of the observed range; on the other hand, a similar steel with normal nitrogen exhibited just as large a shift in transition temperature. When it is considered that an individual transition temperature determination based on the number of specimens employed by Klier, Wagner, and Gensamer is probably uncertain to about ±20° F, at least part of the variation among results for the various steels can be attributed to experimental scatter. The time interval between straining and testing in the above tests was about one month. In order to explore the possibility of variations caused by room-temperature aging, another series of tests in which straining was performed by axial compression was conducted on two of the steels. The specimens were finish-machined, with the exception of notching, to dimensions selected so that the dimensions after straining would be within standard tolerances. This procedure permitted a transition curve to be determined within one hour after straining. Tests were conducted after a series of aging times ranging up to four weeks for two of the ship-plate project steels. While the data are somewhat inconsistent, there is an indication that for one of the steels an increase of 15 to 20° F in transition temperature accompanied the increase in aging time from one hour to four weeks. Inasmuch as no trend was found for the other steel tested, however, the results must be regarded as somewhat inconclusive. It would appear that for the particular steels tested by Klier, Wagner and Gensamer and for the number of tests used in establishing a transition curve, the effect of aging in shifting the transition temperature was no more than 15 to 20° F and was probably within the accuracy of the experiment. For the most precise separation of the effects of cold working and of strain aging following cold working, the time interval between straining and testing should be kept to a minimum and carefully controlled for the specimens that are not deliberately strain aged.

Table 2—Increases in Charpy Keyhole-Notch Transition Temperatures Resulting from Cold Working (in Tension) of Several Ship-Plate Steels (Klier, Wagner and Gensamer)

	Increase in transition temperature (° F)		
Steel*	2% Strain	5% Strain	10% Strain
A	40	55	60
Br	20	45	50
Bn	20	30	55
C	40	55	70
Dr	20	45	75
Dn	− 5	25	40
E	45	40	55
H	−10	25	40

* Designations used by Klier, Wagner and Gensamer.

Epstein[23] reported a series of tests on ship-plate steels in which the effects of straining in compression on the transition temperature in the Charpy keyhole-notch impact test were measured. The temperature corresponding to 20 ft-lb energy absorption was used as the criterion of transition temperature. Epstein tested material from several heats each of American Bureau of Shipping Classes A, B and C hull-plate steel. The carbon and manganese contents are not specified for Class A steel, but usually average about 0.23% C and 0.45% Mn. This steel is used in plates up to 1/2 in. in thickness. In Class B steel, which is used in plates over 1/2 in. and up to 1 in. thick, the carbon content is limited to 0.23% max and the manganese content is from 0.60 to 0.90%. Class C steel is used in plates over 1 in. in thickness. It contains a maximum of 0.25% carbon, 0.60 to 0.90% manganese, and 0.15 to 0.30% silicon and is made by fully aluminum-killed, fine-grain practice. For the purpose of the tests conducted by Epstein, commercial plates of all three grades were rolled to 3/4-in. thickness. No information is given regarding the time interval between straining and testing.

Epstein's results are summarized in Table 3. It can be seen that each grade exhibited about the same shift in transition temperature as a result of straining. The average increases in transition temperature produced by 5% compression were 58, 53 and 52° F for Classes A, B and C, respectively. The average shifts produced by 10% compression were 65, 62 and 63° F for Classes A, B and C, respectively. Thus, on the basis of these data, there do not appear to be significant differences in the response of these three grades of steel to cold work. It should be noted, of course, that the initial transition temperatures prior to cold working are significantly different for the three types of steel as tested by Epstein. The average transition temperatures of the material before straining as reported by Epstein are +26, −1 and −39° F for Classes A, B and C, respectively. Since the shifts in transition temperature produced by cold work were almost the same for all three steels, the differences among the transition temperatures after cold working will be the same as before cold working.

Table 3—Effects of Cold Work (by Compression) on the Transition Temperatures in Charpy Keyhole-Notch Impact Tests of Plates of ABS Classes A, B and C Steel* (Epstein)

		Increase in transition temperature (° F) after 5% strain		*Increase in transition temperature (° F) after 10% strain*	
Steel	*Number of plates tested*	*Range*	*Average*	*Range*	*Average*
A	5	53–66	58		
	4			54–70	65
B	1		53		
	3			48–72	62
C	2	52–52	52		
	2			56–70	63

* All plates rolled to $^3/_4$-in. thickness for comparative purposes.

Markus and Armiento[24] investigated the effect of cold work on the notch toughness of a 1030 cartridge case steel, which contained 0.27% C and 0.64% Mn and was aluminum-killed. Cold rolling was used as a method of straining, with the time interval between straining and testing being held constant at 30 days. The material was tested in the four following conditions that were produced by variations in heat treatment: (1) spheroidized, fine-grained; (2) spheroidized, coarse-grained; (3) pearlitic, fine-grained; and (4) pearlitic, coarse-grained. The test specimen employed was a Charpy-type impact test specimen with a notch root equivalent to that of the keyhole-notch specimen but with the notch machined by a U-shaped milling cutter rather than by drilling and slotting. Transition temperatures were selected at the highest temperature at which a brittle fracture (low-energy absorption) was obtained. Usually groups of five specimens were broken at 5° F temperature intervals in the vicinity of the transition temperature. Curves illustrating the effect of various amounts of cold work on the transition temperatures selected in the indicated manner are shown in Fig. 5. It can be seen that the transition temperatures increase more rapidly at low strains. For three of the conditions, the curves very nearly parallel one another. The fine-grained, spheroidized material, however, shows somewhat smaller increases in transition temperature with increasing cold work than do the other three materials. It is interesting to note that at 10% strain the average increase in transition temperature for these materials amounts to slightly more than 50° F, agreeing well with values observed by Klier, Wagner and Gensamer as well as by Epstein for different methods of straining.

On the basis of the foregoing analysis, it appears that, for open-hearth steels having compositions in the range of 0.15 to 0.30% C and 0.40 to 0.90% Mn, a strain of about 10% results in an increase of transition temperature in the Charpy keyhole-notch test of about 50 to 70° F.

Limited data indicate that capped or semikilled bessemer steel may undergo a much greater increase in transition temperature when cold worked, because of the combination of high phosphorus and high nitrogen. In one experiment,[25] cold rolling 10% increased the transition temperature of a semikilled bessemer steel containing 0.15% C and 0.45% Mn by about 150° F in the Charpy keyhole-notch impact test. Because of the high nitrogen content, this steel may have aged appreciably in even a short period at room temperature after straining and before testing.

Limited information suggests that steels having a tempered martensitic microstructure may be less susceptible than pearlitic steels to a decrease of notch toughness as a result of cold work. In tests of material from two heats of "T-1" steel, which is a low-carbon quenched-and-tempered alloy steel,[26] increases of 35 and 20° were observed after 10% strain produced by cold rolling.[27] Material from a $^1/_2$-in.-thick plate of AISI 4815 ($3^1/_2$% Ni, 0.25% Mo) steel, that had been quenched and tempered, exhibited an increase of 28° F after similar straining, but an increase of about 100° F in the normalized and tempered condition.[28] Work currently in progress under the auspices of the Materials Division of PVRC on higher strength steels (at 50,000, 70,000 and 90,000 psi yield point levels) will add to the fund of information on the effects of cold work on notch toughness.

The methods of straining discussed up to this point have been of such a nature that the strains produced were essentially uniform throughout the specimen. Cold work introduced in actual forming operations, on the other hand, is more likely to vary from point to point in a manner determined by the contour being formed and the method of forming. For example, in a cylindrical bend, the strains will vary from a tensile value on the convex side of the bend to a compressive value on the concave side. For a given plate thickness, the maximum values of strain depend on the radius of the bend, being larger for smaller radii. The question naturally arises as to what effect the type of cold work introduced in actual forming operations has on notch toughness. Only a limited amount of work aimed at clarification of this problem has been reported.

Stout and co-workers[29] studied the effects of cylindrical bending using a modified version of the Lehigh slow notched-bend test specimen. A cylindrical bend was introduced in the specimen in such a way that a tensile strain of 5% was obtained at a depth of 0.08 in. below the surface. This depth corresponded to the depth of the Izod notch which was machined after bending. The testing procedure was the same as for the Lehigh slow notch-bend test. Transition temperatures determined in this manner for the A-285 and A-201 steels, which were mentioned previously in connection with the Lehigh program, agreed within experimental error with values obtained using specimens axially strained 5% in tension.

The effects of spherical pressing were also studied in the Lehigh program.[29] For this purpose a special specimen and testing jig were developed. Circular plates $^3/_8$ in. thick and 16 in. in diam of A-285 and A-201 steels were both cold pressed and hot pressed to a spherical radius of 16 in. A circular V-notch, 0.12 in. deep was machined at a radius of $2^1/_4$ in. after completion of the forming operation. During testing, the central portion of the specimen bounded by the notch was supported, and a load was applied around the periphery of the specimen so that the root of the notch

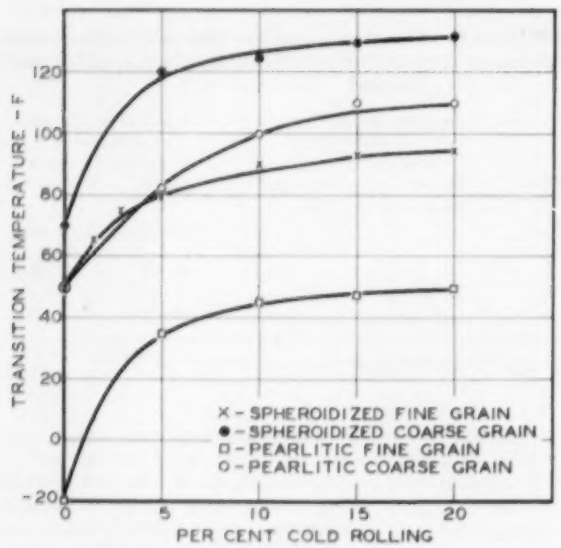
TRANSITION TEMPERATURE - F
PER CENT COLD ROLLING
X - SPHEROIDIZED FINE GRAIN
● - SPHEROIDIZED COARSE GRAIN
□ - PEARLITIC FINE GRAIN
○ - PEARLITIC COARSE GRAIN

Fig. 5. Effect of cold work on the transition temperature of a 1030 cartridge-case steel in the Charpy keyhole-notch impact test (Markus and Armiento[24])

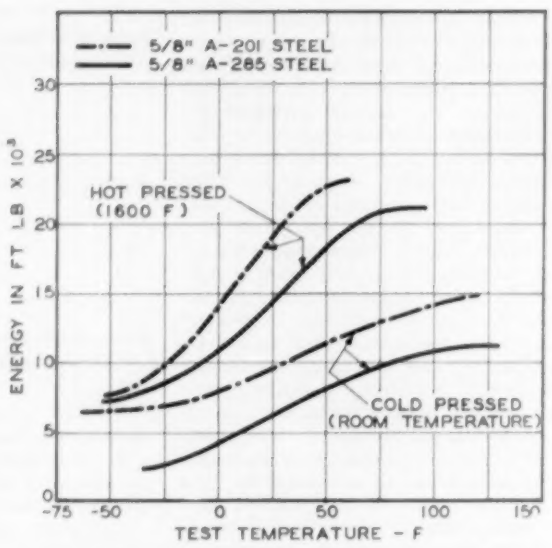

Fig. 6. Effect of cold pressing on the transition from tough to brittle behavior of 16-in. radius spherical heads of A-285 and A-201 steels (Stout[29])

was placed in tension. Total energy to fracture was recorded and used in constructing the transition curves shown in Fig. 6. It is clear that in this test cold pressing shifted the transition curves to higher temperatures, in addition to lowering the ability of the material to absorb energy at any particular temperature. Unfortunately, insufficient testing was conducted to permit correlation of results of this test with results of other tests conducted in the Lehigh program.

At this juncture, it should be pointed out that, although a great deal of attention has been directed toward the effects of strain aging on notch toughness, surprisingly little work has been carried out in an effort to evaluate the effects of prolonged aging at atmospheric temperatures. Although strain aging is not to be discussed at length in this report, it should again be indicated that the property changes discussed up to this point are essentially the effects of cold working alone, with at most a few days of aging at room or atmospheric temperatures. Most studies of the effect of aging on toughness have made use of elevated temperature aging treatments. While such experiments indicate the effects to be expected from heating at the selected temperatures, the effects that would result from prolonged atmospheric temperature aging are not necessarily revealed. Smith and Garofalo[28] studied the effect of aging at 75° F after straining 10% in tension for exposure times ranging from 1 hr to 25,000 hr for three steels indicated in Table 4. A Charpy V-notch specimen of one-half standard width (parallel to notch axis) was used. Energy absorption vs. temperature curves for various aging times at 75° F are shown in Fig. 7. Transition temperatures were selected at the 10 ft-lb level. For steels A and B, a shift of from 25–30° F was produced by an increase of aging time from 5 hr to 25,000 hr. For steel C, the transition temperatures for the cold-worked and aged conditions were above room temperature and it is likely that aging occurred during testing. Aging was also carried out at 450° F for times up to 25,000 hr. In Table 4 the maximum shifts in transition temperature after aging at the two temperatures are indicated. In every instance, aging at 450° F produced a much larger increase in transition temperature than did aging at 75° F. Furthermore, for steels A and B, the increase resulting from 5 hr aging at 450° F was greater than the increase produced by 25,000 hr at 75° F.

Effect of Prior Strain on the Performance of Weldments

When a weld is made on a cold-worked plate, the properties of the cold-worked base material will be altered throughout the zone in which the temperature is raised by the heat of welding. The change at any particular location will depend on the time-temperature cycle experienced by the material in that location. In much of the heated zone the notch toughness will be impaired as a result of strain aging. The changes so produced will contribute to the performance of the weldment as a whole in a manner depending on the extent of the changes and the volumes of metal affected. Stout and co-workers[29] conducted Lehigh slow notch-bend tests on a series of A-285 and A-201 steels that had been strained 5% in tension prior to welding. The results of tests on these specimens are compared in Fig. 8 with results of tests on welded but un-

Table 4—Maximum Increase in Transition Temperature (Modified V-Notch Charpy Test) After Straining 10% in Tension and Aging at 75 or 450° F for Three Carbon Steels (Garofalo and Smith)

		Chemical composition							*Maximum increase in transition temp. After straining and aging*	
							Acid sol.			
Steel	*Melting practice*	*C*	*Mn*	*P*	*S*	*Si*	*Al*	*N*	*75° F*	*450° F*
A	Liquid metal deoxidized with silicon and aluminum	0.25	0.56	0.017	0.028	0.13	0.013	0.011	86	112
B	Open hearth, capped	0.07	0.43	0.006	0.026	0.007	0.005	0.005	73	116
C	Bessemer, capped	0.08	0.47	0.075	0.032	0.012	0.006	0.016	147	209

strained specimens. It can be seen that the transition temperature (based on percent lateral contraction) for material strained prior to welding was higher than for material unstrained prior to welding. Loss of toughness in cold-worked zones heated by welding contributed to an overall loss of toughness of the specimen as a whole. The increase in transition temperature so produced, however, was much less than that produced by welding alone, relative to the transition temperature of unwelded material.

Effects of Heating Cold-Worked Material

As mentioned earlier, cold-worked metals are not stable. The properties tend to change with time, the rate of change being faster the higher the temperature. Cold-worked ferritic steels tend to strain age at atmospheric and moderately elevated temperatures. As discussed in previous interpretive reports, strain aging tends to produce a further increase in strength and a further loss of ductility and toughness above and beyond that produced by cold work alone.

Another process, known as recrystallization, also tends to occur in all cold-worked metals.[21] The individual grains or crystals of a polycrystalline metal are distorted by cold work to an extent depending upon the nature and degree of cold working, and become considerably harder as a result of strain hardening. Furthermore, a system of residual stresses is set up on a microscopic scale in addition to any macroscopic residual stresses that may have been produced. If a cold-worked metal is heated to a sufficiently high temperature, or held for a sufficiently long time at somewhat lower temperatures, recrystallization occurs, i.e., new strain-free grains are formed and begin to grow. For a given degree of cold work, the time required for complete recrystallization depends on temperature, being shorter the higher the temperature. The changes in properties brought about by recrystallization are in the direction of restoration of the original properties. The final properties of the recrystallized material may not be identical to those of the original material, however, because the grain size of the recrystallized material may differ from that of the original material.

Cold working has been defined earlier by implication as deformation under conditions such that strain hardening occurs. A definition can also be stated in terms of recrystallization, i.e., that cold work is plastic deformation carried out under conditions such that recrystallization does not occur as the material is being deformed. Hot work, on the other hand, is deformation carried out under conditions such that recrystallization occurs as the metal is being deformed.

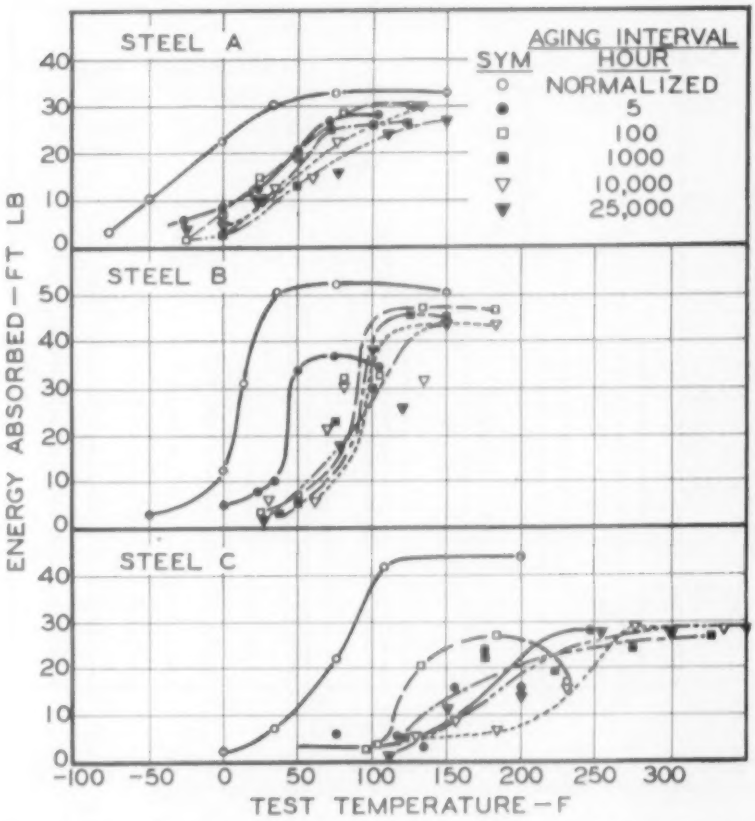

Fig. 7. Effect of straining in tension and aging at 75° F on the transition from tough to brittle behavior (modified V-notch Charpy test) for three carbon steels (Garofalo and Smith[29])

Prior to the onset of actual recrystallization, a process known as recovery occurs, which may result in changes in some properties prior to the rapid softening accompanying the formation of new strain-free grains. Recovery is associated with the relaxation of microscopic residual stresses. A slight decrease in hardness may accompany recovery, but more noticeable changes are manifested as an increased proportional limit, decreased damping capacity, decrease in electrical resistivity, and other changes in physical properties.

The processes of recovery and recrystallization are of especial interest in their relationship to changes in properties that might occur upon heating cold-worked steel, for example, in the range of temperatures customarily used in stress relieving. The question naturally arises: Can the deleterious effects of cold work be removed by heating?

From a knowledge of the changes that occur during recrystallization, it would appear that the only certain method of removing the effects of cold work would be to bring about complete recrystallization of the material. Whether the notch toughness of the recrystallized material would be better than that of the original material would depend on the relative hardnesses and grain sizes. Under some conditions, for example in the recrystallization of very lightly cold-worked material, exaggerated grain growth may occur, so that the final grain size is a great deal larger than that of the original material, thereby partially offsetting the improvement brought about by recrystallization. Normalizing would be expected to eliminate the effects of cold work in that, not only would recrystallization and relief of cold-working effects occur on heating to the normalizing temperature, but also a completely new set of ferrite grains would be formed as the austenite existing at the normalizing temperature is transformed upon cooling.

Stout and co-workers investigated the effect of reheating cold-worked material for 1 hr at 500, 800, 1150 and 1600° F on various properties, including notch toughness as measured in the Lehigh slow notch-bend test.[8] Typical results are shown in Fig. 9, which illustrates the behavior of $1^1/_2$-in. A-201 steel. The criterion of percent lateral

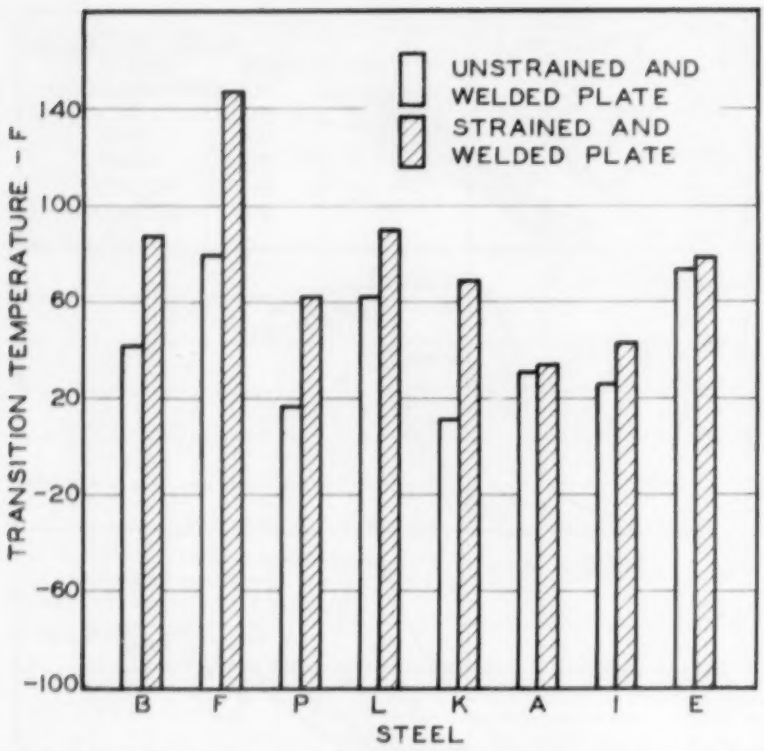

Fig. 8. Effect of prior strain on the transition temperatures for a group of welded A-285 and A-201 steels in the Lehigh slow notch-bend test (Stout[30])

contraction was used in evaluating transition temperatures. It can be seen that the maximum increase in transition temperature occurred at 800° F. The increased transition temperatures at 500 and 800° F can be attributed to strain aging. The transition temperatures observed after heating at 1150° F are almost the same as for the cold-worked material. A similar observation was made by Smith and Garofalo[29] on the steels listed in Table 4 after heating 10 hr at 900° F or 2 hr at 1200° F. This behavior might be attributed either to the possibility that strain aging is not occurring in this temperature range or to the possibility that the effects of strain aging are alleviated by changes associated with recovery. Examination of the steels indicated that recrystallization had not occurred. It is interesting to note that the yield stress of the Lehigh A-201 steel cold worked 5% drops from 58,800 psi to 49,400 psi as a result of heating at 1150° F. The corresponding change in the material cold worked 10% was from 68,600 psi to 46,800 psi, strongly suggesting that recovery or incipient recrystallization has indeed occurred. More pronounced effects are evident in results of the notch toughness tests[29] conducted on $^5/_8$-in. plates strained 20%, and heated for 1 hr at 1150° F. In the Lehigh slow notch-bend test, the transition temperature (on basis of percent lateral contraction) of the A-201 material was raised from −93 to −12° F by 20% strain, but was lowered from −12 to −34° F by heating at 1150° F after cold working. The response of the A-285 steel was even more pronounced, the transition temperature after treatment at 1150° F being about the same as that of unstrained material. The transition temperature was raised from −46 to +43° F by 20% strain, and was lowered to −56° F by heating at 1150° F.

Other limited data indicate that recovery possibly exerts a significant effect on notch toughness and in some instances may permit almost complete recovery of the notch toughness of the original material. In Table 5 are shown results of Charpy keyhole-notch impact tests on three steels: "T-1" steel,[27] quenched-and-tempered AISI 4815, and normalized-and-tempered 2315.[28] It can be seen that in every instance the transition temperature of the cold-worked material is very markedly lowered by heating at 1050° F. On the basis of other tests, recrystallization is not believed to have occurred in these treatments. While it is not possible to advance an explanation at this time for the more pronounced response of these materials to heating, it may be significant that all of these steels have very fine ferritic grain sizes. It is known that for a given amount of cold work, fine-grained metals recrystallize more rapidly or will recrystallize at a lower temperature than coarser-grained material. It seems possible that changes associated with recovery also occur more rapidly in fine-grained material.

Table 5—Effect of Heating for One Hr at 1050° F After 10% Strain on the Charpy Keyhole-Notch Transition Temperature for Three Alloy Steels

Steel	*Initial transition temperature*	*Transition temperature After 10% strain*	*Transition temperature After straining 10% and heating for 1 hr at 1050° F*
"T-1," heat A	−175	−155	−180
"T-1," heat B	−255	−222	−273
AISI 4815 (3.5% Ni, 0.25% Mo) (quenched and tempered)	−275	−247	−263
AISI 2315 (3.5% Ni) (normalized)	−250	−157	−220

Effect of Cold Work on Elevated Temperature Properties

The increase in strength at atmospheric temperature produced by cold working has already been discussed. At moderately elevated temperatures the increased strength will be retained and may be augmented by strain aging. As the temperature is further increased, however, the processes of recovery and recrystallization come into play and the contribution of cold work begins to be lost. Since the temperature at which recovery and recrystallization proceed at an appreciable rate depends on the amount of cold work, it follows that for a particular service temperature there will be an optimum degree of cold work with respect to the increased strength that can be realized.[22] This principle is illustrated in Fig. 10[23] for a high-temperature alloy, N 155.* Creep rates were determined at 1200° F under a stress of 50,000 psi after various amounts of reduction at 80° F by cold rolling. It can be seen that a minimum in the creep-rate curve occurs at about 25% reduction.

Effect of Cold Work on Fatigue

The significance of fatigue in the service performance of pressure vessels is discussed by Dolan in the interpretive

* The nominal composition of N 155 is 20% Cr, 20% Ni, 20% Co, 3% Mo, 2% W, 1% Cb, 1% N, bal. Fe.

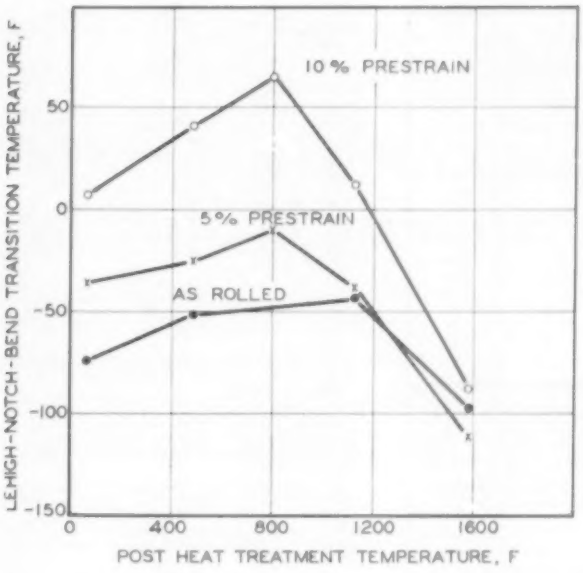

Fig. 9. Effect of heating after prior tensile strain on the transition temperature of A-201 steel in the Lehigh slow notch-bend test (Stout[8])

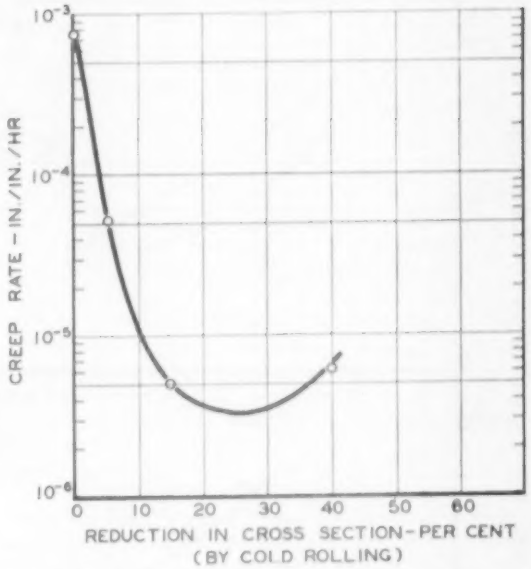

Fig. 10. Effect of cold work on the creep rate of N-155 alloy under 50,000 psi at 1200° F (Frey and Freeman[22])

report "Fatigue as a Factor in Pressure Vessel Design."[24] In a discussion of the basic features of fatigue behavior, it is pointed out that for ferritic steels a "fatigue limit" exists, i.e., there is a stress below which the material will not fail in fatigue even though the stress cycle is repeated indefinitely. As the stress is raised above the "fatigue limit," the lifetime decreases, with lifetime of several million cycles generally being observed at stresses only slightly above the endurance limit. Lifetimes of primary interest in connection with pressure vessels are of the order of 100,000 cycles and less, since it is not likely that a greater number of pressure cycles would be experienced in the lifetime of most vessels. The stresses corresponding to these lifetimes would generally be in the plastic region, at least in the early stages of cycling. Most of the work on fatigue of steels, on the other hand, has been concerned with the effect of different variables on the "fatigue limit" or the stresses corresponding to very long lifetimes. It is very well known, for example, that cold working raises the fatigue limit and that in steels susceptible to strain aging still further strengthening accrues from aging. Surface peening or cold rolling is commonly used to strengthen machine parts to be subjected to large numbers of cyclic stress application. A double benefit results from these treatments in that surface compressive stresses are set up in addition to the increased strength resulting from cold working.

In the range of lifetimes of concern in pressure vessel service, only recently has the fatigue problem been intensively studied, and work in this field is still in progress under the sponsorship of the Pressure Vessel Research Committee. Stout and co-workers[25,26] have reported limited data as shown in Fig. 11 on the effect of cold work on the fatigue of A-201 and A-302 steels in the plastic region. Some increase in lifetime is observed as a result of 10% prestrain for the A-201 steel. For the A-302 steel, however, an increased lifetime was noted only at the lowest strain amplitude of slightly under 0.50%.

Conclusion

In conclusion it should again be emphasized that, from the practical point of view of material performance in a completed pressure vessel, the effects of cold work must be considered to include not only the direct and immediate changes, but also the subsequent changes for which the material is conditioned when cold worked. If logical steps are to be taken to minimize undesirable effects it is obviously important to understand the contributions to the overall change that are made by all the factors involved.

Some of the more important gaps in existing information can be summarized as follows:

1. Most of the studies of the effect of strain aging on notch toughness have been concerned with elevated-temperature aging. While elevated-temperature aging is naturally of great importance when cold-worked steels are subjected to elevated temperatures in subsequent fabrication operations, it is also of importance to know more about the effects produced by atmospheric-temperature aging. Changes in properties produced by elevated-temperature aging for short times are not necessarily the same as those produced by extended atmospheric-temperature aging. In instances where stress relieving is not used and elevated service temperatures are not encountered, the notch toughness of cold-worked steel in service will be established by the combined effects of cold work, *per se*, and aging at atmospheric temperature. It would appear worthwhile to study the relationship between notch toughness and time of aging at atmospheric temperature for a number of widely used pressure-vessel steels. Not only would the results be of interest from a practical point of view, but also a better basis for setting up accelerated aging tests for simulating atmospheric-temperature aging would be provided.

2. The metallurgical changes occurring in cold worked steels in the range of customarily used stress-relieving temperatures and their effects on notch toughness are not well understood. While it appears that normalizing is the only certain way of restoring the original toughness of the material prior to cold working, heating at temperatures that would be encountered when stress-relieving in the temperature range of 1000° F and slightly above may be very beneficial under certain circumstances. Since in a few instances heating in this range appears to restore almost completely the original notch toughness, it is believed that the metallurgical factors influencing changes in this temperature region for pressure-vessel steels would be worthy of study.

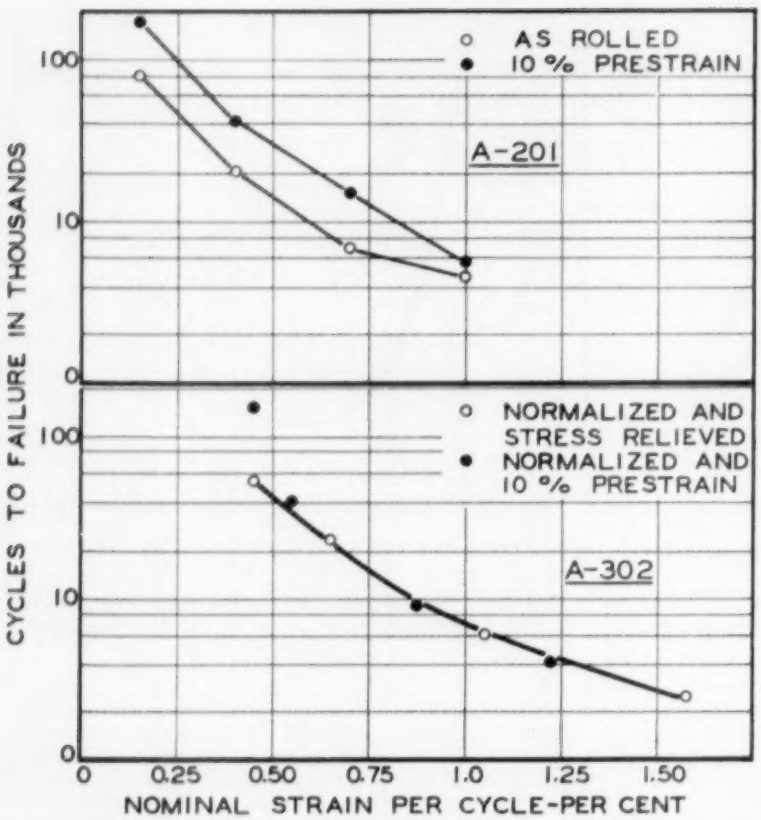

Fig. 11. Effect of prior strain on the plastic fatigue resistance of A-201 and A-302 steels (Stout[35,36])

3. Information on the effect of microstructure on the change in notch toughness produced by cold working is rather meager. With the current interest in the use of higher strength steels in pressure vessel construction, this question becomes one of practical interest. A systematic study of the effects on the response to cold work of variations in microstructure deliberately produced by control of heat treatment would be of value.

4. A better correlation of the effects of cold work produced in actual forming operations and effects of cold work produced by homogeneous straining in the laboratory would be very desirable. What are the amounts of cold work that are of primary interest? How does a non-uniform distribution of strain through the thickness of a plate affect the resistance of that plate to the propagation of a crack? Can the effect be adequately predicted from laboratory tests?

Acknowledgment

The many valuable suggestions and criticisms made by the author's associates in the Research and Technology Division of United States Steel Corporation and by various members of the Pressure Vessel Research Committee are hereby gratefully acknowledged. Mr. F. E. Foster of the Riley Stoker Corp. acted as Coordinator for this report; his guidance in preparing the revisions is greatly appreciated by the author.

References

The following list of references is provided for those readers interested in more detailed information regarding investigations referred to in the body of the report. References 1, 6, 8, 10, 21, and 29 are especially recommended for further reading in this general field.

1. Thielsch, Helmut, "Strain Aging of Pressure Vessel Steels," THE WELDING JOURNAL, **30,** Research Suppl., 283-s to 290-s (1951).

2. Mehringer, F. J., and MacGregor, C. W., "Effects of Cold Rolling on the True Stress-Strain Properties of a Low-Carbon Steel," *Trans. AIME*, **162,** 291–309 (1945).

3. Nadai, A., *Theory of Flow and Fracture of Solids*, McGraw-Hill Book Co., (1950).

4. Jackson, L. R., and Lankford, W. T., "The Experimental Exploration of Plastic Flow in Sheet Metals," Symposium on Plasticity and Creep of Metals, American Society for Testing Materials Special Technical Publication No. 107, 3 to 12 (1949).

5. Jackson, L. R., "Work Hardening and Rupture in Metals," *Trans. AIME*, **171,** 622–637 (1947).

6. Low, John R., Jr., "How Plastic Deformation Influences Design and Forming of Metal Parts," Welding Research Council Bulletin Series, No. 5 (1950).

7. Unpublished Research, United States Steel Corp.

8. Osborn, C. J., Scotchbrook, A. F., Stout, R. D., and Johnston, B. G., "Effect of Plastic Strain and Heat Treatment," THE WELDING JOURNAL, **28,** Research Suppl., 337-s to 353-s (1949).

9. Ripling, E. J., and Baldwin, W. M., Jr., "Rheotropic Embrittlement of Steel," *Trans. ASM*, **43,** 778–805 (1951).

10. Sachs, George, "Effect of Strain on Fracture," *Seminar on Fracturing of Metals, ASM*, 51–67 (1948).

11. Geil, G. W., and Carwile, N. L., "Effect of Strain-Temperature History on the Flow and Fracture of Ingot Iron at Low Temperatures," *Journal of Research, National Bureau of Standards*, **48,** 399–406 (1952).

12. Gensamer, M., Private communication.

13. Bridgman, P. W., *Studies in Large Plastic Flow and Fracture*, McGraw-Hill Book Co. (1952).

14. Hollomon, J. H., and Zener, C., "Conditions of Fracture of Steel," *Trans. AIME*, **158,** 283–296 (1944).

15. McAdam, D. J., Jr., Geil, G. W., and Jenkins, W. H., "Influence of Plastic Extension and Compression on the Fracture Stress of Metals," *Proceedings of ASTM*, **47,** 554–567 (1947).

16. Zener, Clarence, "The Micro-Mechanism of Fracture," *Seminar on Fracturing of Metals, ASM*, 3–31 (1948).

17. Armstrong, T. N., Kahn, N. A., and Thielsch, Helmut, "Transition from Ductile to Brittle Behavior in Pressure Vessel Steels," THE WELDING JOURNAL, **31,** Research Suppl., 371-s to 380-s (1952).

18. Pellini, W. S., "Evaluation of the Significance of Charpy Tests," "Symposium on Effect of Temperature on the Brittle Behavior of Metals with Particular Reference to Low Temperatures," ASTM Special Technical Publication No. 158 (1954).

19. Vanderbeck, R. W., and Gensamer, M., "Evaluating Notch Toughness," THE WELDING JOURNAL, **29,** Research Suppl., 37-s to 48-s (1950).

20. Tör, S. S., Stout, R. D., and Johnston, B. G., "Further Tests on Effects of Plastic Strain and Heat Treatment," *Ibid.*, **16,** Research Suppl., 576-s to 584-s (1951).

21. Tör, S. S., and Stout, R. D., "Investigations of Effect of Fabrication Operations upon Pressure Vessel Steels," Welding Research Council Bulletin Series, No. 11 (1952).

22. Klier, E. P., Wagner, F. C., and Gensamer, M., "The Correlation of Laboratory Tests with Full Scale Ship Plate Fracture Tests," THE WELDING JOURNAL, **27,** Research Suppl., 71-s to 96-s (1948).

23. Epstein, Samuel, "Notch Resistance of Carbon Steel Ship Plate," AISI Technical Committee Activities, 139–181 (1951).

24. Markus, H., and Armiento, D. F., "Mild Steel May be Subject to Unexpected Shock Failure," Machine Design, 123–126, November, 1946.

25. Unpublished research, United States Steel Corp.

26. Bibber, L. C., Hodge, J. M., Altman, R. C., and Doty, W. D., "A New High-Yield Strength Alloy Steel for Welded Structures," *Trans. ASME*, **74** (3), 269–285 (1952).

27. Doty, W. D., "The Properties and Characteristics of a Quenched and Tempered Steel for Pressure Vessels," THE WELDING JOURNAL, **34,** Research Suppl., 425-s to 441-s (1955).

28. Unpublished research, United States Steel Corp.

29. Garofalo, F., and Smith, G. V., "The Effect of Time and Temperature on Various Mechanical Properties During Strain Aging of Normalized Low Carbon Steels," *Trans. ASM*, **47,** 957–983 (1955).

30. Scotchbrook, A. F., Eriv, L., Stout, R. D., and Johnston, B. G., "Effect of Welding on Pressure Vessel Steels," *Trans. ASME*, **72,** 539–548 (1950).

31. Mehl, Robert F., "Recrystallization," Metals Handbook, *ASM*, (1948).

32. Smith, G. V., "Metallurgical Effects on High Temperature Properties of Metals," Proceedings for Short Course—High Temperature Properties of Metals, Pennsylvania State University, 61–77 (1954).

33. Frey, D. N., and Freeman, J. W., "Fundamental Effects of Cold Working on the Creep Resistance of an Austenitic Alloy," *Trans. AIME*, **191,** 755–760 (1951).

34. Dolan, T. J., "Fatigue as a Factor in Pressure Vessel Design," THE WELDING JOURNAL, **33,** Research Suppl., 265-s to 275-s (1954).

35. Gross, J. H., Tsang, S., and Stout, R. D., "Factors Affecting Resistance of Pressure Vessel Steels to Repeated Overloading," *Ibid.*, **32,** Research Suppl., 23-s to 30-s (1953).

36. Gross, J. H., Gucer, D. E., and Stout, R. D., "The Plastic Fatigue Strength of Pressure Vessel Steels," *Ibid.*, **33,** Research Suppl., 31-s to 39-s (1954).

37. Pellini, W. S., "Notch Ductility of Weld Metal," Interpretive Report, Welding Research Council, to be published in THE WELDING JOURNAL, Research Suppl., May, 1956.

INERT SHIELDING GASES FOR WELDING ALUMINUM

Shielding gas containing 50–65% helium, balance argon found to be superior to argon, helium, or other mixtures of argon and helium for both tungsten-arc and consumable-electrode welding of aluminum

BY J. D. DOWD

Introduction

In little more than a decade, the inert-gas-shielded arc-welding processes have almost completely displaced all others for welding aluminum. During this time, much has been written concerning the nature of the arc in argon, helium, and mixtures of argon and helium.[1–8] Little has been published, however, showing the effect of inert gas composition on such practical considerations as ease of welding, porosity in welds, susceptibility to hot-short cracking during welding, deposition rate, and welding costs. The results of an investigation conducted at Aluminum Research Laboratories to obtain such information are presented in this paper.

Porosity in Consumable-Electrode Welds

Weld porosity is probably the most serious problem in the consumable-electrode welding of aluminum. It was, therefore, the first factor considered in evaluating the effect of shielding-gas composition. In this evaluation, overhead, multipass welds were used so as to obtain maximum porosity. The welds were deposited in $^5/_8$ in. diam x $^5/_{16}$ in. deep longitudinal grooves machined in $^1/_2$ x 6 x 12-in. plates of annealed 5052 alloy using a $^3/_{32}$ in. diam 5154 inert gas electrode. Immediately prior to welding, the plates were caustic etched and wire brushed, and the electrodes were caustic etched.

The welding procedure consisted of running down-hand test welds to establish the equipment settings required to obtain the desired voltage, current, travel speed and gas flow. The overhead welds were then run, using automatic controls to maintain constant voltage and travel speed. The arc current, arc voltage, and welding time were recorded on appropriate meters. The gas flow, travel speed, ease with which the filler metal flowed and wetted the plate, and any pertinent observations were also noted.

The equipment used was a welding machine equipped with a consumable-electrode torch, all of which were mounted on an automatic travel carriage. Reverse polarity direct current was supplied by a 400-amp welding rectifier. The argon and helium flows were controlled by metering regulators.

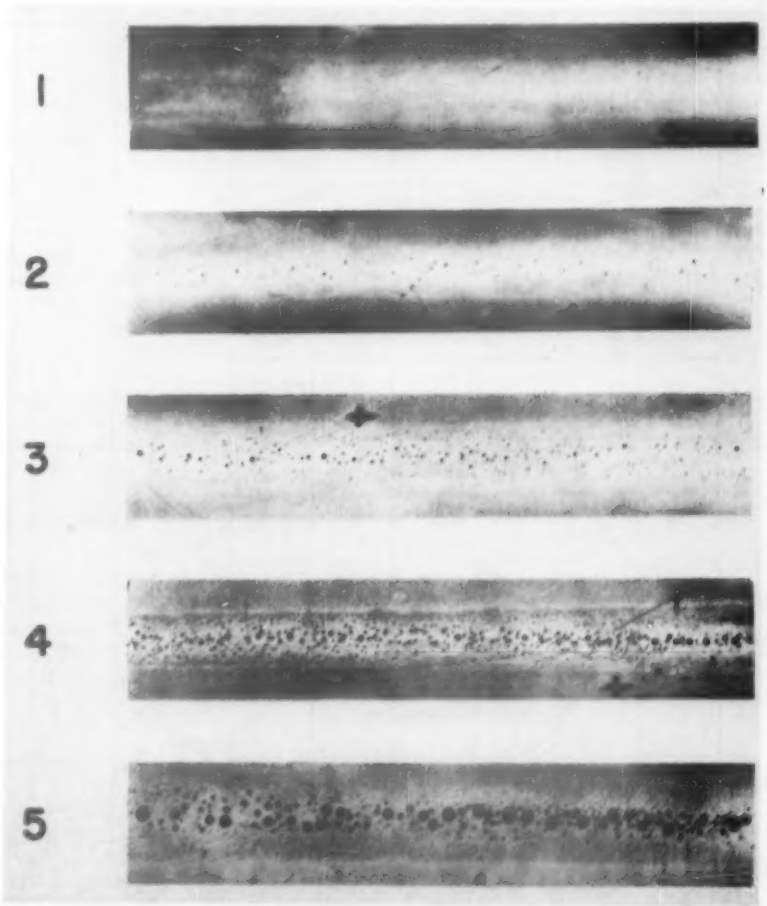

Fig. 1 Weld porosity ratings

J. D. Dowd is associated with Aluminum Research Laboratories, Aluminum Company of America, New Kensington, Pa.

Presented at AWS 1955 National Fall Meeting in Philadelphia, Pa., Oct., 17–21, 1955.

Mixing of the gases was accomplished using a simple Y-connection.

Porosity was evaluated by comparing radiographs of the welds with the series of standard radiographs shown in Fig. 1. Half-ratings were used for intermediate porosity levels. Thus, a rating of $2^1/_2$ would indicate porosity intermediate between ratings 2 and 3.

The shielding gas compositions investigated were 100% argon, 75% argon, 25% helium, 50% argon–50% helium, 35% argon–65% helium, 20% argon–80% helium and 100% helium. With each atmosphere, the voltage and current were varied throughout the ranges in which it was physically possible to deposit a bead in the overhead position. For most of the atmospheres, these ranges were 200 to 280 amp and 22 to 30 v. Since it would have been too time-consuming to make welds at all of the combinations of current, voltage, travel speed, and gas flow, the travel speed was held constant at 40 ipm and the gas flow at 70 cfh.

The results are presented as current-voltage-porosity diagrams in Figs. 2 to 7. In these diagrams, the porosity ratings are plotted at the points corresponding to the voltages and currents used in making the welds. Examination of the diagrams shows that the amount of porosity is dependent upon arc voltage and welding current in a manner such that each diagram can be divided into regions of varying soundness. This has been done using the following arbitrary divisions:

Porosity classification	*Average porosity rating*
Sound	Less than $1^1/_2$
Slight porosity	$1^1/_2$ to $2^1/_2$
Moderate porosity	$2^1/_2$ to $3^1/_2$
Severe porosity	Greater than $3^1/_2$

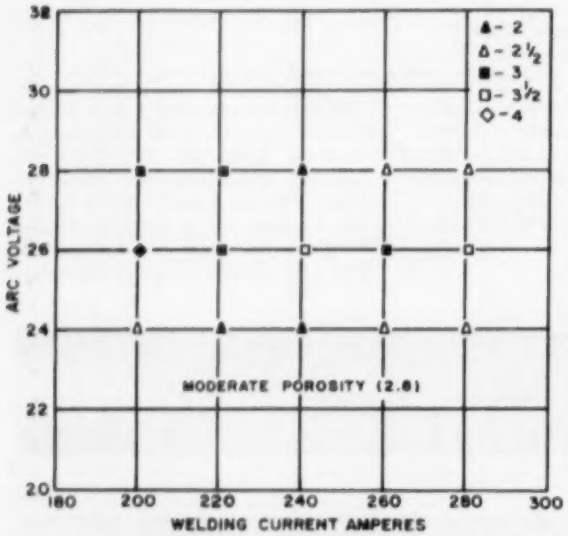

Fig. 2 Current-voltage-porosity diagram for 100% argon atmosphere

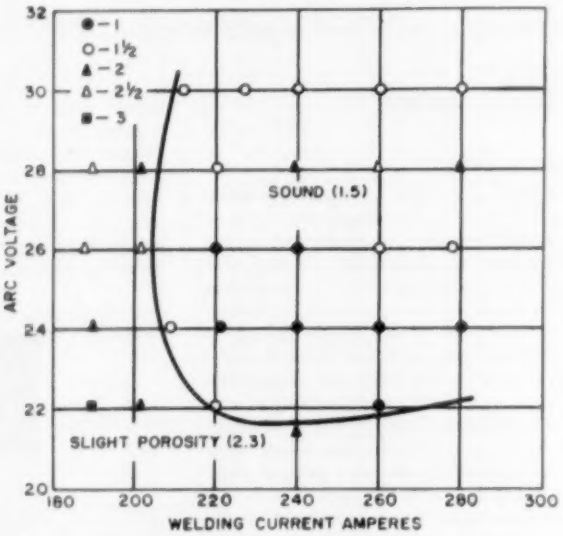

Fig. 4 Current-voltage-porosity diagram for 50% A – 50% He atmosphere

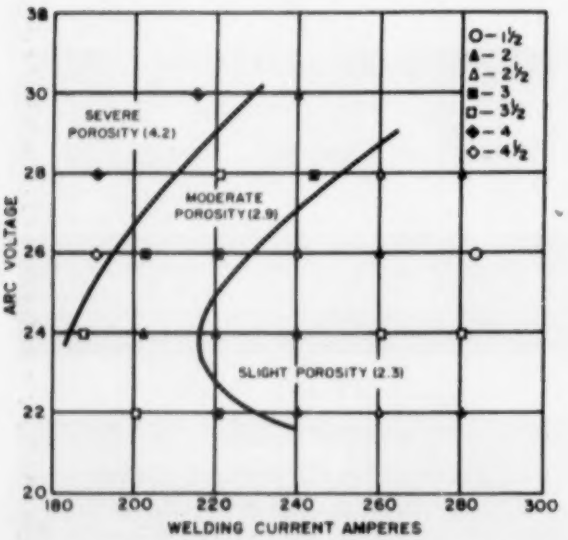

Fig. 3 Current-voltage-porosity diagram for 75% A – 25% He atmosphere

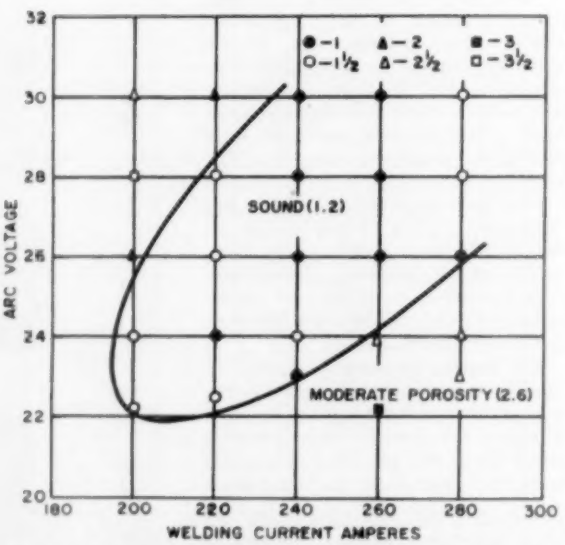

Fig. 5 Current-voltage-porosity diagram for 65% He – 35% A atmosphere

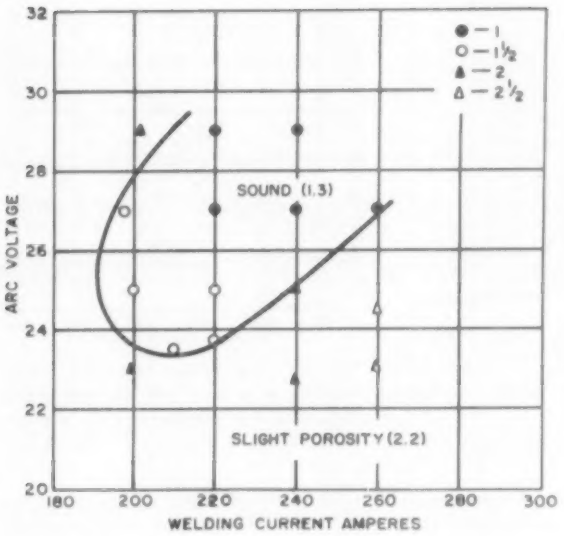

Fig. 6 Current-voltage-porosity diagram for 80% He–20% A atmosphere

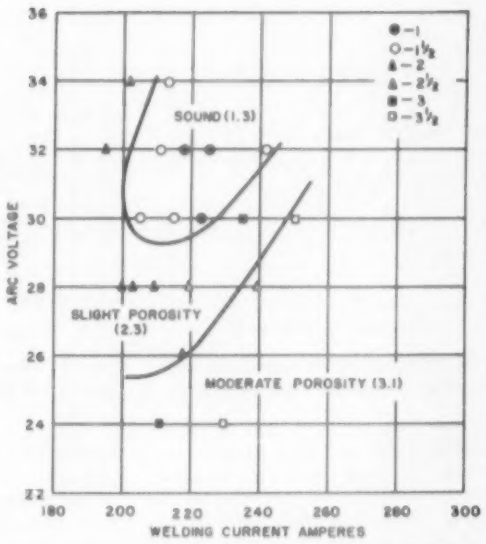

Fig. 7 Current-voltage-porosity diagram for 100% helium atmosphere

At a welding speed of 40 ipm, it was impossible to obtain sound welds at any voltage or current using pure argon or the 75% argon–25% helium mixture. Sound welds were obtained, however, over very wide current and voltage ranges using atmospheres containing 50% and 65% helium, balance argon. Increasing the helium content to 80% or more decreased the current and voltage ranges within which sound welds were obtained. These results clearly show that the 50–65% helium, balance argon atmosphere gives sound welds over the widest ranges of arc voltage and welding current.

While making the welds using argon, it was observed that the wetting of the base plate by the filler metal was much better at slow travel speeds than at fast travel speeds. Since wetting was affected by travel speed, it was thought that the voltage range within which sound consumable-electrode welds could be made might also be affected by travel speed. To check this, overhead, multi-pass welds were made in argon and 65% helium–35% argon atmospheres. To minimize the number of tests, all welds were made at 240 amp, the current that gave the soundest and best appearing welds at 40 ipm. The results, which are plotted in Fig. 8, show that sound welds were obtained at travel speeds between 24 and 60 ipm in the 65% helium–35% argon atmosphere. In argon alone, however, sound welds were only obtained over a very narrow voltage range and at travel speeds of about 25 ipm. Maintaining the arc voltage within the narrow range indicated for argon is not possible with most of the power sources in use today unless expensive electronic control equipment is employed. Therefore, it is not surprising that sound argon-shielded consumable-electrode welds are difficult to make in the overhead position using standard power sources not having voltage control.

Hot-Short Cracking

Hot-short cracking sometimes occurs during the welding of certain combinations of aluminum alloy plate and electrode. Previous work has indicated that the heat input during welding affects the magnitude of such cracking.[9] Since it was observed while making the porosity tests that heat input and welding time were less with the helium–argon mixture than with argon alone, it was reasoned that weld cracking might also be less in that mixture. To check this, cracking tests were run in 100% argon and 65% helium–35% argon atmospheres using aluminum–magnesium alloys for the base plates and electrodes. These alloys were selected because they are the best aluminum alloys for welded assemblies.

The procedure, which was essentially the same as that described previously,[9] consisted of fillet welding a $^{1}/_{2}$- x 4- x 10-in. vertical plate to a 1- x 4- x 10-in. base plate to form an inverted T-type specimen. Base plates of 3004, 5052, 5154 and 5056 alloys and electrodes of 1100, 3004, 5052, 5154 and 5056 alloys were used. The combinations of plate, electrode and atmosphere were tested in a random order. The 100% argon welds were made using 300 amp current; the 65% helium–35% argon welds were made using 200 amp current. The gas flow for both the argon and the helium–argon atmospheres was 50 cfh. The total longitudinal cracking in both fillets was used as a measure of the susceptibility to hot-short cracking.

The results are summarized in Fig. 9 in which cracking is plotted as a function of the magnesium content of the weld bead. Although the curves for argon and the 65% helium–35% argon mixture are similar in shape, the amount of cracking in the helium–argon atmosphere was much less than that in argon alone. From the weld-cracking standpoint, these data indicate that the helium–argon mixture is superior to argon, especially when using plate-electrode combinations susceptible to weld cracking.

Deposition Rate

Deposition rates during consumable-electrode welding with 100% argon and 65% helium–35% argon shielding gases were determined at various arc currents using $^{3}/_{32}$ in. diam 5154 electrode. The results, which are plotted in Fig. 10, show that the deposition rate in the helium–argon mixture is significantly greater than in pure argon, with the difference becoming more pronounced as the welding current is increased. It is evident from this that the time required to make a weld would be appreciably less with the mixture than with argon alone.

Ease of Welding

The ease with which a weld can be made will markedly affect both the quality and the cost of the weld. Any evaluation of ease of welding must include both the operator skill and the degree of control of welding conditions required to make a good weld.

The operator skill required to make a good weld is largely dependent upon the

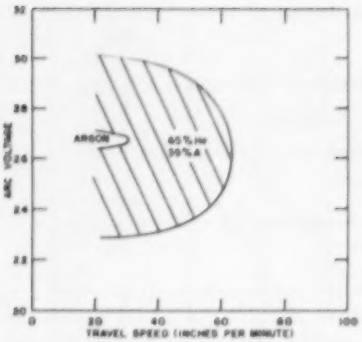

Fig. 8 Effect of travel speed on voltage range for sound overhead weld

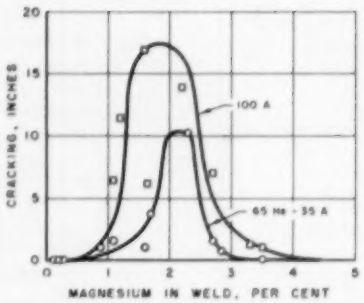

Fig. 9 Weld cracking of Al-Mg alloys in 100% A and 65% He–35% A

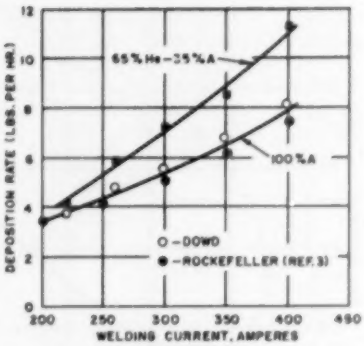

Fig. 10 Deposition rates for 5154 welding wire in 100% A and 65% He–35% A atmospheres ($^3/_{32}$-in. diam wire, 27 v)

ease with which the filler metal flows and wets the base metal. It was observed in both the porosity and weld-cracking tests that the filler metal flowed and wetted the base plate much more readily when the 65% helium–35% argon mixture was used than when argon alone was used. Because of this superior wetting, both tungsten-arc and consumable-electrode welding is physically easier using this mixture than it is using argon alone.

The good wetting obtained in the helium–argon mixture was also advantageous because it permitted the use of edge contours having small groove angles; with argon alone it was often necessary to use larger groove angles because of the poor wetting. The narrow angle contour is superior in that it reduces the amount of welding required to make a given joint.

Pure helium and mixtures high in helium also gave good wetting, but the arc in these shielding gases has poor stability and produces a lot of spatter. The arc in the 50–65% helium, balance argon mixture has neither of these disadvantages, being similar in these respects to the arc in pure argon.

It has already been pointed out that satisfactory welds can be made over much wider ranges of welding current, arc voltage and travel speed in the 50–65% helium, balance argon mixture than in argon, helium or other mixtures. This means that much wider variations in these conditions can be tolerated during welding in this mixture than in argon alone. Furthermore, with this helium–argon mixture machine settings are not critical; consequently fewer test welds have to be made to establish the proper settings.

Penetration with the helium–argon mixture is appreciably greater than with argon alone. In making most welds this would be an advantage; but in welds where shallow penetration is desired, it would be a disadvantage.

From the above it can be seen that welding is easier in the 50–65% helium, balance argon mixture than in argon, helium or other mixtures of helium and argon because of the superior metal flow and wetting; the good arc stability and freedom from spatter; the wider ranges of arc current, arc voltage and travel speed that can be used; and the deeper penetration of filler metal obtained.

Welding Cost

The cost of the shielding gas should generally be less with the helium–argon mixture than with argon alone. One reason is that the mixture costs about 10% less per cu ft than pure argon, based on an argon cost of 9.4 cents per cu ft and a helium cost of 8.0 cents per cu ft. Since the flow rates generally used with argon can also be used with the mixture, this 10% savings would usually be realized. A second and more important reason for lower gas costs is that the welding time using the mixture is appreciably less because of its higher deposition rate.

Other costs should also be less when welding with the helium-argon mixture. The higher deposition rate should reduce labor, power and burden costs. The small groove angle that can be used with the mixture would in many cases reduce gas, labor, power, burden and electrode costs. The decreased porosity obtained with the mixture would mean fewer repairs and lower inspection costs, as might also the decreased susceptibility to hot-short cracking. These savings, when added together, constitute a very real and worthwhile reduction in welding costs.

Summary

A shielding gas containing 50–65% helium, balance argon is superior to argon, helium, or other mixtures of argon and helium for both tungsten-arc and consumable-electrode welding of aluminum. This helium-argon shielding-gas mixture gives sounder welds, decreases the susceptibility to hot-short cracking, permits the use of wider ranges of voltages, current, and travel speed, makes welding easier and faster, and reduces welding costs.

References

1. Muller, A., Gibson, G. J., and Roper, E. H., "The Aircomatic Welding Process," The Welding Journal, **29** (6), 458–482 (1950).
2. Rockefeller, H. E., "Fundamentals of Inert-Gas-Shielded-Arc Welding," *Ibid.*, **30** (8) 711–716 (1951).
3. Moen, W. B., and Gibson, G. J., "Schlieren Analysis of Inert-Gas Arc Shields," *Ibid.*, **31** (3) 208–213 (1952).
4. Breymeier, R. T., "Metal Transfer in Sigma Welding," *Ibid.*, **31** (5) 393–399 (1952).
5. Rockefeller, H. E., "Inert-Gas-Shielded Arc Consumable Electrode Welding," *Ibid.*, **31** (7) 575–580, (1952).
6. Skolnil, Merrill, and Jones, T. B., "High-Current Tungsten Arc in Argon, Helium, and Their Mixtures," *Ibid.*, **32** (1), Research Suppl., 55-s–64-s (1953).
7. Gibson, G. J., "Gas Flow Requirements for Inert-Gas-Shielded Arc Welding," *Ibid.*, **32** (4) Research Suppl., 198-s–208-s (1953).
8. Cunningham, J. W., and Cook, H. C., "A Comparison of Shielding Mixtures for Gas-Shielded Arc Welding," *Ibid.*, **32** (9) 834–841 (1953).
9. Dowd, J. D., "Weld Cracking of Aluminum Alloys," *Ibid.*, **31** (10), Research Suppl., 448-s–456-s (1952).

MECHANICAL PROPERTIES OF BUTT JOINTS BRAZED WITH BAg-1, BAg-3 AND BCu FILLER METALS

The room temperature, impact, tensile and fatigue properties of brazed butt joints are presented in a manner that will enable designer to design properly these joints for specific applications

BY G. HANSEL

Occasionally the designer encounters a joining application for which one of the brazing processes would be best suited. However, the nature of the joint may be such that questions are raised about little known properties, such as the impact or fatigue values which may be obtained from brazed butt joints. A large amount of brazing involves the use of hardenable ferritic-base materials, with the filler metal used being selected partially due to the relationship that the brazing cycle bears to the heat treatment of the base material.

This investigation has been conducted to establish the physical properties of brazed butt joints in a manner which will enable the designer to properly design butt joints for specific applications. A hardenable ferritic steel of the 2½% Ni, ½% Mo variety, and filler metals BAg-1, BAg-3 and BCu have been chosen to represent the field of joining applications which often arise. The room temperature, impact, tensile and fatigue properties of joints prepared with these materials are presented in this paper.

Materials

Filler metal* BAg-1 was selected for tests on joints which may be prepared without exceeding a temperature of 1200° F. Filler metal BAg-3 flows well at 1300° F, and was chosen to obtain data on the properties of joints which are prepared below the 1340° F transformation temperature range which characterizes many ferritic materials. For a joining situation which would permit fully heat treating the brazed assembly, the use of BCu filler metal is possible, and was selected for the third series of tests.

The characteristics of the materials selected for this investigation are shown in the table below.

Nominal Composition

Brazing filler metal, %	Ag	Cu	Zn	Cd	Ni	Solidus, °F	Liquidus, °F
BAg-1	45.0	15.0	16.0	24.0		1125	1145
BAg-3	50.0	15.5	15.5	16.0	3.0	1193	1270
BCu		99.9				1982	1982

Base metal	
C, %	0.22
Mn, %	0.61
Ni, %	2.25
Mo, %	0.41
V, %	0.04
Ac_1, °F	1240

Although the Ac_1 of the base material used for this investigation is lower than the 1300° F brazing temperature of BAg-3, this steel is hardenable during furnace cooling, and was used throughout for this reason. The extensive grain growth which occurs in most steels during the copper brazing cycle makes a grain refinement heat treatment desirable. Grain refinement is accomplished by austenitizing slightly above the A_3. The assembly is then cooled rapidly enough to obtain hardening, and then tempered. The fact that the 2.5% Ni – 0.5% Mo steels are furnace hardenable made their use desirable in order to eliminate the need for handling the austenitized and brazed parts for quenching in some other media.

Brazing Procedure

Using the Silver Alloy Filler Metals, BAg-1 and BAg-3

The BAg-1 and BAg-3 test specimens were to be brazed using an acid-fluoride paste flux instead of the controlled atmosphere employed in many brazing cycles. The problem of obtaining sound joints while using a paste flux (Type No. 3*) indicated the desirability of selecting, from two brazing procedures, the better procedure to be used in the preparation of test specimens. One procedure would involve the use of a specimen having the joint clearance fixed by the depth of the recess ground into the butting specimen halves, with filler metal fed into the joint during brazing (as shown by Fig. 1). In the second procedure to be investigated, the joint surfaces of both specimen halves are precoated with filler metal and the specimen is brazed in the vertical position, under a mechanically applied pressure of 100 psi. No effort is made to fix the thickness of the filler metal with this technique, except that the pressure on the joint, the thermal cycle for brazing, and the alignment of the specimen were kept uniform throughout.

Procedure 1. Figure 1 shows the specimen employing a fixed joint clearance. Flux is applied to the joint sur-

G. Hansel is associated with General Electric Co., Materials and Processes Laboratory, Schenectady, N. Y.

Presented at AWS 1955 National Fall Meeting held in Philadelphia, Pa., Oct. 17–21.

* AWS-ASTM classification of brazing filler metal.

* AWS Brazing Flux Type No. 3 (see *AWS Brazing Manual*).

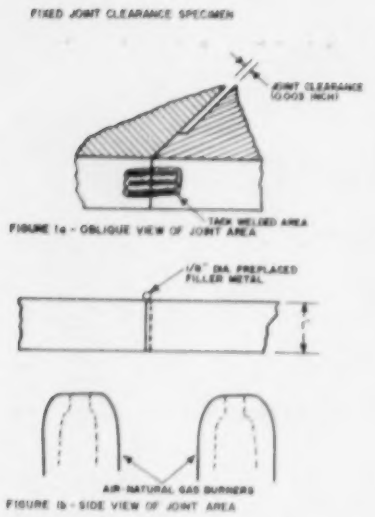
FIXED JOINT CLEARANCE SPECIMEN
JOINT CLEARANCE (0.003 INCH)
TACK WELDED AREA
FIGURE 1a - OBLIQUE VIEW OF JOINT AREA
1/8" DIA PREPLACED FILLER METAL
AIR-NATURAL GAS BURNERS
FIGURE 1b - SIDE VIEW OF JOINT AREA

Fig. 1 Oblique and side views of specimen employing fixed joint clearance

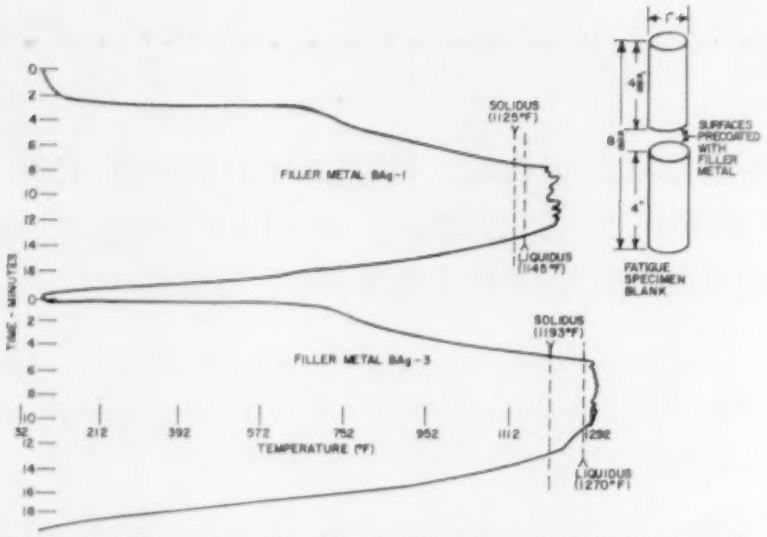

Fig. 3 Time-Temperature plot of the brazing cycles recorded when preparing blanks to be machined into fatigue specimens

faces before they are assembled in position and tack welded as shown. Heat is applied by air-natural gas radiant burners positioned as shown. Although the method of heating proved rapid and provided uniform heat distribution, unsatisfactory joints resulted. The BAg-1 and BAg-3 filler metals displayed a strong tendency to fill the very tight clearances at the shoulders of the specimen, but would not fill the 0.003-in. interstice of the test area. It appeared that a joint clearance could be selected which would result in more satisfactory joints. This investigation would not serve its purpose, however, if data were obtained using a technique that involves a critical relationship between joint clearance and the ability to consistently produce quality joints.

Procedure 2. Investigation of a second procedure proved that it provided better joints and did so with greater consistency. This is the procedure which was used and is as follows:

1. Prepare the base material in blanks whose size is determined by the size of the specimen to be machined from the brazed assembly. All surfaces which parallel the joint are ground flat and maintained in parallel with each other.

2. Degrease the specimen halves and grit blast the two joint surfaces with No. 80 steel grit.

3. Precoat the two joint surfaces with BAg-1 or BAg-3 filler metals. After the specimen halves have cooled remove all flux residues and apply a fresh, thin coating of acid fluoride paste flux to each surface.

4. Place the specimen halves in a mandrel press and arrange burners, thermocouple, etc. Apply 100 psi to the joint, and proceed with the brazing operation, using the equipment set up as shown by Fig. 2. (The alignment of the bottom part of the specimen is fixed by a locating pin in the center of the flat plate clamped to the press.)

5. Bring the work to brazing temperature using air-natural gas radiant heating and a temperature recording unit. Figure 3 shows representative thermal cycles for brazing with filler metals BAg-1 and BAg-3.

Procedure

Using the BCu Filler Metal

The tight joint fits which are requisite to successful brazing with copper filler metal were maintained by clamping the specimen halves tightly together and welding them in place. Larger specimens were used for the preparation of samples brazed with BCu and several test specimen blanks were obtained from each.

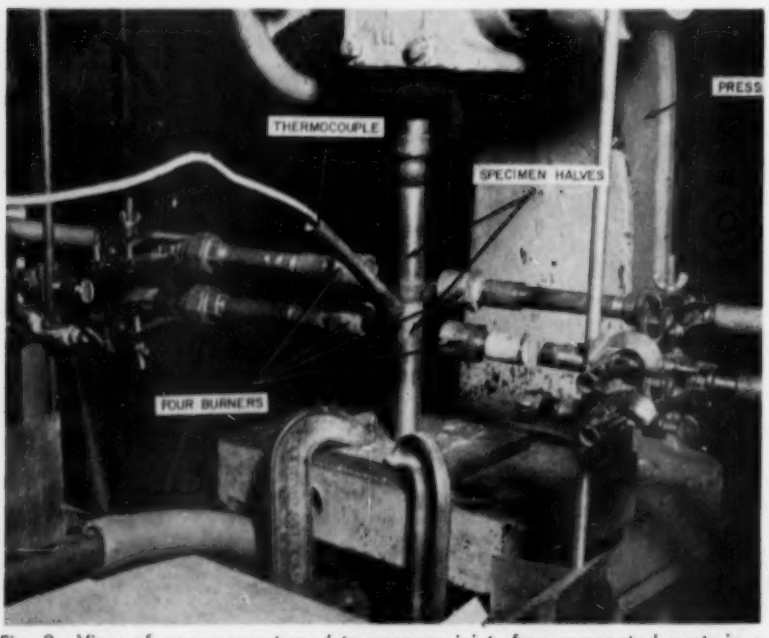

Fig. 2 View of arrangement used to prepare joints from precoated parts in a mandrel press

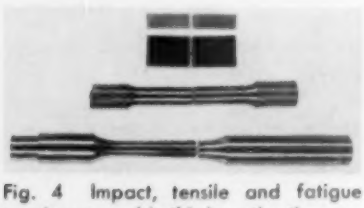

Fig. 4 Impact, tensile and fatigue specimens used in this investigation

The duration of the furnace brazing cycle was 4 hr, in hydrogen atmosphere (dewpoint −40° F), including 1 hr hold time at 2100° F. After cooling from 2100° F, the base metal is fully hardened, with an extremely large grain size. Subsequent grain refinement is accomplished by austenitizing at 1545° F for 2 hr and furnace cooling to 750° F at a rate of 200° F per hour. Tempering at 1180° F for 2 hr returned the material to a hardness of 190 (Bhn).

Testing

The specimens and procedures used in obtaining impact, tensile and fatigue values for this investigation are standard for tests on homogenous specimens, with the exception that all impact specimens were unnotched. The standard 0.505-in. tensile specimens were machined from 1-in. square blanks and loaded at 40,000 psi per minute. The impact specimens (0.394 x 0.394 x 2.2 and 0.394 x 0.788 x 2.2) were evaluated in a 110 ft-lb testing machine. Figure 4 is a view of each of the specimens used, including the rotating cantilever fatigue specimen. The fracture in the fatigue specimen may occur at any point throughout the tapered region of uniform stress. For reasons of uniformity, however, all specimens were prepared with the joint located as shown by the fracture.

Test Results

One of the purposes of this investigation was to evaluate a selected set of conditions suitable for the brazing of large parts. It is emphasized that one of the most valuable findings of this investigation was learning the extent to which scatter exists in tests conducted on specimens which have been prepared by this set of conditions.

The charts in Figs. 5 and 6 present impact and tensile test results as a function of joint clearance, and serve to illustrate this scatter. An unnotched specimen, such as that shown in Fig. 4, was used for impact testing.

It is important to note that the chart in Fig. 6 shows a uniformity of tensile strength values for specimens prepared with BCu and BAg-1 filler metals. Impact specimens prepared with these filler metals, however, displayed results whose inconsistency resembled that of specimens prepared with BAg-3, a filler metal whose tensile specimens displayed a considerable variation in properties.

The observation that impact-tested joints displayed inconsistencies which were not shown in similarly prepared tensile specimens poses an interesting problem. Joint quality as shown by an examination of the fractures is equal in both the tensile and impact specimens. Similarly, no useful correlation between joint clearance and impact strength seems to exist for the joint clearances

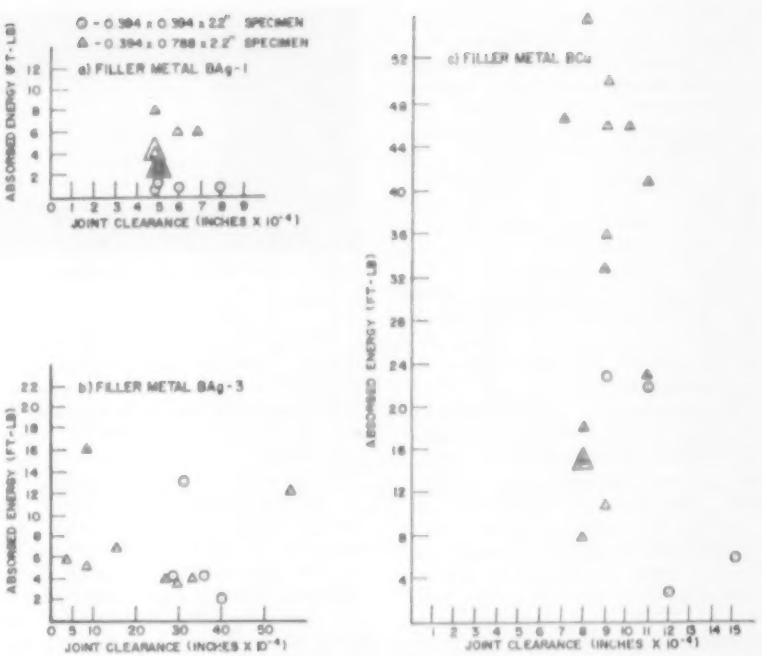
○ - 0.394 x 0.394 x 2.2" SPECIMEN
△ - 0.394 x 0.788 x 2.2" SPECIMEN
a) FILLER METAL BAg-1
b) FILLER METAL BAg-3
c) FILLER METAL BCu
ABSORBED ENERGY (FT-LB)
JOINT CLEARANCE (INCHES X 10⁻⁴)

Fig. 5 Scatter plots showing the joint clearance and absorbed energy values obtained from the investigation of impact properties

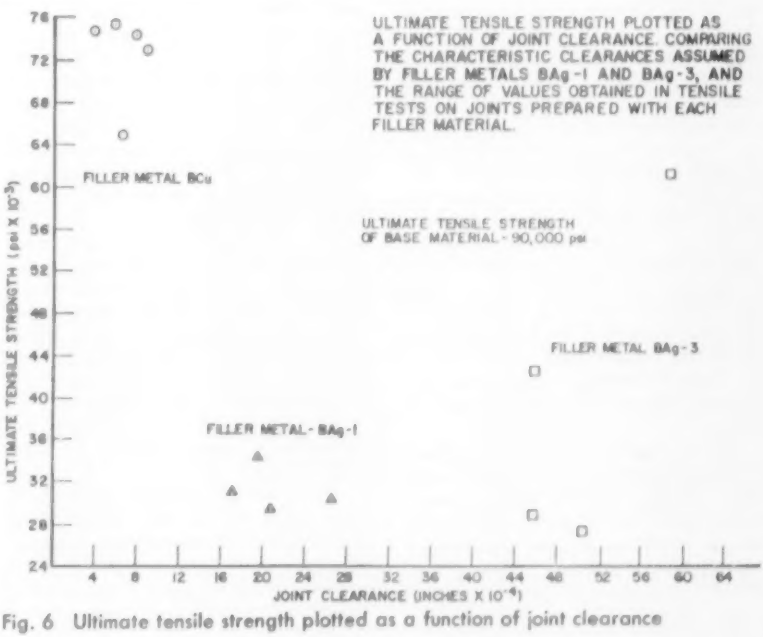
ULTIMATE TENSILE STRENGTH PLOTTED AS A FUNCTION OF JOINT CLEARANCE. COMPARING THE CHARACTERISTIC CLEARANCES ASSUMED BY FILLER METALS BAg-1 AND BAg-3, AND THE RANGE OF VALUES OBTAINED IN TENSILE TESTS ON JOINTS PREPARED WITH EACH FILLER MATERIAL.
FILLER METAL BCu
ULTIMATE TENSILE STRENGTH OF BASE MATERIAL - 90,000 psi
FILLER METAL BAg-3
FILLER METAL - BAg-1
ULTIMATE TENSILE STRENGTH (psi X 10³)
JOINT CLEARANCE (INCHES X 10⁻⁴)

Fig. 6 Ultimate tensile strength plotted as a function of joint clearance

which were tested. The difference in the consistency of test results, however, is striking, and it is concluded that impact testing has subjected these brazed joints to a stress condition which, for them is severe, being capable of detecting flaws, imperfections or other differences much more effectively than will tensile testing.

The nature of the stress condition which exists in a brazed joint under load is first illustrated by considering the "metallurgical notch" which exists when a thin, weak member joins two materials of higher strength. The weaker member, having a lower yield point, will elongate as far as possible before it either (1) work hardens until it reaches the strength level of the base material and causes it to elongate, or (2) fails in the joint. It is assumed that the weakest plane in the joint will be at

its center, in the region of lowest base metal alloy content. Bredzs and Rostoker[1] have discussed the manner in which the tensile strength of a material may be increased by the biaxial constraint occurring when this material is in a brazed joint as a filler metal. The "neck down" effect which is common to specimens in tension, and which is suppressed by biaxial constraint, occurs in the impact testing of unnotched ductile materials such as that shown in Fig. 7 (solid Charpy). Suppression of the neck down effect will lessen the amount of filler metal elongation which may occur before the tensile strength of the base metal is reached.

The high rate of strain to which a specimen is subjected during impact testing contrasts sharply with the strain rate imposed on a specimen in tensile test. This is very significant when one considers that an imperfection, under the standard conditions of tensile testing, has more opportunity to alter its geometry, thus alleviating the notch severity which it originally possessed, than is allowed under impact conditions. In applying this to the variation in absorbed energy values obtained from impact testing, it can be seen that the bend angle which an impact specimen can attain before fracture occurs is dependent upon the ability of those fibers which are under tensile stress to elongate. Of the impact specimens brazed with BCu filler metal, some joints contained imperfections which rendered the surface fibers too weak to cause elongation in the base metal on each side of the joint. As these fibers fail, a very sharp notch results, and the fracture proceeds to completion with almost no further absorption of impact energy. It appears that the contrast between the uniformity of impact and tensile test results for BCu, BAg-1 and BAg-3 joints may be explained on the basis of the above discussion, as applied to the inherent characteristics of each type of joint.

Figure 8 contains a view of typical impact fractures in joints brazed using BAg-1, BAg-3 and BCu filler metals. Variations in joint efficiency* occur only among specimens brazed with BAg-3 filler metal. The small, uniformly distributed gas voids in BCu joints are quite visible in this photograph. All joints prepared with BAg-1 exhibited a joint efficiency of approximately 50% and consisted of small areas in which flux had been entrapped, uniformly dispersed between small bonded areas free of flux entrapment. This condition contrasts sharply with that existing in BAg-3 joints where a nonuniform distribution of large voids and large bonded areas coexist.

* Joint efficiency is the percentage of a given joint area which is completely bonded to its mating surface.

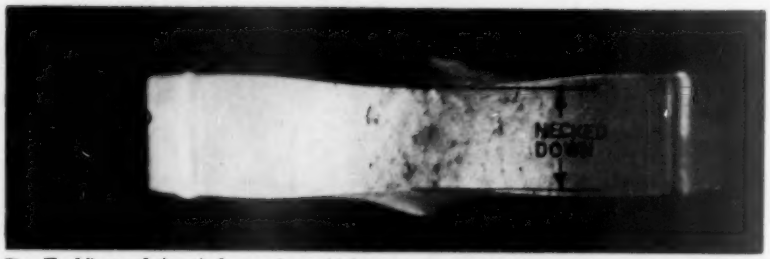

Fig. 7 View of the deformation which exists in a solid impact bar after testing

In reviewing the above joint characteristics from the standpoint of their performance during impact testing, it will be seen that the amount of scatter, and the impact strength level in which this scatter occurs, may be discussed with respect to the type and frequencies of surface imperfections which are peculiar to each filler metal. BAg-1, for example, produced joints containing a very large number of small voids. Although this filler metal produced tensile specimens which were superior to some of the tensile specimens brazed with BAg-3, and were much more uniform, the impact test results were low due to the fact that each specimen possessed surface flaws. The characteristic nature of void formation in specimens brazed with BAg-3, however, indicates that more variation will occur in the values obtained by impact testing since not all joints will contain voids at their edges. By virtue of the corollary possibility that individual voids may or may not be sufficiently large, less uniformity is to be found in the tensile data for BAg-3.

The observations which are made regarding the factors affecting impact and tensile values, apply equally well to an understanding of their fatigue properties, with fatigue test and tensile test results each being dependent upon the characteristics of the joint in a similar manner. The charts in Figs. 9, 10, and 11 show the fatigue curves which have been obtained for each filler metal.

The rotating cantilever test which was employed in this investigation places alternating tensile and compressive stresses on the specimen fibers according to the pattern of a sine curve of 1500–1700 wave lengths per minute. Examination of failed BAg-3 tensile specimens revealed no dependable correlation between the incidence of surface imperfections at the joint and the performance of the joint in fatigue test. This finding contrasts sharply with the fact that the fatigue properties of a homogenous part improve with its smoothness.

The two fatigue specimens prepared with BAg-1 which were somewhat above the fatigue curve for these specimens had a joint clearance of 0.0015 in., whereas the remainder of these joints were approximately 0.0025 in. thick. The uniform condition of flux entrapment probably makes joint clearance the only significant factor in influencing the minor variation existing in this set of test values.

In examining the fatigue testing of BAg-3 specimens, each of two variables, joint efficiency and joint clearance, have an influence on the test result. The presence of two variables prevents an attempt to explain the single variation which occurred in fatigue testing these specimens. It was generally observed, however, that joint efficiency is more important than joint clearance in determining fatigue performance.

Joint Fractures

Figure 12, (*a*), (*b*), and (*c*), shows representative photomicrographs at 250 × of joint fractures prepared with BAg-1, BAg-3 and BCu, respectively. Each specimen has been nickel plated for the polishing operation. Evidence of the grit-blasting operation remains apparent in Fig. 12 (*a*) and (*b*). Note the thorough coverage of the base metal by BAg-3 in contrast to that shown in

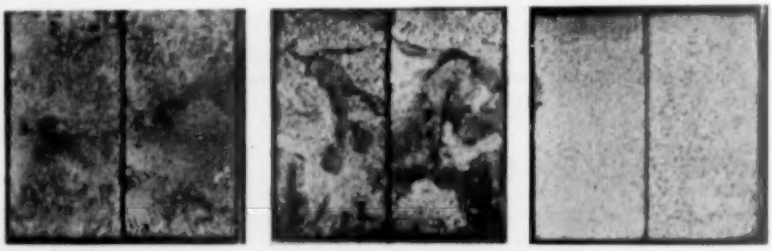

Fig. 8 Shown is the appearance of fractures in impact specimens prepared with BAg-1, BAg-3 and BCu

the fractured BAg-1 specimen. Flux entrapment in the presence of BAg-1 results in areas which are not wet by filler metal, the precoated filler metal having been displaced by flux. In the case of the more sluggish BAg-3, however, flux is entrapped, as for instance between the two joint surfaces which remain wetted by the filler metal.

The contrast between the size and nature of the voids is shown in Figs. 13 and 14, which are radiographs of joints prepared using BAg-1 and BAg-3 filler metals. Note the fine, granular dispersement of void characterizing BAg-1 filler metal and contrasted with the irregular large dispersement of voids shown for BAg-3 filler metal in Fig. 14. Figure 12 (*c*) reveals the extensive alloying which has occurred between the BCu filler metal and the base metal.

It is interesting to note the characteristic mode of the failure occurring in a fatigue specimen brazed with BCu. The observations which were made on fractures in BAg-1 and BAg-3 fatigue specimens do not show that this discussion may be extended to the case of the silver alloy filler metals.

Figure 15 is a photograph of a BCu specimen which has been fatigue tested to failure. The wormlike areas of gas entrapment are typical of those which were found in all specimens which were prepared for this investigation using BCu filler metal. Of interest, is the manner in which darkening of the filler metal is related to the progression of failure through the joint. In this specimen, the failure was clearly started from the left of the sample shown in Region A. From the bright areas in Region A in the upper half of the joint, it can be seen that the filler metal pulled away from the base metal to provide the beginning of failure. As failure progressed through the joint to the right, it accelerated through Region B until failure occurred almost instantaneously upon reaching the edge of this region. This observation is based upon the manner in which the discoloration in Region B gradually lessens until the salmon color characteristic of tensile and impact failures in joints brazed with BCu filler metal is reached.

In examining the fractures in all specimens which were prepared using the silver alloy filler metals and paste flux type No. 3, the importance of eliminating flux entrapment in brazed joints is very striking. The statement that there are possibilities for butt brazed joints received strong support when one considers that tensile strength values of 30,000 psi were obtained on BAg-1 specimens have a joint efficiency of only 50%, or that a BAg-3 specimen of only 60% joint efficiency fractured at 60,000 psi. The need for better, more practical methods of consistently ob-

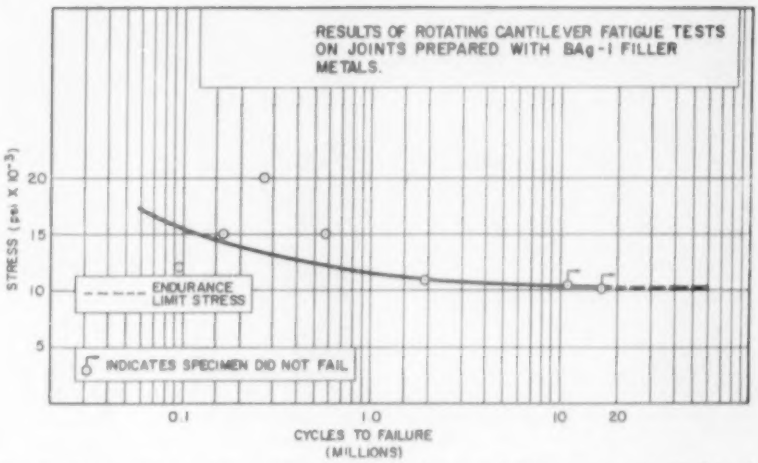

Fig. 9 Results of rotating centilever fatigue tests on joints prepared with BAg-1

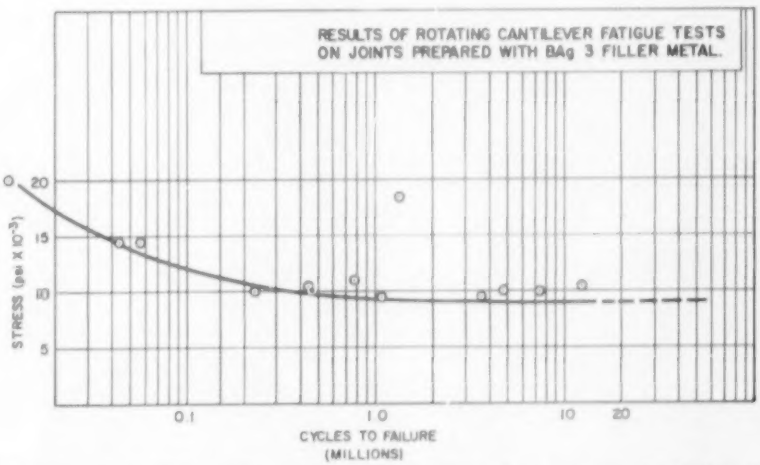

Fig. 10 Results of rotating centilever fatigue tests on joints prepared with BAg-3

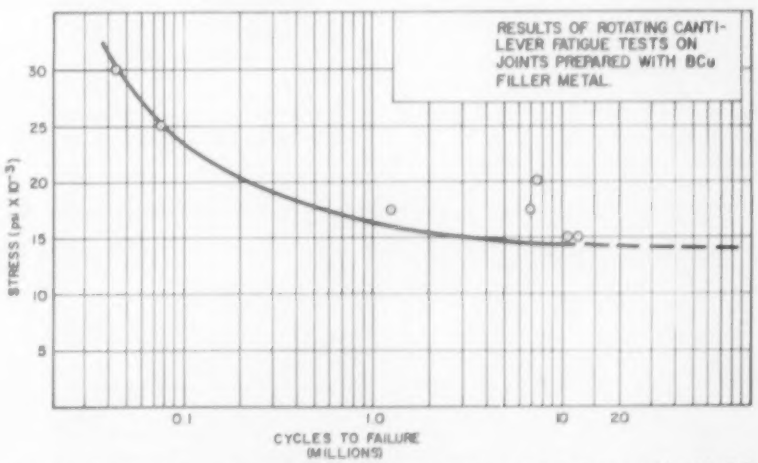

Fig. 11 Results of rotating centilever fatigue tests on joints prepared with BCu

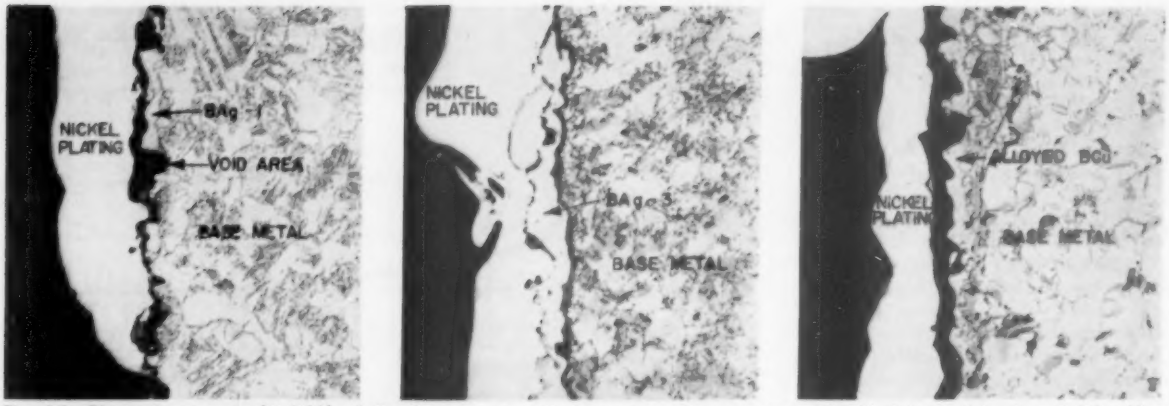

Fig. 12 Photomicrographs (X 250) of the fracture area in impact specimens prepared with BAg-1, BAg-3 and BCu filler metals. Each of these specimens was nickel plated for the polishing operation. (Reduced by 1/2 upon reproduction).

taining sound brazed joints is great, and is now under further study on a practical basis.

Conclusions

1. The impact properties of sound brazed joints will vary according to the ability of those joint fibers which are under tensile stress to cause elongation of the base material. The amount of scatter to be found in impact tests on brazed joints will depend in part upon the incidence of joint imperfections occurring at the joint surface under tensile stress.

2. The tensile strength of joints which are brazed under the conditions selected for this investigation is approximately 30,000 psi for BAg-1 and ranged from 27,600 to 60,400 psi for BAg-3. Specimens brazed with BCu provide tensile strengths of approximately 74,000 psi at a joint clearance of 0.0004–0.0008 in.

3. Although BAg-3 joints show higher strength potential than those prepared with BAg-1, they are quite inconsistent. For this reason, the endurance limit stress established by this investigation for joints brazed with BAg-1 was 11,000 psi, and 9000 psi for joints prepared with BAg-3. The endurance limit stress of joints prepared with BCu filler metal is 14,000 psi.

4. This investigation has shown that the field of silver-alloy filler-metal brazing has an outstanding need for fluxes and techniques which may be used with the flexibility required by many manufacturing operations to provide consistently void-free joints.

Acknowledgment

The author expresses his appreciation to Wesley J. Van Natten and Dr. W. H. Chang of the Materials and Processes Laboratory, General Electric Co., Schenectady, for their helpful suggestions and review.

Reference

1. Bredzs, N., and Rostoker, W., "Fundamentals of Brazing," Final Report (June 1952–June 1953), Armour Research Foundation.

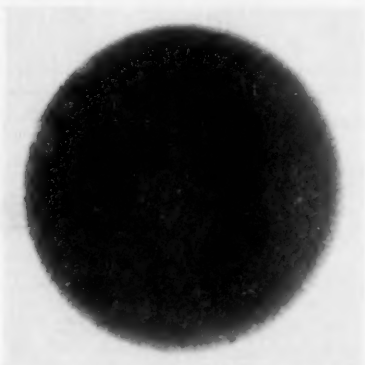

Fig. 13 Radiograph of joint brazed with BAg-1 filler metal

Fig. 14 Radiograph of joint brazed with BAg-3 filler metal

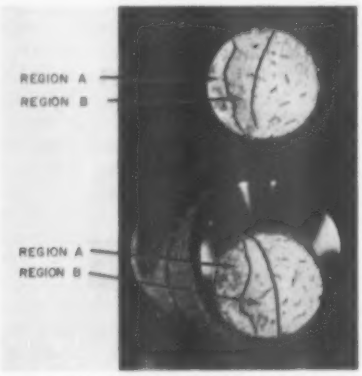

Fig. 15 View of a typical fracture in a fatigue specimen prepared with BCu filler metal

RESEARCH NEWS

(*Continued from page 194-s*)

certified for nine trace elements: aluminum, boron, copper, molybdenum, niobium, lead, vanadium, tungsten, and zinc. These are available in the form of rods 4/32 in. in diam and 4 in. long.

The rods have a uniform grain structure resulting from hot-rolling and annealing the cast metal. The surfaces of the rods were finished by centerless grinding. The homogeneity of the rods, both in cross and longitudinal sections, was studied by spectrochemical analysis at the Bureau and was found satisfactory with respect to the concentrations of the certified elements.

The standards can be applied directly to the analysis of stainless steel rods prepared in a similar manner and with similar dimensions. However, when the standards are applied to the analysis of steel samples prepared by other procedures, adjustments may be required to correct for variations introduced by physical differences.

The stainless steel standards may be obtained from the National Bureau of Standards for a fee of $8.00 each.